

# Spontaneous Symmetry Breaking and Exotic Quantum Order in Integer Quantum Hall Systems under a Tilted Magnetic Field

Daw-Wei Wang<sup>1,2</sup>, Eugene Demler<sup>2</sup>, and S. Das Sarma<sup>1</sup>

<sup>1</sup>*Condensed Matter Theory Center, Department of Physics, University of Maryland, College Park, MD 20842*

<sup>2</sup>*Physics Department, Harvard University, Cambridge, MA 02138*

(November 19, 2018)

We use the microscopic Hartree-Fock approximation to investigate various quantum phase transitions associated with possible spontaneous symmetry breaking induced by a tilted magnetic field in the integral quantum Hall regime of wide parabolic wells and zero width double well (bilayer) systems. Spin, isospin (associated with the layer index in the bilayer systems), and orbital dynamics all play important roles in the quantum phase transitions being studied. We propose a general class of variational wavefunctions that describe several types of parity, spin, and translational symmetry breaking, including spin and charge density wave phases. In wide well systems at odd filling factors, we find a many-body state of broken parity symmetry for weak in-plane magnetic fields and an isospin skyrmion stripe phase, which simultaneously has isospin and charge modulation, for strong in-plane fields. In wide well systems at even filling factors, we find direct first order transitions between simple (un)polarized QH states with several complex many-body states that are only slightly higher in energy (within the Hartree-Fock theory) than the ground state. We suggest that going beyond the approximations used in this paper one may be able to stabilize such many-body phases with broken symmetries (most likely the skyrmion stripe phase). In a bilayer system at the filling factor  $\nu = 4N \pm 1$ , where  $N$  is an integer, we obtain an isospin spiral stripe phase in addition to the known (in)commensurate phases and the stripe phase without isospin winding. We do not find a charge or spin density wave instability in the bilayer system at  $\nu = 4N + 2$ , except for the known commensurate canted antiferromagnetic phase. Zero temperature quantum phase diagrams for these systems are calculated in the parameter regime of experimental interest. We discuss the symmetry properties of our predicted quantum phase diagrams and give a unified picture of these novel many-body phases. We point out how quantum level crossing phenomena in many situations (tuned by the applied tilted magnetic field) may lead to interesting quantum phases and transitions among them. A conceptually new aspect of our theory is the predicted possibility for the spontaneous breaking of parity symmetry, which indicates a “ferroelectric” quantum order in integer quantum Hall systems and has not been considered in the literature before.

## I. INTRODUCTION

Unidirectional charge density wave order (also called stripe order) in quantum Hall (QH) systems has been extensively studied [1] since the first theoretical prediction in 1996 [2,3] and the first experimental observation in high Landau levels via the magnetoresistance anisotropy measurement in 1999 [4,5]. Many related phenomena, e.g. transport via internal edge state excitations [6–8], liquid crystal phases [1,9], reorientation of stripe directions [10–12], and re-entrant integer quantum Hall effect [13], have been widely explored both theoretically and experimentally in this context. Stripe formation at fractional filling factors,  $\nu = (2N + 1)/(4N + 4)$ , corresponding to the composite fermion filling factor,  $\nu^* = N + 1/2$ , was also proposed to have energy lower than the conventional Laughlin liquid, composite-fermion Fermi sea or paired composite-fermion state [14]. (Throughout this paper  $N$  is zero or an integer,  $N = 0, 1 \dots$ , and  $\nu = 1, 2, 3 \dots$  is the Landau level filling factor of the whole system.) However, most of the stripe phases discussed in the literature so far are formed by electrons in the top (half-filled) level of the QH system at high half-odd-integer (HOI) filling factors (e.g.  $\nu = N + 1/2$  for  $N \geq 4$ ), while the stripe formation at integer filling factors is seldom studied either theoretically or experimentally.

We develop a detailed theory in this paper for possible spontaneous symmetry breaking and associated exotic quantum order in wide-well and double-well integer quantum Hall systems by considering all the symmetry properties of the realistic system Hamiltonians. The great advantage of the quantum Hall systems in studying quantum critical phenomena is, however, the existence of various energy gaps (at the Fermi level) which enables us to carry out reasonable energetic calculations (within a mean-field Hartree-Fock theory) to quantitatively check whether the various possible quantum phase transitions and exotic quantum order allowed by symmetry considerations are actually energetically favored in realistic systems. We therefore construct explicit variational wavefunctions for various

possible (exotic) quantum states, and carry out energetic calculations to find the optimal ground state. Using an in-plane parallel magnetic field (in addition to the perpendicular field necessary in the quantum Hall problem) to tune system parameters, we find a surprisingly rich quantum phase diagram in our systems of interest. We believe that the symmetry-broken states with exotic quantum order predicted by our theory should be experimentally observable in transport and inelastic light scattering experiments. We emphasize that the salient feature of our work (making it particularly significant from the experimental perspective) is that we not only identify spontaneous symmetry breaking and exotic quantum order allowed by the system Hamiltonian, but also carry out Hartree-Fock energetic calculations to obtain the quantum phase diagrams using realistic system Hamiltonians. Among the spontaneous symmetry breakings predicted in this paper are, in addition to the usual translational and spin symmetries, the spontaneous breaking of discrete parity symmetry in a number of interesting situations.

Very recently, magnetoresistance anisotropy was observed in both doped GaAs/AlGaAs [15] and Si/SiGe [16] based semiconductor quantum well systems at even integer filling factors, when a strong in-plane magnetic field ( $B_{\parallel}$ ), in addition to the perpendicular magnetic field ( $B_{\perp}$ ) producing the 2D Landau levels, is applied. In Refs. [15,16], it is proposed that the strong in-plane magnetic field increases the electron Zeeman energy so much that the highest filled Landau level (with spin down) has a level crossing with the lowest empty Landau level (with spin up), and then a charge density wave (CDW) phase may be stabilized by electron Coulomb interaction. Our recent work [17] on the magnetoplasmon energy dispersion of a wide well system in the presence of a strong in-plane magnetic field finds a near mode softening in the spin-flip channel, suggesting the possibility of a spin density wave (SDW) instability near the degeneracy point. As a result, we proposed a spin-charge texture (skyrmion [18]) stripe phase [8,17] to explain the magnetoresistance anisotropy observed in the experiments [15,16]. In an earlier theoretical work, Brey [19] also found a charge density wave instability in a wide well at  $\nu = 1$  *without* any in-plane magnetic field. Murthy [20] recently considered the the coexistence of quantum Hall order and density wave order in a single well at  $\nu = 2$  with zero Zeeman energy and strong level mixing. To the best of our knowledge, however, systematic theoretical analyses of these candidate stripe phases at integer QH systems have not yet been carried out and need to be further developed.

A double well (bilayer) quantum Hall system is another system where one may see a stripe phase order at integral filling factors. At total filling factor  $\nu = 4N \pm 1$ , electrons are equally distributed in the two layers if no gate voltage or in-plane magnetic field is applied. We note that the bilayer systems of filling factor  $\nu = 4N - 1$  ( $N > 0$ ) can be understood to be equivalent to  $\nu = 4(N - 1) + 1 = 4N - 3$  system by electron-hole symmetry in the top filled Landau levels, if the Landau level mixing is negligible. Therefore all of our results shown in this paper for bilayer  $\nu = 4N + 1$  quantum Hall systems can be applied to  $\nu = 4(N+1) - 1 = 4N - 3$  system as well. We will not distinguish these two systems and will mention  $\nu = 4N + 1$  case only in the rest of this paper. When the layer separation,  $d$ , is small compared to the 2D magnetic length,  $l_0$ , spontaneous interlayer coherence can be generated by interlayer Coulomb interaction even in the absence of any interlayer tunneling [21,22], and the ground state is therefore best understood as a Halperin (1,1,1) coherent phase with finite charge gap [23]. When  $d$  is comparable to or larger than  $l_0$ , however, there should be a transition to two decoupled compressible  $\nu = 2N + 1/2$  systems or one of the competing many-body phases. A detailed analysis of all competing phases is still lacking, although it is commonly believed that for  $N = 0$  there is a direct first order transition from the (1,1,1) phase to the compressible states, although for  $N > 0$  there may be intermediate quantum Hall phases with stripe order [24]. Other more exotic phases, including the ones with electron pairing [25], have also been proposed in the literature. This interlayer coherence and the corresponding Goldstone mode of the symmetry-broken phases have been extensively studied theoretically [26–28] as well as experimentally [29,30] in the literature. In addition to the layer separation, the in-plane magnetic field is another important controlling parameters for the double well QH systems. In the presence of an in-plane magnetic field, an Aharonov-Bohm phase factor, associated with the gauge invariance, has to be considered for the electron tunneling amplitude between the two layers and may cause a commensurate-to-incommensurate (C-I) phase transition at a critical magnetic field strength [26,31,32]. Such C-I phase transition arises as a result of competition of the interlayer tunneling and Coulomb interlayer exchange interaction. The former favors a commensurate phase, in which the phase of the order parameter winds at a rate fixed by the parallel magnetic field; whereas the latter favors an incommensurate phase, in which the order parameter is more nearly uniform in space [22]. Taking into account the stripe order associated with the layer separation ( $d$ ) and the spiral order associated with the in-plane magnetic field ( $B_{\parallel}$ ) the possibility exists for a very complex and rich phase diagram with many competing phases occurring for various values of  $d$  and  $B_{\parallel}$  in the bilayer double well system at  $\nu = 4N + 1$ . Following our earlier work based on the collective mode dispersion [8,17], in this paper we carry out the ground state energetic calculation within the Hartree-Fock approximation to obtain and describe these exotic phases, which break isospin rotation, parity, and/or translational symmetries. We will also investigate the possibility of stripe formation at the even filling factor,  $\nu = 4N + 2$ , where a nonstripe canted antiferromagnetic phase (CAF) has been proposed and extensively studied in the literature [33–41]. The goal of our work is to discuss possible symmetry broken exotic quantum phases in bilayer and wide-well quantum Hall systems.

In this paper, we use the idea of isospin to label the two (nearly) degenerate energy levels at the Fermi energy,

and construct trial many-body wavefunctions that have various kinds of (possibly exotic) isospin order. The relevant isospin quantum number can be associated with Landau level index, layer index, spin index, or any other good quantum numbers describing the corresponding noninteracting system. Within Hartree-Fock approximation we investigate phases with isospin spiral and/or stripe orders and discuss their relevance for various systems. In Table I we summarize the definition of the isospin up(down) components for each system individually. For the convenience of discussion, we use following notations and labels to denote the systems in the rest of this paper (see also Fig. 2):  $W1(W2)$  and  $W1'(W2')$  denote the intersubband and intrasubband level crossing (or level near degeneracy in  $W1'$  case) in a wide well system with filling factor  $\nu = 2N + 1(2N + 2)$  respectively;  $D1$  and  $D2$  are for the level crossing (or level near degeneracy in  $D1$  case) in a double well system at total filling factor,  $\nu = 4N + 1$  and  $4N + 2$ , respectively. (Note that the distinction between intrasubband and intersubband level crossing of a wide well system in the presence of an in-plane magnetic field is somewhat ambiguous and will be clarified in the next section.) By "level crossing" we mean a point in the parameter space of noninteracting electrons, for which the energy difference between the highest filled Landau level and the lowest empty Landau level vanishes, while by "level near degeneracy" we mean a region in the parameter space, in which the energy difference between the above noninteracting electron levels is not zero, but relatively small compared to the interlevel interaction energy, which can strongly mix the two close noninteracting Landau levels in certain situations. In this paper, we consider the following six quantum phases generated by our trial wavefunction: conventional incompressible integer QH liquid (i.e. isospin polarized), isospin coherent, isospin spiral, isospin coherent stripe, isospin spiral stripe and isospin skyrmion stripe phases, classified by the behaviors of the expectation values of their isospin components,  $\langle \mathcal{I}_\pm \rangle$  and  $\langle \mathcal{I}_z \rangle$ . More precise definitions and the related physical properties of these phases will be discussed in Section III. In the last two columns of Table I we list the exotic many-body phases that become the ground states near the appropriate degeneracy points and the associated broken symmetries. For a wide well system at  $\nu = 2N + 1$  near the intersubband level crossing (i.e.  $W1$  in small in-plane field region), we find that interactions stabilize the isospin coherent phase, which breaks the parity (space inversion) symmetry and can be understood as a quantum Hall ferroelectric state [42]. For the same system near the intrasubband level near degeneracy region (i.e.  $W1'$  in large in-plane field region), we obtain the isospin skyrmion stripe phase, which breaks both parity and translational symmetries of the system. For wide well systems at even filling factors we find that many-body states with isospin coherence and/or stripe order are not favored at either the intersubband ( $W2$ ) or the intrasubband ( $W2'$ ) degenerate points within the HF approximation, exhibiting instead a trivial first order phase transition at the level crossing points. However, we find the calculated HF energy difference between the uniform ground state and the phases of spiral and stripe orders to be rather small, indicating the possibility of a spontaneous symmetry breaking in more refined approximations. Therefore, based on our HF calculation results, we suggest the existence of skyrmion stripe phase, breaking both spin rotational and translational symmetries near the degenerate point of  $W2'$  systems, may be responsible for the resistance anisotropy observed recently in Ref. [15]. (As for the magnetoresistance anisotropy observed in Si/SiGe semiconductor [16], the complication of valley degeneracy in Si makes a straightforward comparison between our theory and the experiments difficult.) For a double well system at  $\nu = 4N + 1$  ( $D1$ ), several interesting phases can be stabilized in the parameter range of interest (see Table I), while only a commensurate CAF phase is stabilized for even filling factor,  $\nu = 4N + 2$  ( $D2$ ), being consistent with the earlier results [36]. All of our calculation are carried out at zero temperature without any disorder or impurity scattering effects. We suggest that these symmetry broken phases discussed in this paper should be observable in transport and inelastic light scattering experiments.

We note that the presence of an in-plane magnetic field  $B_{\parallel}$  (in the 2D plane) automatically introduced a tilted magnetic field of amplitude  $B_{tot} = \sqrt{B_{\parallel}^2 + B_{\perp}^2}$  at an angle of  $\tan^{-1}(B_{\parallel}/B_{\perp})$  tilted with respect to the normal vector of the 2D plane since the field  $B_{\perp}$ , perpendicular to the 2D plane, is always present in order to produce the 2D Landau level system. The presence of  $B_{\parallel}$  (or more generally, the tilted field) introduces qualitatively new physics to 2D quantum Hall systems by allowing a tuning parameter (i.e.  $B_{\parallel}$ ) without affecting the basic Landau level structure. Changing  $B_{\parallel}$  in a continuous manner may enable the 2D system to undergo various quantum phase transition which would not otherwise be possible. Thus the physics of quantum Hall systems becomes considerably richer in the presence of a continuously tunable parallel (or tilted) magnetic field. The general (and somewhat ambitious) goal of our theoretical work present in this paper is to study this rich quantum phase diagram of 2D quantum Hall systems as a function of the in-plane field (used as a tuning parameter). As such we concentrate in the two most promising candidate systems, namely the (single) wide quantum well system and the (bilayer) double quantum well system, where the tilted field configuration is expected to give rise to exotic symmetry-broken quantum orders in the quantum Hall ground states. The underlying idea is to use the in-plane magnetic field as a tuning parameter to cause level crossing (or almost level degeneracy) in the noninteracting system (around the Fermi level) to see if the interaction effects then drive the system to non-trivial symmetry-broken many-body ground states (particularly with exotic quantum order) which can be experimentally studied. Earlier examples of such exotic symmetry-broken ground states (arising from level crossing phenomena) include, in addition to our prediction [17] of a skyrmion stripe phase, the bilayer canted

antiferromagnetic phase predicted in Ref. [33] where a tilted field is not necessary.

This paper is organized as follows: in Section II we introduce the Hamiltonians of interest, for both wide well and double well systems in the presence of a finite in-plane magnetic field. In Section III we propose various trial many-body wavefunctions incorporating both isospin stripe and isospin spiral orders. Physical features of the six typical phases generated by the wavefunctions will also be discussed in detail. For the systems of even filling factors, we propose trial wavefunctions that involve the four Landau levels closest to the Fermi energy simultaneously. (Including four rather than two levels in many-body wavefunctions was shown to be crucial for establishing the many-body canted antiferromagnetic state in bilayer systems at  $\nu = 2$  [33].) We will then divide the Hartree-Fock variational energies and the related numerical results into the following four sections: wide well systems at  $\nu = 2N + 1$  (Section IV) and at  $\nu = 2N + 2$  (Section V); double well systems at total filling factor  $\nu = 4N + 1$  (Section VI) and at  $\nu = 4N + 2$  (Section VII). For the sake of convenience (and relative independence of different sections), results of each section are discussed independently and then compared with each other in Section VIII, where we also make connections to the earlier works in the literature. Finally we summarize our paper in Section IX, and discuss some open questions.

## II. HAMILTONIANS

In this section, we present the Hamiltonians of the systems we will study in this paper, including both the single wide (parabolic) well systems and the double (thin) well (or bilayer) systems. Most of the formulae given in this section exist in the literature (perhaps scattered over many publications) and hence we will not derive them in details unless absolutely necessary. To make the notations consistent throughout this paper, we use the superscript  $W$  to denote physical variables or quantities for the wide well system and the superscript  $D$  for the double well systems. We will also describe the symmetry properties of these systems, which are crucial in formulating the many-body trial wavefunctions in the next section and in discussing the nature of the spontaneous symmetry breaking and the associated exotic quantum order in our various proposed phases.

### A. Wide Well System

For a wide well system we consider a parabolic confinement potential [17] in the growth direction ( $z$ ),  $U_c(z) = \frac{1}{2}m^*\omega_0^2z^2$ , where  $m^*$  is electron effective mass and  $\omega_0$  is the confinement energy. The advantage of using a parabolic well model is that we can easily diagonalize the noninteracting Hamiltonian even in the presence of in-plane magnetic field. We will use eigenstates of the non-interacting Hamiltonian as the basis functions for writing variational Slater determinant states for the many-body wavefunctions that may be stabilized by Coulomb interactions. We believe that our wide well results obtained in this paper for parabolic confinement should be qualitatively valid even for nonparabolic quantum wells. To incorporate both the in-plane magnetic field ( $B_{\parallel}$ ), which we take to be along the  $x$  axis in this section, and the perpendicular (along the  $z$  axis) magnetic field ( $B_{\perp}$ ) in the Hamiltonian, we choose two kinds of Landau gauges for the vector potential: in one of them,  $\vec{A}_{[y]}(\vec{r}) = (0, B_{\perp}x - B_{\parallel}z, 0)$ , particle momentum is conserved along  $y$  direction, and in the other one,  $\vec{A}_{[x]}(\vec{r}) = (-B_{\perp}y, -B_{\parallel}z, 0)$ , particle momentum is conserved along  $x$  direction. The final physical results are of course independent of the choice of the gauge. However, as will be clear from the discussion below, various phases may be more conveniently discussed in different gauges, since the physical or the mathematical description of particular many-body states may be more natural in specific gauges. For the consistency of notations, all the explicit calculations presented in this paper will be done in the gauge  $\vec{A}_{[y]}(\vec{r})$ . Since the generalization of these equations to the other case is straightforward (see Appendix A), we will only present the final results for the  $\vec{A}_{[x]}(\vec{r})$  gauge. The noninteracting (single electron) Hamiltonian in the parabolic potential with both perpendicular and in-plane magnetic fields in gauge  $\vec{A}_{[y]}(\vec{r})$  is (we choose  $\hbar = 1$  throughout this paper)

$$H_0^W = \frac{p_x^2}{2m^*} + \frac{1}{2m^*} \left( p_y + \frac{eB_{\perp}x}{c} - \frac{eB_{\parallel}z}{c} \right)^2 + \frac{p_z^2}{2m^*} + \frac{1}{2}m^*\omega_0^2z^2 - \omega_z S_z, \quad (1)$$

where  $S_z$  is the  $z$  component of spin operator and  $\omega_z$  is Zeeman energy, proportional to the total magnetic field,  $B_{tot} = \sqrt{B_{\perp}^2 + B_{\parallel}^2}$ . It has been shown [17] that the one electron energies and wavefunctions of Eq. (1) can be obtained analytically even in the presence of an in-plane magnetic field by rotating to a proper coordinate. The resulting noninteracting Hamiltonian is a sum of two decoupled one-dimensional simple harmonic oscillators with energies [17],

$$\omega_{1,2}^2 = \frac{1}{2} \left[ (\omega_b^2 + \omega_{\perp}^2) \pm \sqrt{(\omega_b^2 - \omega_{\perp}^2)^2 + 4\omega_{\perp}^2\omega_{\parallel}^2} \right], \quad (2)$$

where  $\omega_{\perp,\parallel} = eB_{\perp,\parallel}/m^*c$  (i.e.  $\omega_{\perp}$  is the conventional cyclotron frequency), and  $\omega_b \equiv \sqrt{\omega_0^2 + \omega_{\parallel}^2}$  is the effective confinement energy. Using  $(\vec{n}, s, k)$  as the noninteracting eigenstate quantum numbers, where  $\vec{n} = (n, n')$  is the orbital Landau level index for the two decoupled 1D simple harmonic oscillators,  $s = \pm 1/2$  the electron spin eigenvalues along the total magnetic field,  $\vec{B}_{tot} \equiv (B_{\parallel}, 0, B_{\perp})$  and  $k$  the guiding center coordinate, one can obtain the following noninteracting eigenenergies,  $E_{\vec{n},s}^{0,W}$ , for  $H_0^W$  of Eq. (1):

$$E_{\vec{n},s}^{0,W} = \omega_1 \left( n + \frac{1}{2} \right) + \omega_2 \left( n' + \frac{1}{2} \right) - \omega_z s, \quad (3)$$

and the noninteracting orbital wavefunction:

$$\phi_{\vec{n},s,k}^W(\vec{r}) = \frac{e^{iky}}{\sqrt{L_y}} \underbrace{\psi_n^{(1)}(\cos \theta(x + l_0^2 k) - \sin \theta z) \cdot \psi_{n'}^{(2)}(\sin \theta(x + l_0^2 k) + \cos \theta z)}_{\equiv \Phi_{\vec{n}}^W(x + l_0^2 k, z)} \quad (4)$$

where  $L_y$  is the system length in  $y$  direction and the function  $\Phi_{\vec{n}}^0(x + l_0^2 k, z)$  has  $x$  and  $z$  components only;  $\tan(2\theta) \equiv -2\omega_{\perp}\omega_{\parallel}/(\omega_b^2 - \omega_{\perp}^2)$ . In Eq. (4), the function  $\psi_n^{(i)}(x)$  is

$$\psi_n^{(i)}(x) = \frac{1}{\sqrt{\pi^{1/2} 2^n n! l_i}} \exp \left[ -\frac{x^2}{2l_i^2} \right] H_n \left( \frac{x}{l_i} \right), \quad (5)$$

with  $l_i \equiv \sqrt{1/m^*\omega_i}$  for  $i = 1, 2$ , and  $H_n(x)$  is Hermite polynomial.

A typical noninteracting energy spectrum as a function of in-plane magnetic field,  $B_{\parallel}$ , is shown in Fig. 1 (with system parameters similar to the experimental values of Ref. [15]). In Fig. 1, two kinds of level crossing can be observed, one is in the weak  $B_{\parallel}$  ( $< 5$  Tesla) region and the other in the strong  $B_{\parallel}$  ( $> 19$  Tesla) region. In this paper we will denote the former to be an "intersubband level crossing" and the latter to be an "intrasubband level crossing" (see Table I) [43]. In this paper we adopt a convention that all single particle states in Eqs. (3) and (4) that have the same quantum number  $n$  (the first index of  $\vec{n}$ ) correspond to the same subband. With this definition of "subbands", the characteristic energy separation of intersubband levels,  $\omega_1$ , is always larger than the energy separation of intrasubband levels,  $\omega_2$ . It is useful to emphasize that the states of Eqs. (3)-(5) are the exact noninteracting eigenenergies for *arbitrary* values of in-plane field, perpendicular field, and confinement energy. In the second quantization notation, the noninteracting Hamiltonian can be written to be

$$H_0^W = \sum_{\vec{n},s,k} E_{\vec{n},s}^{0,W} c_{\vec{n},s,k}^{W,\dagger} c_{\vec{n},s,k}^W, \quad (6)$$

where  $c_{\vec{n},s,k}^{W,\dagger}(c_{\vec{n},s,k}^W)$  creates(annihilates) an electron in the state  $(\vec{n}, s, k)$ .

Before showing the full many-body interaction Hamiltonian, it is convenient to define the form functions [17],

$$\begin{aligned} A_{\vec{n}_i \vec{n}_j}^W(\vec{q}) &\equiv \int d\vec{r} e^{-i\vec{q} \cdot \vec{r}} \phi_{\vec{n}_i, s, -q_y/2}^W(\vec{r}) \phi_{\vec{n}_j, s, q_y/2}^W(\vec{r}) \\ &= \int dx \int dz e^{-iq_x x} e^{-iq_z z} \tilde{\Phi}_{\vec{n}_1}^W(x - l_0^2 q_y/2, z) \tilde{\Phi}_{\vec{n}_2}^W(x + l_0^2 q_y/2, z), \end{aligned} \quad (7)$$

which are constructed from the noninteracting electron wavefunctions (Appendix B). In principle one could use the electron wavefunctions obtained either from a self-consistent Hartree-Fock approximation [17,19] or from a self-consistent local density approximation [44,45] in Eq. (7) to calculate the form function. However, in Ref. [17] we have shown that the difference in the form function between using the noninteracting single electron wavefunctions and the self-consistent Hartree-Fock wavefunctions is very small. Therefore we define the form function by using the noninteracting wavefunctions and consider only the diagonal part of the Hartree-Fock potential (i.e. the first order Hartree-Fock approximation) in calculating the ground state energy. In addition, we include the screening effect of positively charged donors by using the statically screened Coulomb interaction,  $V(\vec{q}) = e^2/\epsilon_0(|\vec{q}|^2 + (2\pi/l_s)^2)$  for convenience, where  $l_s$  is the effective screening length by donors outside the well and  $\epsilon_0 = 12.7$  is the static lattice dielectric constant of GaAs. We believe this simple approximation should give reasonable results compared with the

more complicated calculation by including the donor density in a self-consistent approximation [44,45]. Using the notations defined above, the interaction Hamiltonian can be expressed as follows [17]:

$$H_1^W = \frac{1}{2\Omega} \sum_{\vec{n}_1, \dots, \vec{n}_4} \sum_{\sigma_1, \sigma_2} \sum_{k_1, k_2, \vec{q}} V_{\vec{n}_1 \vec{n}_2, \vec{n}_3 \vec{n}_4}^W(\vec{q}) e^{-iq_x(k_1-k_2)l_0^2} c_{\vec{n}_1, \sigma_1, k_1+q_y/2}^{W, \dagger} c_{\vec{n}_2, \sigma_1, k_1-q_y/2}^W c_{\vec{n}_3, \sigma_2, k_2-q_y/2}^{W, \dagger} c_{\vec{n}_4, \sigma_2, k_2+q_y/2}^W \\ = \frac{1}{2\Omega_\perp} \sum_{\vec{n}_1, \dots, \vec{n}_4} \sum_{\sigma_1, \sigma_2} \sum_{k_1, k_2, \vec{q}_\perp} \tilde{V}_{\vec{n}_1 \vec{n}_2, \vec{n}_3 \vec{n}_4}^W(\vec{q}_\perp) e^{-iq_x(k_1-k_2)l_0^2} c_{\vec{n}_1, \sigma_1, k_1+q_y/2}^{W, \dagger} c_{\vec{n}_2, \sigma_1, k_1-q_y/2}^W c_{\vec{n}_3, \sigma_2, k_2-q_y/2}^{W, \dagger} c_{\vec{n}_4, \sigma_2, k_2+q_y/2}, \quad (8)$$

where  $V_{\vec{n}_1 \vec{n}_2, \vec{n}_3 \vec{n}_4}^W(\vec{q}) \equiv V(\vec{q}) A_{\vec{n}_1 \vec{n}_2}^W(-\vec{q}) A_{\vec{n}_3 \vec{n}_4}^W(\vec{q})$  and  $\tilde{V}_{\vec{n}_1 \vec{n}_2, \vec{n}_3 \vec{n}_4}^W(\vec{q}_\perp) \equiv L_z^{-1} \sum_{q_z} V_{\vec{n}_1 \vec{n}_2, \vec{n}_3 \vec{n}_4}^W(\vec{q})$ .  $\Omega = L_x L_y L_z$  is the usual normalization volume and  $\Omega_\perp = L_x L_y$  is the 2D normalization area. If we choose the alternate Landau gauge,  $\vec{A}_{[x]}(\vec{r})$ , the expression of  $H_1^W$  will have the phase factor,  $e^{-iq_y(k_1-k_2)l_0^2}$ , rather than  $e^{iq_x(k_1-k_2)l_0^2}$  above.

For the convenience of later discussion, we can express the Hamiltonians shown in Eq. (6) and Eq. (8) as follows:

$$H_{tot}^W = \sum_{\vec{n}, \sigma} E_{\vec{n}, \sigma}^{0, W} \rho_{\vec{n}\sigma, \vec{n}\sigma}^W(0) + \frac{1}{2\Omega_\perp} \sum_{\vec{q}_\perp} \sum_{\vec{n}_1, \dots, \vec{n}_4} \sum_{\sigma_1, \sigma_2} \tilde{V}_{\vec{n}_1 \vec{n}_2, \vec{n}_3 \vec{n}_4}^W(\vec{q}_\perp) \rho_{\vec{n}_1 \sigma_1, \vec{n}_2 \sigma_1}^W(-\vec{q}_\perp) \rho_{\vec{n}_3 \sigma_2, \vec{n}_4 \sigma_2}^W(\vec{q}_\perp), \quad (9)$$

where

$$\rho_{\vec{n}_i \sigma_1, \vec{n}_j \sigma_2}^W(\vec{q}_\perp) \equiv \sum_k e^{iq_x k l_0^2} c_{\vec{n}_i, \sigma_1, k-q_y/2}^{W, \dagger} c_{\vec{n}_j, \sigma_2, k+q_y/2}^W \quad (10)$$

is the density operator for the wide well system.

## B. Double Well System

For a double well (bilayer) system, we assume both wells are of zero width in their growth direction so that the in-plane magnetic field does not change the electron orbital wavefunctions as in wide well systems. For most bilayer problems of physical interest, neglecting the individual layer width is an extremely reasonable approximation. In the presence of an in-plane (parallel) magnetic field, the tunneling amplitude in the Hamiltonian acquires an Aharonov-Bohm phase factor to satisfy the gauge invariance of the whole system [22,36,27]. This, in fact, is the main effect of the in-plane field in the double well system for our purpose. To describe this important effect, we first express the Hamiltonians of a double well system in a special gauge [26]:  $\vec{A}'_{[y]}(\vec{r}) = (0, B_\perp x, B_{xy} - B_y x)$ , where  $B_x$  and  $B_y$  are the  $x$  and  $y$  components of the in-plane field (i.e.  $\vec{B}_\parallel = (B_x, B_y, 0)$ ), by using a conventional basis of electron states,  $(n, l, s, k)$ , where  $n$  is Landau level index in a single layer,  $l = \pm$  is the layer index for right(left) layer (sometimes also called up/down layers in analogy with electron spin), and  $s$  and  $k$  are the same as before. The Aharonov-Bohm phase factor,  $\exp[-i\Phi_0^{-1} \int_{\pm d/2}^{\mp d/2} A'_{[y], z}(\vec{r}_\perp, z) dz]$  (where  $d$  is layer separation and  $\Phi_0 = hc/e$  is fundamental flux quantum), is then introduced for electron tunneling from one layer to the other. In the bilayer Hamiltonian we need to keep the tunneling term only for the electrons in the highest filled Landau level, and therefore the noninteracting Hamiltonian in the second quantization representation becomes:

$$H_0^D = \sum_{n, l, k, s} \left[ \left( n + \frac{1}{2} \right) \omega_\perp - \omega_z s \right] c_{n, l, s, k}^{D, \dagger} c_{n, l, s, k}^D \\ - t_{N, P} \sum_{s, k} \left[ e^{-ikP_y l_0^2} c_{N, +1, s, k-P_x/2}^{D, \dagger} c_{N, -1, s, k+P_x/2}^D + e^{ikP_y l_0^2} c_{N, -1, s, k+P_x/2}^{D, \dagger} c_{N, +1, s, k-P_x/2}^D \right], \quad (11)$$

where  $c_{n, l, s, k}^{D, \dagger}(c_{n, l, s, k}^D)$  is the electron creation(annihilation) operator of state  $(n, l, s, k)$ , described by  $L_y^{-1/2} e^{iky} \psi_n^{(0)}(x + kl_0^2) \delta(z \mp d/2)$ , where  $\psi_n^{(0)}(x)$  is the same as Eq. (5) with  $l_i$  replaced by magnetic length  $l_0$ .  $\vec{P}_\perp = (P_x, P_y) \equiv 2\pi d \vec{B}_\parallel / \Phi_0$  is a characteristic wavevector introduced by the in-plane field. The effective tunneling amplitude  $t_{N, P}$  is  $t e^{-P^2 l_0^2/4} L_N^0(P^2 l_0^2/2)$  with  $t$  being a parameter for interlayer tunneling, where  $P = |\vec{P}_\perp|$  and  $L_n^0(x)$  is the generalized Laguerre polynomial. Following the convention in most of the existing literature, we will treat  $t_{N, P}$  as a whole to be an independent variable in this paper and hence neglect all its level and magnetic field dependence for simplicity [46,47].

Similar to Eq. (7) we define the following form function for the double well system:

$$A_{n_i n_j}^D(\vec{q}_\perp) = \int d\vec{r}_\perp e^{-i\vec{q}_\perp \cdot \vec{r}_\perp} \phi_{n_i, -q_y/2}^{D,\dagger}(\vec{r}_\perp) \phi_{n_j, q_y/2}^D(\vec{r}_\perp), \quad (12)$$

where  $\phi_{n,k}^D(\vec{r}_\perp) = L_y^{-1/2} e^{iky} \psi_n^{(0)}(x + kl_0^2)$  is the one electron wavefunction of Landau level  $n$  in a single well. The  $z$  component of the wavefunction can be integrated first and the resulting explicit formula of  $A_{n_i n_j}^D(\vec{q}_\perp)$  is shown in Appendix B. The interaction Hamiltonian in this basis is then

$$\begin{aligned} H_1^D &= \frac{1}{2\Omega_\perp} \sum_{n_1 \dots n_4} \sum_{l_1, l_2} \sum_{s_1, s_2} \sum_{k_1, k_2, \vec{q}_\perp} V_{n_1 n_2, n_3 n_4}^{D, l_1, l_2}(\vec{q}_\perp) e^{-i q_x (k_1 - k_2) l_0^2} c_{n_1, l_1, s_1, k_1 + q_y/2}^{D,\dagger} c_{n_2, l_1, s_1, k_1 - q_y/2}^D c_{n_3, l_2, s_2, k_2 - q_y/2}^{D,\dagger} c_{n_4, l_2, s_2, k_2 + q_y/2}^D \\ &= \frac{1}{2\Omega_\perp} \sum_{\vec{q}_\perp} \sum_{l_1, l_2} V_{n_1 n_2, n_3 n_4}^{D, l_1, l_2}(\vec{q}_\perp) \rho_{n_1 l_1, n_2 l_1}^D(-\vec{q}_\perp) \rho_{n_3 l_2, n_4 l_2}^D(\vec{q}_\perp) \end{aligned} \quad (13)$$

where  $V_{n_1 n_2, n_3 n_4}^{D, l_1, l_2}(\vec{q}_\perp) = V(\vec{q}_\perp) A_{n_1 n_2}^D(-\vec{q}_\perp) A_{n_3 n_4}^D(\vec{q}_\perp) \exp(-\frac{1}{2}|l_1 - l_2|d|\vec{q}_\perp|)$ , including the contribution of the  $z$  component of the electron wavefunction;  $\rho_{n_1 l, n_2 l}^D(\vec{q}_\perp) = \sum_{s,k} e^{iq_x k l_0^2} c_{n_1, l, s, k - q_y/2}^{D,\dagger} c_{n_2, l, s, k + q_y/2}^D$  is the electron density operator of layer  $l$  and spin  $s$ .

Sometimes it is more convenient to rewrite the Hamiltonian in terms of the eigenstates of the noninteracting Hamiltonian, which are defined as:

$$\begin{aligned} c_{n,+1,s,k}^\dagger &= \frac{e^{i(k+P_x/2)P_y l_0^2/2}}{\sqrt{2}} \left( a_{n,+1,s,k+P_x/2}^\dagger + a_{n,-1,s,k+P_x/2}^\dagger \right) \\ c_{n,-1,s,k}^\dagger &= \frac{e^{-i(k-P_x/2)P_y l_0^2/2}}{\sqrt{2}} \left( a_{n,+1,s,k-P_x/2}^\dagger - a_{n,-1,s,k-P_x/2}^\dagger \right), \end{aligned} \quad (14)$$

where  $a_{n,\alpha,s,k}^\dagger$  is the new electrons creation operator of a symmetric ( $\alpha = +1$ ) or an antisymmetric ( $\alpha = -1$ ) noninteracting state, because they are also the eigenstates of parity (space inversion) transformation ( $c_{n,l,s,k}^\dagger \rightarrow c_{n,-l,s,-k}^\dagger$ ). Note that the description in terms of the left/right layer index  $l$  (in Eq. (11)) or the symmetric/antisymmetric state  $\alpha$  are completely equivalent since they are simple linear combinations of each other (cf. Eq. (14)).

In the  $\alpha$  basis, the noninteracting Hamiltonian of Eq. (11) is

$$H_0^D = \sum_{n,\alpha,k,s} E_{n,\alpha,s}^{0,D} a_{n,\alpha,s,k}^\dagger a_{n,\alpha,s,k}, \quad (15)$$

where the noninteracting electron eigenenergy,  $E_{n,\alpha,s}^{0,D}$ , is

$$E_{n,\alpha,s}^{0,D} = (n + 1/2)\omega_\perp - \alpha\Delta_{SAS}/2 - s\omega_z, \quad (16)$$

and  $\Delta_{SAS} = 2t$  is the tunneling energy. The interacting Hamiltonian in Eq. (13) then becomes

$$\begin{aligned} H_1^D &= \frac{1}{2\Omega_\perp} \sum_{\alpha_1, \alpha_2, \vec{q}_\perp} \sum_{n_1 \dots n_4} \left[ \tilde{V}_{n_1 n_2, n_3 n_4}^I(\vec{q}_\perp) \rho_{n_1 n_2}^{\alpha_1 \alpha_1}(-\vec{q}_\perp) \rho_{n_3 n_4}^{\alpha_2 \alpha_2}(\vec{q}_\perp) + \tilde{V}_{n_1 n_2, n_3 n_4}^o(\vec{q}_\perp) \rho_{n_1 n_2}^{-\alpha_1 \alpha_1}(-\vec{q}_\perp) \rho_{n_3 n_4}^{-\alpha_2 \alpha_2}(\vec{q}_\perp) \right. \\ &\quad \left. + \tilde{V}_{n_1 n_2, n_3 n_4}^s(\vec{q}_\perp) \sum_{\lambda=\pm 1} \lambda \rho_{n_1 n_2}^{-\lambda \alpha_1 \alpha_1}(-\vec{q}_\perp) \rho_{n_3 n_4}^{\lambda \alpha_2 \alpha_2}(\vec{q}_\perp) \right], \end{aligned} \quad (17)$$

where the new density operator,  $\rho_{n_1 n_2}^{\alpha_1 \alpha_2}(\vec{q}_\perp) = \sum_{s,k} e^{iq_x k l_0^2} a_{n_1, \alpha_1, s, k - q_y/2}^\dagger a_{n_2, \alpha_2, s, k + q_y/2}$  and the three interaction matrix elements in Eq. (17) are as follows:

$$\tilde{V}_{n_1 n_2, n_3 n_4}^{I,o}(\vec{q}_\perp) \equiv \frac{1}{2} \left( \tilde{V}_{n_1 n_2, n_3 n_4}^{D,++}(\vec{q}_\perp) \pm \cos((\vec{q}_\perp \cdot \vec{P}_\perp) l_0^2) \tilde{V}_{n_1 n_2, n_3 n_4}^{D,+-}(\vec{q}_\perp) \right) \quad (18)$$

$$\tilde{V}_{n_1 n_2, n_3 n_4}^s(\vec{q}_\perp) \equiv \frac{i}{2} \sin((\vec{q}_\perp \cdot \vec{P}_\perp) l_0^2) \tilde{V}_{n_1 n_2, n_3 n_4}^{D,+-}(\vec{q}_\perp). \quad (19)$$

As will become clear from the later discussion in this paper the basis described by Eqs. (15)-(19)) is often more convenient for constructing trial wavefunctions, especially for an even filling system in the presence of in-plane magnetic field.

### C. Symmetry properties of the systems

We now discuss the symmetry properties of the wide well systems and the double well systems in the presence of in-plane field. We first consider parity (full space inversion) symmetry, translational symmetry and spin rotational symmetry individually, which exist in both the systems of interest (i.e. wide well and double well). Then we discuss the  $z$ -parity (reflection about  $x - y$  plane) and the isospin rotation symmetries, which exist only in the double well system in certain situations.

In this paper, we define the parity operator,  $\hat{\mathcal{P}}$ , so that it reverses the *full* space coordinates from  $\vec{r} = (x, y, z)$  to  $-\vec{r} = (-x, -y, -z)$ . Therefore, in the second quantization notation, we have

$$\hat{\mathcal{P}}c_{\vec{n},s,k}^W\hat{\mathcal{P}}^{-1} = (-1)^{n+n'}c_{\vec{n},s,-k}^W \quad (20)$$

for the wide well system (see Eq. (4)), and

$$\hat{\mathcal{P}}c_{n,l,s,k}^D\hat{\mathcal{P}}^{-1} = (-1)^n c_{n,-l,s,-k}^D \text{ or } \hat{\mathcal{P}}a_{n,\alpha,s,k}\hat{\mathcal{P}}^{-1} = (-1)^n \alpha a_{n,\alpha,s,-k} \quad (21)$$

for the double well system in the two different basis. It is easy to see that the Hamiltonians of these two systems shown above are not changed under the parity transformation by using the identities (see Eq. (B1)):  $A_{\vec{n}_1\vec{n}_2}^W(-\vec{q}) = (-1)^{n_1+n'_1}(-1)^{n_2+n'_2}A_{\vec{n}_1\vec{n}_2}^W(\vec{q})$  and  $A_{n_1n_2}^D(-\vec{q}_\perp) = (-1)^{n_1+n_2}A_{n_1n_2}^D(\vec{q}_\perp)$ . This simple result is valid even in the presence of the tilted magnetic field, if only we consider a symmetrically confined (but not necessary parabolic) potential well in the wide well system and no external bias voltage in the double well systems. Thus, parity is rather general symmetry property of the physical systems under consideration.

To consider the 2D translational symmetry in the  $x - y$  plane, it is more convenient to consider the many-body system in the first quantization representation, and introduce the total “momentum” operator,  $\hat{\mathcal{M}}$  [48,17]:

$$\hat{\mathcal{M}} \equiv \sum_i \left[ \vec{p}_i + \frac{e}{c} \vec{A}(\vec{r}_i) - \frac{e}{c} \vec{B}_{tot} \times \vec{r}_i \right], \quad (22)$$

where  $\vec{p}_i$  and  $\vec{r}_i$  are the momentum and position operators of the  $i$ th electron.  $\vec{A}$  is the vector potential and  $B_{tot} = (B_{\parallel}, 0, B_{\perp})$  is the total magnetic field. Then it is straightforward to see that the  $x$  and  $y$  components of  $\hat{\mathcal{M}}$  commute with the Hamiltonian,  $H = \frac{1}{2m^*} \sum_i (\vec{p}_i + e\vec{A}(\vec{r}_i)/c)^2 + \sum_i U_c(z_i) + \frac{1}{2} \sum_{i \neq j} V(\vec{r}_i - \vec{r}_j)$ . This result is true even in the presence of an in-plane magnetic field and for arbitrary shape of the electron confinement potential in  $z$  direction. Therefore it applies equally well to wide well systems and double well systems. We can then define the 2D translation operators in the  $x$  and  $y$  directions as

$$\hat{\mathcal{T}}_x(R_x) \equiv \exp \left( -iR_x \hat{\mathcal{M}}_x \right), \quad (23)$$

$$\hat{\mathcal{T}}_y(R_y) \equiv \exp \left( -iR_y \hat{\mathcal{M}}_y \right), \quad (24)$$

which form closed translational symmetry group individually [49] (they do not commute with each other due to the presence of the magnetic field). We first study how  $\hat{\mathcal{T}}_{x,y}(R_{x,y})$  can transform a noninteracting electron eigenstate of a wide well system,  $\phi_{\vec{m},k}^W(\vec{r}) = L_y^{-1/2} e^{iky} \Phi_{\vec{m}}^W(x + l_0^2 k, z)$ , with a shift,  $\vec{R}_{\perp} = (R_x, R_y)$ , in the  $x - y$  plane. In the Landau gauge,  $\vec{A}_{[y]}(\vec{r})$ , we obtain

$$\hat{\mathcal{T}}_x(R_x) \phi_{\vec{m},k}^W(\vec{r}) = e^{-iR_x y / l_0^2} \phi_{\vec{m},k}^W(x - R_x, y, z) = \phi_{\vec{m},k-R_x/l_0^2}^W(\vec{r}), \quad (25)$$

$$\hat{\mathcal{T}}_y(R_y) \phi_{\vec{m},k}^W(\vec{r}) = \phi_{\vec{m},k}^W(x, y - R_y, z) = e^{-ikR_y} \phi_{\vec{m},k}^W(\vec{r}). \quad (26)$$

In the second quantization representation, it is equivalent to

$$\hat{\mathcal{T}}_x(R_x) c_{\vec{m},s,k}^W \hat{\mathcal{T}}_x(R_x)^{-1} = c_{\vec{m},s,k+R_x/l_0^2}^W, \quad (27)$$

$$\hat{\mathcal{T}}_y(R_y) c_{\vec{m},s,k}^W \hat{\mathcal{T}}_y(R_y)^{-1} = e^{-ikR_y} c_{\vec{m},s,k}^W. \quad (28)$$

In other words,  $\hat{\mathcal{T}}_x(R_x)$  shifts the guiding center coordinate and  $\hat{\mathcal{T}}_y(R_y)$  adds an additional phase factor of the electron operators respectively. As discussed in Section II B, in the case of double well systems we use the gauge

$\vec{A}'_{[y]}(\vec{r}) = (0, B_{\perp}x, B_xy - B_yx)$  (see the paragraph above Eq. (11)). Therefore the “momentum” operator in this gauge becomes  $\hat{\mathcal{M}} = (p_x + y/l_0^2 - zP_y/d, p_y + zP_x/d, p_z)$  and the translational operators are

$$\hat{\mathcal{T}}_x(R_x)\phi_{n,k}^D(\vec{r}_{\perp})\delta(z - ld/2) = e^{ilR_xP_y/2}\phi_{n,k-R_x/l_0^2}^D(\vec{r}_{\perp})\delta(z - ld/2), \quad (29)$$

$$\hat{\mathcal{T}}_y(R_y)\phi_{n,k}^D(\vec{r}_{\perp})\delta(z - ld/2) = e^{-ilR_yP_x/2}e^{-ikR_y}\phi_{n,k}^D(\vec{r}_{\perp})\delta(z - ld/2). \quad (30)$$

In the second quantization representation, they are equivalent to

$$\hat{\mathcal{T}}_x(R_x)c_{n,l,s,k}^D\hat{\mathcal{T}}_x(R_x)^{-1} = e^{ilR_xP_y/2}c_{n,l,s,k+R_x/l_0^2}^D, \quad (31)$$

$$\hat{\mathcal{T}}_y(R_y)c_{n,l,s,k}^D\hat{\mathcal{T}}_y(R_y)^{-1} = e^{-ilR_yP_x/2}e^{-ikR_y}c_{n,l,s,k}^D. \quad (32)$$

Comparing Eqs. (31)-(32) to Eqs. (27)-(28), we find that an additional phase factor appears in the layer index basis, which is related to the Aharonov-Bohm phase factor and hence confirms that the tunneling Hamiltonian in Eq. (11) commutes with the translational operator,  $\hat{\mathcal{T}}_{x,y}$ . If we use Eq. (14) to change the above results (Eqs. (31)-(32)) to the symmetric-antisymmetric basis, we obtain

$$\hat{\mathcal{T}}_x(R_x)a_{n,\alpha,s,k}\hat{\mathcal{T}}_x(R_x)^{-1} = a_{n,\alpha,s,k+R_x/l_0^2}, \quad (33)$$

$$\hat{\mathcal{T}}_y(R_y)a_{n,\alpha,s,k}\hat{\mathcal{T}}_y(R_y)^{-1} = e^{-ikR_y}a_{n,\alpha,s,k}, \quad (34)$$

which are the same as Eqs. (27)-(28) obtained by replacing  $c_{\vec{m},s,k}^W$  by  $a_{n,\alpha,s,k}$ .

As for the spin rotational symmetry about the total magnetic field direction with an angle  $\chi$ , we can simply apply the following operator on the spin wavefunction,

$$\hat{\mathcal{U}}(\chi) = e^{-i\chi S_z}, \quad (35)$$

where  $S_z$  is the  $z$  component of spin operator with the spin  $z$  axis being along the direction of total magnetic field. Since our noninteracting eigenstate is always the eigenstate of  $S_z$ , the spin rotational operator,  $\hat{\mathcal{U}}(\chi)$ , just gives an additional prefactor,  $e^{\mp i\chi/2}$  for spin up(down) electron annihilation operators. The spin rotational symmetry is conserved by the Hamiltonians that we consider.

Now we discuss the symmetry properties that exist only in the double well system but *not* in the wide well system. First, if there is no in-plane magnetic field ( $B_{\parallel} = 0$ ), the double well system has two separate parity symmetries: one is the  $z$ -parity symmetry,  $\hat{\mathcal{P}}_z$  (changing  $z$  to  $-z$ ) and the other one is the in-plane parity symmetry,  $\hat{\mathcal{P}}_{xy}$  (changing  $(x, y)$  to  $(-x, -y)$ ). In the second quantization representation, we have  $\hat{\mathcal{P}}_z c_{n,l,s,k}^D \hat{\mathcal{P}}_z^{-1} = c_{n,-l,s,k}^D$  and  $\hat{\mathcal{P}}_{xy} c_{n,l,s,k}^D \hat{\mathcal{P}}_{xy}^{-1} = (-1)^n c_{n,l,s,-k}^D$ . It is easy to show that both  $\hat{\mathcal{P}}_z$  and  $\hat{\mathcal{P}}_{xy}$  commute with the total Hamiltonian of the double well system in the absence of in-plane magnetic field. When an in-plane magnetic field is applied, however, none of them is conserved due to the Aharonov-Bohm phase shift in the tunneling amplitude (see Eq. (11)), while their product, the full space inversion  $\hat{\mathcal{P}} = \hat{\mathcal{P}}_z \hat{\mathcal{P}}_{xy}$ , is still conserved as discussed above. Second, if there is no electron interlayer tunneling ( $\Delta_{SAS} = 0$ ) in the double well system, the electron number in each layer is also a constant of motion. In the isospin language of the layer index basis, such conservation is described by an isospin rotational symmetry about the isospin  $z$  axis,  $\hat{\mathcal{U}}_{iso}(\xi) \equiv \exp[-i\xi(c_{n,+s,k}^{D,\dagger}c_{n,+s,k}^D - c_{n,-s,k}^{D,\dagger}c_{n,-s,k}^D)/2]$ . The spontaneous interlayer coherence will break such continuous symmetry and give rise to a Goldstone mode. Such  $U(1)$  symmetry breaking has been extensively studied in the literature (see Ref. [22] and references therein), and hence we will not seriously address this issue in this paper. However, since our interest in this paper is to study the charge and spin density wave phases induced by the in-plane magnetic field, we will always consider systems with finite tunneling and finite in-plane magnetic field throughout, so that the above unique symmetries ( $\hat{\mathcal{P}}_z$ ,  $\hat{\mathcal{P}}_{xy}$ , and  $\hat{\mathcal{U}}_{iso}$ ) actually do not exist in the double well systems we consider in this paper. As a result, both the wide well systems and the double well systems we study will have full space parity symmetry ( $\hat{\mathcal{P}}$ ), two-dimensional translational symmetry ( $\hat{\mathcal{T}}_{x,y}$ ), and spin rotational symmetry about the total magnetic field ( $\hat{\mathcal{U}}$ ). We will then discuss how a stabilized many-body coherent wavefunction can break these symmetries near the level crossing (or level near degeneracy) regions.

### III. VARIATIONAL WAVE FUNCTIONS

In this section, we propose trial many-body wavefunctions to variationally minimize the Hartree-Fock energy of the integer quantum Hall systems in the level degeneracy region: a wide parabolic well and a double well system at both

even and odd filling factors. Stripe phases, that we are primarily interested in, have translational symmetry along the longitudinal direction of the stripes. They are conveniently discussed in the Landau gauge, for which particle momentum is a good quantum number in the direction of the stripe. In this paper we only consider stripes that are parallel or perpendicular to the direction of the in-plane magnetic field. Therefore for the in-plane field in the  $x$  direction we choose gauges  $\vec{A}_{[y]}(\vec{r}) = (0, B_{\perp}x - B_{\parallel}z, 0)$  and  $\vec{A}_{[x]}(\vec{r}) = (-B_{\perp}y, -B_{\parallel}z, 0)$  to describe phases with stripes along  $y$  and  $x$  axes respectively. By comparing the HF energies of these two stripes phases (one is along  $y$  direction obtained by using gauge  $\vec{A}_{[y]}(\vec{r})$ , and the other one is along  $x$  direction obtained by using gauge  $\vec{A}_{[x]}(\vec{r})$ ) and the HF energies of other nonstripe phases (discussed later), we can determine if a stripe phase can be stabilized and which direction is energetically more favorable for stripe formation. If no stripe phase is energetically favorable, the nonstripe phases obtained in these two gauges are identical (as they should be due to symmetry). In the rest of this paper, for the sake of brevity, we will show equations and formulae for the trial wavefunction and the related HF energy of a wide well system only for stripes along  $y$  axis (perpendicular to the in-plane field) in the gauge  $\vec{A}_{[y]}(\vec{r})$ , although (we emphasize that) we always consider both stripe directions in our variational calculations.

For a zero width double well (bilayer) system, the trial wavefunction for a stripe phase along the in-plane field direction ( $x$ ) can be studied in a much easier way. Using the fact that the in-plane magnetic field does not change the electron orbital wavefunctions in the zero width wells, we can simply rotate the in-plane magnetic field,  $\vec{B}_{\parallel}$ , from the direction along  $x$  axis to the direction along  $y$ , keeping all the trial wavefunction obtained by the conventional gauge,  $\vec{A}_{[y]}(\vec{r})$ , the same. We then equivalently obtain the HF energies of a stripe phase with a conserved momentum either perpendicular or parallel to the in-plane magnetic field. Their energy difference results from the Aharonov-Bohm phase factor in the tunneling amplitude, and that is the reason we keep both  $P_x$  and  $P_y$  in the bilayer Hamiltonian in Eq. (11).

In the rest of this section, we first show the trial wavefunction for the two level crossing (or level near degeneracy) situations in Section III A. We also consider several special many-body phases it generates and study their physical properties. In Section III B we propose wavefunctions for the four level degeneracy, involving the second highest filled level and the second lowest empty level about the Fermi energy for the double well system at  $\nu = 4N + 2$  and for the wide well system at  $\nu = 2N + 2$ , leaving out all other lower filled levels and higher empty levels as irrelevant core states. In Section III C we develop a perturbation technique to investigate the possible instability toward the stripe formation from a uniform coherent phase. We can use this method to study the existence of a stripe phase and its basic properties without optimizing the whole HF energy if the stripe formation is a second order phase transition.

### A. Two level degeneracy: variational wavefunctions for odd filling factors

#### 1. Wavefunction

We propose the following trial many-body wavefunction to incorporate both isospin stripe and isospin spiral orders simultaneously:

$$|\Psi_G(\psi_k, \vec{Q}_{\perp}, \gamma)\rangle = \prod_k \tilde{c}_{1,k}^{\dagger} |LL\rangle$$

$$\begin{bmatrix} \tilde{c}_{1,k}^{\dagger} \\ \tilde{c}_{2,k}^{\dagger} \end{bmatrix} = \begin{bmatrix} e^{ikQ_x l_0^2/2+i\gamma/2} \cos(\psi_k/2) & e^{-ikQ_x l_0^2/2-i\gamma/2} \sin(\psi_k/2) \\ -e^{ikQ_x l_0^2/2+i\gamma/2} \sin(\psi_k/2) & e^{-ikQ_x l_0^2/2-i\gamma/2} \cos(\psi_k/2) \end{bmatrix} \cdot \begin{bmatrix} c_{\uparrow,k-Q_y/2}^{\dagger} \\ c_{\downarrow,k+Q_y/2}^{\dagger} \end{bmatrix}, \quad (36)$$

where we use  $\uparrow$  ( $\downarrow$ ) to denote the isospin up(down) state, which can represent subband level, spin and/or layer indices depending on the systems we are considering (see Table I). The spiral winding wavevector,  $\vec{Q}_{\perp}$ , stripe phase function,  $\psi_k$ , and the additional phase,  $\gamma$ , are the variational parameters to minimize the total Hartree-Fock energy. If the system has isospin rotation symmetry around the isospin  $z$  axis (e.g. double well systems at  $\nu = 4N + 1$  in the absence of tunneling), the new ground state energy obtained by the trial wavefunction above will be independent of  $\gamma$ . If the system has no such isospin rotation symmetry (e.g. double well systems at  $\nu = 4N + 1$  in the presence of tunneling or the wide well systems at  $\nu = 2N + 1$ ), the new ground state energy will then depend on  $\gamma$ , selecting some specific values of  $\gamma$  to minimize the total variational energy. We will discuss both of these cases in details in our HF analysis in Sections IV-VII. In general this two level coherence approximation should be good for a system near the degeneracy point, especially for an odd filling factor. For systems with even filling factor, the inclusion of the next nearest two levels about Fermi energy becomes crucial as will be discussed later.

For the convenience of later discussion, we define following functions:

$$\begin{aligned}
\Theta_1(q_x) &\equiv \frac{1}{N_\phi} \sum_k e^{ikq_x l_0^2} \cos^2(\psi_k/2) \\
\Theta_2(q_x) &\equiv \frac{1}{N_\phi} \sum_k e^{ikq_x l_0^2} \sin^2(\psi_k/2) = \delta_{q_x,0} - \Theta_1(q_x) \\
\Theta_3(q_x) &\equiv \frac{1}{N_\phi} \sum_k e^{ikq_x l_0^2} \sin(\psi_k/2) \cos(\psi_k/2),
\end{aligned} \tag{37}$$

Note that when  $\psi_k = \psi_0$  as a constant,  $\Theta_i(q_x) = \Theta_i(0)\delta_{q_x,0}$  (for  $i = 1, 2, 3$ ) and  $\Theta_3(0)^2 = \Theta_1(0)\Theta_2(0)$ . The physical meaning of these functions are the following:  $\Theta_1(0)$  describes the density of isospin-up electrons,  $\Theta_2(0)$  describes the density of isospin-down electrons, and  $\Theta_3(0)$  measures the coherence between isospin up and isospin down electrons. For the periodic function,  $\psi_k$ , without any loss of generality, we can assume that it is a real and even function of the guiding center coordinate  $k$  so that  $\Theta_i(q_x)$  are all real quantities.

## 2. Isospin phases and their physical properties

To understand the physical properties of the trial wavefunction proposed in Eq. (36), we first define the following generalized density operators (isospin index,  $I = \pm 1 = \uparrow (\downarrow)$ ):

$$\rho_{I_1 I_2}(\vec{q}_\perp) \equiv \sum_k e^{ikq_x l_0^2} c_{I_1, k-q_y/2}^\dagger c_{I_2, k+q_y/2}, \tag{38}$$

which generalizes Eqs. (10), (13) and (17)). The isospin operator at the in-plane momentum,  $\vec{q}_\perp$ , can be defined as

$$\begin{aligned}
\vec{\mathcal{I}}(\vec{q}_\perp) &\equiv \frac{1}{2} \int dz \int d\vec{r}_\perp e^{-i\vec{q}_\perp \cdot \vec{r}_\perp} \sum_{I_1, I_2} \sum_{k_1, k_2} c_{I_1, k_1}^\dagger \vec{\sigma}_{I_1, I_2} c_{I_2, k_2} \phi_{I_1, k_1}(\vec{r})^* \phi_{I_2, k_2}(\vec{r}) \\
&= \sum_{I_1, I_2} \vec{\sigma}_{I_1, I_2} \rho_{I_1 I_2}(\vec{q}_\perp) A_{I_1 I_2}(\vec{q}_\perp, 0),
\end{aligned} \tag{39}$$

where  $\vec{\sigma}_{I_1, I_2}$  are the Pauli matrix elements, and  $A_{I_1 I_2}(\vec{q})$  is the generalized form function as has been specifically defined in Eqs. (7) and (12) for wide well systems and double well systems respectively.

Using the trial wavefunction,  $|\Psi_G\rangle$ , in Eq. (36), we obtain the following expectation value of isospin components:

$$\begin{aligned}
\langle \vec{I}_z(\vec{q}) \rangle &= \frac{1}{2} [A_{\uparrow\uparrow}(\vec{q}_\perp, 0) \langle \Psi_G | \rho_{\uparrow\uparrow}(\vec{q}_\perp) | \Psi_G \rangle - A_{\downarrow\downarrow}(\vec{q}_\perp, 0) \langle \Psi_G | \rho_{\downarrow\downarrow}(\vec{q}_\perp) | \Psi_G \rangle] \\
&= \frac{1}{2} N_\phi \delta_{q_y,0} \left[ A_{\uparrow\uparrow}(\vec{q}_\perp, 0) e^{-iq_x Q_y l_0^2/2} \Theta_1(q_x) - A_{\downarrow\downarrow}(\vec{q}_\perp, 0) e^{iq_x Q_y l_0^2/2} \Theta_2(q_x) \right]
\end{aligned} \tag{40}$$

and

$$\langle \mathcal{I}_+(\vec{q}_\perp) \rangle = A_{\uparrow\downarrow}(\vec{q}_\perp, 0) \langle \Psi_G | \rho_{\uparrow\downarrow}(\vec{q}_\perp) | \Psi_G \rangle = N_\phi \delta_{q_y, Q_y} A_{\uparrow\downarrow}(\vec{q}_\perp, 0) \Theta_3(q_x - Q_x) e^{-i\gamma}. \tag{41}$$

There are two classes of interesting phases one can find from Eqs. (40) and (41). First, if  $\psi_k = \psi_0$  is a constant, the  $z$  component of the mean value of isospin,  $\langle \mathcal{I}_z(\vec{q}_\perp) \rangle \propto \delta_{q_x,0} \delta_{q_y,0}$ , is uniform over the 2D well plane, while its transverse components,  $\langle \mathcal{I}_\pm(\vec{q}_\perp) \rangle \propto \delta_{q_x, Q_x} \delta_{q_y, Q_y}$ , select a certain wavevector,  $\vec{Q}_\perp = (Q_x, Q_y)$ , in the guiding center coordinate for winding, i.e. the isospin  $x$  and  $y$  components oscillate in the real space at wavevector,  $\vec{Q}_\perp$  (see Fig. 3(a)). Therefore we define  $\vec{Q}_\perp$  as the wavevector of isospin spiral order. Secondly if  $\psi_k$  is a periodic function of  $k$ , the isospin polarization,  $\langle \mathcal{I}_z(\vec{r}_\perp) \rangle$ , will oscillate along  $x$  direction (but uniform in  $y$  direction) according to Eq. (40), characterizing a stripe phase with normal vector  $\hat{n} \parallel \hat{x}$ . Choosing the other gauge,  $\vec{A}_{[x]}(\vec{r})$ , in which the particle momentum is conserved along  $x$  direction, we can construct a stripe phase along  $x$  direction and isospin  $\langle \mathcal{I}_z(\vec{r}_\perp) \rangle$  then modulates in  $y$  direction as shown in Appendix A.

It is also interesting to investigate the local charge density distribution in the top Landau level,  $\rho_{local}(\vec{r}_\perp)$ , by using the trial wavefunction,  $|\Psi_G\rangle$ , in Eq. (36). It has contributions from both the isospin up and isospin down electrons:

$$\begin{aligned}
\rho_{local}(\vec{r}_\perp) &= \frac{1}{\Omega_\perp} \sum_{\vec{q}_\perp} e^{i\vec{q}_\perp \cdot \vec{r}_\perp} \langle \Psi_G | A_{\uparrow\uparrow}(\vec{q}_\perp, 0) \rho_{\uparrow\uparrow}(\vec{q}_\perp) + A_{\downarrow\downarrow}(\vec{q}_\perp, 0) \rho_{\downarrow\downarrow}(\vec{q}_\perp) | \Psi_G \rangle \\
&= \frac{1}{2\pi l_0^2} - \frac{1}{2\pi l_0^2} \sum_{q_x} \Theta_2(q_x) [A_{\uparrow\uparrow}(q_x, 0, 0) \cos(q_x(x - Q_y l_0^2/2)) - A_{\downarrow\downarrow}(q_x, 0, 0) \cos(q_x(x + Q_y l_0^2/2))], \\
&\equiv \rho_0 + \rho_{ex}(\vec{r}_\perp)
\end{aligned} \tag{42}$$

where  $N_\phi/\Omega_\perp = (2\pi l_0^2)^{-1}$  is the average electron density in each Landau level. Eq. (42) shows that if  $\Theta_2(q_x)$  selects a specific wavevector (i.e.  $\psi_k$  oscillates periodically with a characteristic wavevector) at  $q_x = q_n = 2\pi n/a$ , where  $a$  is the period of stripe, the extra charge density,  $\rho_{ex}(\vec{r}_\perp)$ , will be nonzero and a periodic function in the real space. In Appendix C we will show that this extra charge density is related to the charge density induced by the topological isospin density by generalizing the theory of skyrmion excitations developed in Ref. [18] for a double well system. Therefore in the rest of this paper we will denote such a CDW state as a "skyrmion stripe" phase. In general we should have skyrmion stripe phases whenever the stripe normal vector  $\hat{n}$  (i.e. the modulation direction of  $\langle \mathcal{I}_z \rangle$ ) is perpendicular to the spiral wavevector  $\vec{Q}_\perp$  [8].

According to the above analysis, we can consider the following six different phases obtained from Eq. (36): when  $\psi_k$  is a constant, the wavefunction of Eq. (36) can describe three nonstripe phases: (i) fully (un)polarized uniform quantum Hall phase for  $\psi_k = (0)\pi$  (with  $\vec{Q}_\perp$  being arbitrary), (ii) coherent phase for  $\vec{Q}_\perp = 0$  and  $\psi_k \neq 0, \pi$ , and (iii) spiral phase for finite  $\vec{Q}_\perp$  and  $\psi_k \neq 0, \pi$ . When  $\psi_k$  changes periodically with  $k$ , three kinds of stripe phases arises: (i) when  $\vec{Q}_\perp$  is perpendicular to the stripe normal direction, we have a skyrmion stripe described above; (ii) when  $\vec{Q}_\perp$  is parallel to the stripe normal direction, we have a spiral stripe phase, and (iii) when  $\vec{Q}_\perp = 0$  we have a coherent stripe phase. For simplicity, in this paper we will only consider stripe and spiral orders (if they exist) with characteristic wavevector  $\hat{n}$  and  $\vec{Q}_\perp$  being either perpendicular or parallel to the in-plane magnetic field, which is fixed to be in the positive  $x$  axis. A simple visualized cartoon of the spiral winding and the three stripe phases is shown in Fig. 4. We calculate the HF energy given by the six different phases generated from the trial wavefunction, Eq. (36), and compare them to get the minimum energy for the true ground state.

### 3. Symmetry properties of the trial wavefunction

In Section II C we have shown that the systems we are considering have three kinds of symmetries: parity (full space inversion) symmetry, two-dimensional translational symmetry, and spin rotational symmetry. Here we show how a general isospin trial wavefunction in Eq. (36) is transformed under these symmetry operators defined in Section II C. This will enable us to identify the broken symmetries in each of the isospin phases discussed above.

First it is easy to see that the conventional integer QH state (i.e. isospin polarized with  $\psi_k = 0$  or  $\pi$ ),  $|\Psi_0\rangle = \prod_k c_{\uparrow(\downarrow),k}^\dagger |LL\rangle$ , is an eigenstate of all the three symmetry operators ( $\hat{\mathcal{P}}$ ,  $\hat{\mathcal{T}}_{x(y)}$ , and  $\hat{\mathcal{U}}$ ), by applying the equations in Section II C directly. (For simplicity, in our discussion below, the isospin basis of double well system at  $\nu = 4N+1$  is chosen to be the symmetric-antisymmetric basis, i.e. the noninteracting eigenstate basis. The symmetry properties of the isospin coherent phases constructed in the layer index basis will be discussed later in Section VID). Therefore, the isospin polarized state,  $|\Psi_0\rangle$ , does not break any symmetry properties as expected.

Now we consider a general many-body state described by the wavefunction Eq. (36) with variational parameters obtained from minimizing the HF energy:  $\psi_k = \psi_k^* \neq 0, \pi$ ;  $\vec{Q}_\perp = \vec{Q}_\perp^*$ , and  $\gamma = \gamma^*$ . Applying the parity operator,  $\hat{\mathcal{P}}$ , translation operator,  $\hat{\mathcal{T}}_{x(y)}$ , and spin rotation operator,  $\hat{\mathcal{U}}$ , on  $|\Psi_G(\psi_0^*, \vec{Q}_\perp^*, \gamma^*)\rangle$ , we can obtain respectively

$$\hat{\mathcal{P}}|\Psi_G(\psi_k^*, \vec{Q}_\perp^*, \gamma^*)\rangle = (-i)^{N_\phi} |\Psi_G(\psi_{-k}^*, -\vec{Q}_\perp^*, \gamma^* + \pi)\rangle, \tag{43}$$

$$\hat{\mathcal{T}}_\alpha(R_\alpha)|\Psi_G(\psi_k^*, \vec{Q}_\perp^*, \gamma^*)\rangle = |\Psi_G(\psi_{k-\hat{n} \cdot \vec{R}_\perp/l_0^2}^*, \vec{Q}_\perp^*, \gamma^* - Q_\alpha R_\alpha)\rangle, \tag{44}$$

$$\hat{\mathcal{U}}(\chi)|\Psi_G(\psi_k^*, \vec{Q}_\perp^*, \gamma^*)\rangle = |\Psi_G(\psi_k^*, \vec{Q}_\perp^*, \gamma^* - \chi(s_1 - s_2))\rangle, \tag{45}$$

where  $\alpha = x$  or  $y$ ,  $\vec{R}_\perp = (R_x, R_y)$ ,  $s_{1(2)} = \pm 1/2$  is the spin quantum number of isospin up(down) state, and  $\hat{n}$  is the stripe oscillation direction (it is perpendicular to the direction of stripes, e.g.  $\hat{n} = \hat{x}$  for stripes along  $y$  direction described by the Landau gauge,  $\vec{A}_{[y]}(\vec{r})$ ). In Eq. (43) we have assumed that the signs for the isospin up state and isospin down state are opposite after parity operation (we will show that this is always true in the level crossings considered in this paper). According to Eqs. (43)-(45), we find that only parity symmetry is broken in a coherent phase ( $\psi_k^* = \psi_0^* \neq 0, 2\pi$  and  $\vec{Q}_\perp^* = 0$ ), if  $s_1 = s_2$ . Spin rotation symmetry is also broken if the spin quantum number

of the two crossing levels (isospin up and down) are different ( $s_1 \neq s_2$ ), which is true only for the level crossings in the even filling systems. When we consider the spiral phase with  $\psi_k^* = \psi_0^* \neq 0, \pi$  and  $\vec{Q}_\perp^* \neq 0$ , we find that in addition to the broken symmetries discussed above (parity symmetry and spin rotational symmetry if  $s_1 \neq s_2$ ), it breaks translational symmetry in the direction of isospin winding (i.e. along  $\vec{Q}_\perp^*$ ). From Eq. (44) we immediately see that the wavefunction has a period  $2\pi/|\vec{Q}_\perp^*|$ . For the coherent stripe phase ( $\psi_k^*$  modulated periodically and  $\vec{Q}_\perp^* = 0$ ) we have broken parity, spin rotational symmetry if  $s_1 \neq s_2$ , and translational symmetry in the direction of  $\hat{n}$ . For a spiral stripe, the spiral winding direction is parallel to the stripe oscillation direction ( $\vec{Q}_\perp^* \parallel \hat{n}$ ), and therefore the translational symmetry is broken only in one direction, while a skyrmion stripe ( $\vec{Q}_\perp^* \perp \hat{n}$ ) breaks translational symmetries in both  $x$  and  $y$  directions. Both the spiral stripe and the skyrmion stripe also break the parity symmetry and spin rotational symmetry if  $s_1 \neq s_2$ .

A fundamental quantum mechanical principle stipulates that when a system undergoes a quantum phase transition to break a symmetry (i.e. the ground state wavefunction is not an eigenstate of the symmetry operator), the new symmetry-broken ground state will have additional degeneracy associated with the spontaneously broken symmetry. This result is also obtained in our HF energy calculation shown later. In Table I we list the many-body states obtained by our HF variational calculation and the resulting broken symmetries. We will discuss each of them individually in the following sections for different systems and then compare the results with each other in Section VIII.

## B. Four levels near a degeneracy: variational wavefunctions for even filling factors

### 1. Wavefunction for double well systems

For a double well system at  $\nu = 4N + 2$ , the complete filled core levels are the lowest  $4N$  levels, while the top two filled levels may coherently hybridize in some situations with the empty levels above the Fermi energy (we consider only the two lowest empty Landau levels in the context motivated by the scenario originally discussed in Ref. [33]). We label the states involved in forming a many-body state as follows: the second highest filled level is denoted to be level 3, the highest (top) filled level is level 1, the lowest empty level above the Fermi energy is level 2, and the second lowest empty level is level 4 (see Fig. 5(a)), and the other higher empty levels are assumed to be irrelevant. Naively one may think that we may construct a trial wavefunction similar to Eq. (36) to consider interlevel coherence only between level 1 (the highest filled level) and level 2 (the lowest empty level), because the single electron energy separation between these two levels is the smallest energy scale near level crossing. However, it was explicitly shown that in a double well system at  $\nu = 4N + 2$ , the contribution of the second highest filled level (level 3) and the second lowest empty level (level 4) could make crucial contribution to the coherent hybridization between level 1 and level 2, resulting a novel canted antiferromagnetic phase (CAF) with broken spin symmetry [33]. This symmetry-broken coherent phase cannot be obtained if one considers the coherence between the most degenerate pair only (i.e. level 1 and level 2) via Eq. (36). Another way to understand why it is natural to consider four rather than two levels around the Fermi energy in creating a many-body state for the double well system at  $\nu = 4N + 2$  is to note that these four levels are separated from the other ones by a large cyclotron energy, whereas they are separated from each other only by (much) smaller energies of Zeeman and tunneling splittings. Therefore in this section we will consider the mixing of the four (rather than two) levels closest to the Fermi energy to study the trial wavefunctions for the double well  $\nu = 4N + 2$  system near the level crossing region in the presence of the in-plane field.

Let us first consider the uniform ground state of a double well system at  $\nu = 4N + 2$  *without* any in-plane magnetic field. We assume that the cyclotron resonance energy,  $\omega_\perp$ , is much larger than the tunneling energy,  $\Delta_{SAS}$ , and the Zeeman (spin-splitting) energy,  $\omega_z$ , so that the two highest filled levels and the two lowest empty levels have the same orbital Landau level and all other levels can be treated as incoherent core states not actually participating in the level-crossing hybridization process. Single particle states for noninteracting electrons are shown in Fig. 5(a) in the case when the tunneling energy,  $\Delta_{SAS}$ , is larger than the Zeeman energy,  $\omega_z$ . We use  $(\alpha, s)$  to label the four levels around Fermi level under consideration, where  $\alpha = \pm 1$  is the quantum number of parity symmetry (which in this case is the reflection symmetry about  $x - y$  plane,  $z \rightarrow -z$ , or the interchange of layers, see Section II C), and  $s = \uparrow (\downarrow)$  is the spin quantum number. For convenience of comparison and later discussion, we define level 1 ( $(\alpha, s) = (+, \downarrow)$ ) and level 2 ( $(\alpha, s) = (-, \uparrow)$ ) to be the isospin up and isospin down state respectively as shown in Table I, because these two levels, being closest to the Fermi energy, are obviously the most energetically relevant ones compared to the other two levels in this four level scenario (see Fig. 2(f)). Many-body states that appear in this system correspond to mixing some of these single particle states and describe the breaking of certain symmetries in this problem. As discussed by Das Sarma *et. al.* [33] in the context of the canted antiferromagnetic state in bilayer systems, the states that are most likely to be hybridized by Coulomb interaction are the ones that are closest to each other for the noninteracting system:

state 1 =  $(+, \downarrow)$ , and 2 =  $(-, \uparrow)$ . When the expectation value  $\langle c_{1,k}^\dagger c_{2,k} \rangle$  is finite and independent of  $k$ , the system has canted antiferromagnetic spin order. In the two layers the transverse components of the spin point in the opposite directions. Such an order parameter breaks the spin rotational symmetry around  $z$ -axis and the parity symmetry  $\hat{\mathcal{P}} = \hat{\mathcal{P}}_z \hat{\mathcal{P}}_{xy}$ . (We use the full parity symmetry,  $\hat{\mathcal{P}}$ , rather than  $\hat{\mathcal{P}}_z$ , since the latter is not conserved when we include an in-plane magnetic field later, see Section II C.) More precisely, under the spin rotation,  $\hat{\mathcal{U}}(\chi)$  (defined in Eq. (35)), we have  $\hat{\mathcal{U}}(\chi) a_{1,k}^\dagger a_{2,k} \hat{\mathcal{U}}^{-1}(\chi) = e^{-i\chi} a_{1,k}^\dagger a_{2,k}$ , and under parity transformation, we have  $\hat{\mathcal{P}} a_{1,k}^\dagger a_{2,k} \hat{\mathcal{P}}^{-1} = -a_{1,-k}^\dagger a_{2,-k}$ . So the order parameter has spin  $S_z = 1$  and is odd under parity. However, the operator  $a_{4,k}^\dagger a_{3,k}$  has exactly the same symmetry properties as  $a_{1,k}^\dagger a_{2,k}$ , so in a canted antiferromagnetic phase both of them acquire finite expectation values. Therefore it would be insufficient to consider mixing of the states 1 and 2 only and treat levels 3 and 4 as frozen [33] in the double well system at even filling factors. On the other hand hybridization between any other pair of levels does not take place since the appropriate expectation values would have symmetry properties different from the transverse CAF Neel order. For example  $a_1^\dagger a_4$  has the right parity symmetry but wrong spin symmetry, and  $a_1^\dagger a_3$  has the correct spin symmetry but wrong parity. As was discussed earlier [33–35] and as we will demonstrate below, the physical origin of the CAF phase is the lowering of the exchange energy due to the additional spin correlations associated with  $a_{4,k}^\dagger a_{3,k}$ , present above.

To construct an appropriate trial wavefunction *in the presence of* in-plane field, we first consider a uniform phase. If we make the assumption that the order parameter breaks the same symmetries as in the case  $B_{\parallel} = 0$ , it has to have spin  $S_z = 1$  and be odd under parity. The operators,  $a_{1\dots 4,k}$  defined in Eq. (14), have the same transformation properties under  $\hat{\mathcal{U}}(\chi)$  and  $\hat{\mathcal{P}}$  (see Section II C) with or without  $B_{\parallel}$ . The identical nature of broken symmetries in the cases  $B_{\parallel} = 0$  and  $B_{\parallel} \neq 0$  implies that  $a_{1,k}^\dagger a_{2,k}$  and  $a_{3,k}^\dagger a_{4,k}$  acquire expectation values even in the presence of a finite in-plane magnetic field. Therefore we can still apply the ansatz of Ref. [33] and consider the hybridization of level 1 with level 2 and level 3 with level 4 separately to construct a trial wavefunction wavefunction for the *uniform* phase in the presence of in-plane field. In addition, as suggested by the wavefunction of odd filling system in Eq. (36), this hybridization may be further extended to a slightly more complicated form to reflect the possible uniform winding of the transverse Neel order [36] and/or the stripe order to break the translational symmetry. We then propose a trial wavefunction for a double well system at  $\nu = 4N + 2$  in the presence of in-plane magnetic field as follows:

$$\begin{aligned}
|\Psi_G^{D2}(\psi_k, \psi'_k; \vec{Q}_\perp, \vec{Q}'_\perp; \gamma, \gamma')\rangle &= \prod_k \tilde{a}_{1,+k}^\dagger \tilde{a}_{2,+k}^\dagger |LL\rangle \\
\begin{bmatrix} \tilde{a}_{1,+k}^\dagger \\ \tilde{a}_{1,-k}^\dagger \\ \tilde{a}_{2,+k}^\dagger \\ \tilde{a}_{2,-k}^\dagger \end{bmatrix} &= \begin{bmatrix} e^{ikQ_x l_0^2/2+i\gamma/2} \cos(\psi_k/2) & e^{-ikQ_x l_0^2/2-i\gamma/2} \sin(\psi_k/2) & 0 & 0 \\ -e^{ikQ_x l_0^2/2+i\gamma/2} \sin(\psi_k/2) & e^{-ikQ_x l_0^2/2-i\gamma/2} \cos(\psi_k/2) & 0 & 0 \\ 0 & 0 & e^{ikQ'_x l_0^2/2+i\gamma'/2} \cos(\psi'_k/2) & e^{-ikQ'_x l_0^2/2-i\gamma'/2} \sin(\psi'_k/2) \\ 0 & 0 & -e^{ikQ'_x l_0^2/2+i\gamma'/2} \sin(\psi'_k/2) & e^{-ikQ'_x l_0^2/2-i\gamma'/2} \cos(\psi'_k/2) \end{bmatrix} \\
\cdot \begin{bmatrix} a_{N,+1,\downarrow,k-Q_y/2}^\dagger \\ a_{N,-1,\uparrow,k+Q_y/2}^\dagger \\ a_{N,+1,\uparrow,k-Q'_y/2}^\dagger \\ a_{N,-1,\downarrow,k+Q'_y/2}^\dagger \end{bmatrix}, & \quad (46)
\end{aligned}$$

where  $\psi'_k$ ,  $\vec{Q}'_\perp = (Q'_x, Q'_y)$ , and  $\gamma'$  are four additional parameters to be determined variationally. We allow  $\psi_k$  and  $\psi'_k$  to be arbitrary periodic functions of  $k$ , in order to consider the possible stripe formation. Note that the original  $4 \times 4$  matrix representation of an unitary transformation has been reduced to an effective block-diagonalized matrix form, and reduces to the uniform wavefunction originally proposed in Ref. [33] if we put  $\vec{Q}_\perp = 0$  and  $\psi_k = \psi_0$ , a constant. The fact that the uniform wavefunction ( $Q_\perp = 0$ ,  $\psi_k = \psi_0$ ) turns out to be an excellent description [33–35] for the corresponding  $B_{\parallel} = 0$  case leads us to believe that the variational symmetry-broken wavefunction defined by Eq. (46) should be a reasonable generalization to study the many-body phases in the *presence* of an in-plane magnetic field, for the  $\nu = 4N + 2$  bilayer system.

The specific symmetry-broken form of the wavefunction in Eq. (46) allows us to introduce the concept of "double isospinors" to describe the coherence in the four levels near degeneracy, because each degenerate pair (i.e. levels 1 and 2, and levels 3 and 4) form two distinct isospinors in the state defined by Eq. (46). The exchange energy between the two isospinors may stabilize a symmetry-broken phase, and it reaches its maximum value if the two isospinors have the same stripe period but have opposite spiral winding wavevectors. (This result is explicitly obtained later in our numerical calculations of Section VII.) The symmetry properties of this four level mixing coherent wavefunction (Eq. (46)) are identical to those discussed in Section III A 3, and we do not discuss it further here.

To develop a deeper understanding of the trial wavefunction proposed in Eq. (46), it is instructive to transform Eq. (46) back into the layer index basis, which, while not being a noninteracting energy eigenbasis, is physically more appealing and easier to visualize conceptually. For the convenience of comparison, we let  $P_x = Q_y = Q'_y = 0$  and  $\gamma = \gamma' = 0$ , i.e. the in-plane magnetic field chosen to be in the  $y$  direction. (Here we have used a known result that the winding vector is always perpendicular to the in-plane magnetic field in the double well system, which is justified by the numerical results shown later in this paper.) Combining Eq. (14) and Eq. (46) we obtain the ground state wavefunction as follows (the Landau level index,  $N$  is omitted):

$$|\Psi_G^{D2}\rangle = \prod_{i=1,2} \prod_k \left( \sum_{l,s} z_{l,s,k}^{(i)} e^{ikQ_{l,s}^{(i)} l_0^2} c_{l,s,k}^{D,\dagger} \right) |LL\rangle, \quad (47)$$

where  $z_{\pm,\uparrow,k}^{(1)} = \cos(\psi_k/2)$ ,  $z_{\pm,\downarrow,k}^{(1)} = -\sin(\psi_k/2)$ ,  $z_{\pm,\uparrow,k}^{(2)} = \pm \sin(\psi'_k/2)$ , and  $z_{\pm,\downarrow,k}^{(2)} = \cos(\psi'_k/2)$ , and their phases are respectively

$$\begin{aligned} Q_{\pm,\uparrow}^{(1)} &= (\mp P_y + Q_x)/2 \\ Q_{\pm,\downarrow}^{(1)} &= (\mp P_y - Q_x)/2 \\ Q_{\pm,\uparrow}^{(2)} &= (\mp P_y - Q'_x)/2 \\ Q_{\pm,\downarrow}^{(2)} &= (\mp P_y + Q'_x)/2. \end{aligned} \quad (48)$$

One can see that the phase difference between the right ( $l = +$ ) and the left ( $l = -$ ) layers of the same spin is always  $-P_y$  as in a commensurate phase, while it is  $Q_x$  or  $Q'_x$  between up spin electrons and down spin electrons within the same layer. In other words the wavefunction proposed in Eq. (46) can only give a commensurate phase, because the effect of in-plane magnetic field has been automatically taken into account by transforming the layer index basis into the noninteracting energy eigenstate basis as shown in Section II B. More precisely, following Ref. [36], we can define three different states according to the phase difference of electrons in different layer and spin quantum states: (i) fully commensurate state, if  $Q_x = Q'_x = 0$ , and hence spin up and spin down electrons in the same layer have the same winding phase determined by the in-plane field; (ii) partially commensurate/incommensurate state, if  $Q_x \neq 0$  or  $Q'_x \neq 0$ , and hence spin up and spin down electrons in the same layer have different winding frequency, although the phase difference between electrons of the same spin but in different layers still oscillates with a wavevector determined by the in-plane field  $P_y$ ; (iii) fully incommensurate state, if  $Q_{+,\uparrow(\downarrow)}^{(1,2)} - Q_{-,\uparrow(\downarrow)}^{(1,2)} \neq -P_y$ , and therefore the tunneling energy becomes ineffective. According to Eq. (48), the fully incommensurate cannot be obtained from the trial wavefunction of Eq. (46), and only the fully commensurate and partially commensurate/incommensurate phases are the possible solutions. We note, however, that the fully incommensurate phase can be formally described by Eq. (46) if we use operators defined in Eq. (14) with  $P_x = P_y = 0$  and set  $\Delta_{SAS} = 0$  in the HF energy. Symmetry properties of the wavefunction, Eq. (46), may be easily described in analogy with Section III A 3 (see Eqs. (43)-(45)).

## 2. Wavefunction for wide well systems

For a wide well system at  $\nu = 2N + 2$ , we have to separate the two kinds of level crossing possibilities in different regimes of the in-plane magnetic field: (i) the intersubband level crossing ( $W2$ ) at small  $B_{\parallel}$  (see Figs. 1 and 2(c)), and (ii) the intrasubband level crossing ( $W2'$ ) at larger  $B_{\parallel}$  (see Figs. 1 and 2(d)). In the first case, the intersubband level crossing for noninteracting electrons at even filling factors, there are two separate possible level crossings close to each other:  $((1,0),\downarrow)$  with  $((0,N),\uparrow)$  and  $((1,0),\uparrow)$  with  $((0,N),\downarrow)$ . The in-plane magnetic field (and hence Zeeman energy) is so small (for realistic situations in GaAs-based 2D systems) in this case that the two level crossings are actually very close, and therefore it is better to consider both of them simultaneously in a single trial wavefunction (constructed by the four degenerate levels) rather than consider them separately as two independent crossings. The simplest wavefunction in this case should be similar to Eq. (46), where the  $4 \times 4$  matrix is block-diagonalized as two separate isospinors for each pair of the crossing levels. According to the symmetry arguments of the last section and the parity symmetry properties shown in Eq. (20), such simple block-diagonalized  $4 \times 4$  matrix representation of the trial wavefunction is further justified when considering a uniform phase only (i.e.  $\vec{Q}_{\perp} = \vec{Q}'_{\perp} = 0$ , and  $\psi_k$  and  $\psi'_k$  are constants), if the two crossing levels have different parity symmetries. As a result, we just consider the even- $N$  case in this paper (so that level  $(1,0)$  and  $(0,N)$  have different parity and spin rotational symmetries), and speculate that the results for the odd- $N$  case should be similar. Therefore, for the intersubband level crossing of a wide well system at even filling factors, we propose the following trial wavefunction, similar to Eq. (46):

$$\begin{aligned}
|\Psi_G^{W2}(\psi_k, \psi'_k; \vec{Q}_\perp, \vec{Q}'_\perp; \gamma, \gamma')\rangle &= \prod_k \tilde{c}_{1,+k}^{W,\dagger} \tilde{c}_{2,+k}^{W,\dagger} |LL\rangle \\
\begin{bmatrix} \tilde{c}_{1,+k}^\dagger \\ \tilde{c}_{1,-k}^\dagger \\ \tilde{c}_{2,+k}^\dagger \\ \tilde{c}_{2,-k}^\dagger \end{bmatrix} &= \begin{bmatrix} e^{ikQ_x l_0^2/2+i\gamma/2} \cos(\psi_k/2) & e^{-ikQ_x l_0^2/2-i\gamma/2} \sin(\psi_k/2) & 0 & 0 \\ -e^{ikQ_x l_0^2/2+i\gamma/2} \sin(\psi_k/2) & e^{-ikQ_x l_0^2/2-i\gamma/2} \cos(\psi_k/2) & 0 & 0 \\ 0 & 0 & e^{ikQ'_x l_0^2/2+i\gamma'/2} \cos(\psi'_k/2) & e^{-ikQ'_x l_0^2/2-i\gamma'/2} \sin(\psi'_k/2) \\ 0 & 0 & -e^{ikQ'_x l_0^2/2+i\gamma'/2} \sin(\psi'_k/2) & e^{-ikQ'_x l_0^2/2-i\gamma'/2} \cos(\psi'_k/2) \end{bmatrix} \\
\cdot \begin{bmatrix} c_{\vec{n}_1,\downarrow,k-Q_y/2}^{W,\dagger} \\ c_{\vec{n}_2,\uparrow,k+Q_y/2}^{W,\dagger} \\ c_{\vec{n}_1,\uparrow,k-Q'_y/2}^{W,\dagger} \\ c_{\vec{n}_2,\downarrow,k+Q'_y/2}^{W,\dagger} \end{bmatrix}, & \tag{49}
\end{aligned}$$

where  $\vec{n}_1 = (1, 0)$  and  $\vec{n}_2 = (0, N) = (0, 2)$  are the Landau level indices of the crossing levels (see Fig. 2(c)).

For the intrasubband level crossing at large  $B_\parallel$  region ( $W2'$ ), only two noninteracting levels participate in level crossing (see Figs. 2(d) and 5(a)): level 1 =  $((0, N), \downarrow)$  and level 2 =  $((0, N+1), \uparrow)$ , and all the other levels remain separated by a finite gap. In this situation one is allowed to consider only two degenerate levels when discussing the formation of a many-body state created by hybridization of levels 1 and 2. We will, however, still include mixing the next nearest levels, levels 3 =  $((0, N), \uparrow)$  and 4 =  $((0, N+1), \downarrow)$ , in the theory, and consider the block-diagonal wavefunctions of the type given in Eq. (49) (but with  $\vec{n}_1 = (0, N)$  and  $\vec{n}_2 = (0, N+1)$ ). In the lowest order in Coulomb interaction they agree with the two-level coupling wavefunction (c.f. Eq. (36)), but have an advantage that they allow us to discuss  $W2'$  level crossing point at the same footing as  $W2$ . The parity symmetry argument for a *uniform* phase can also be applied in this case, since levels  $(0, N)$  and  $(0, N+1)$  are always of different parity symmetry and the corresponding Zeeman-split levels obviously have different spin polarizations. Therefore we believe Eq. (49) to be a reasonable trial wavefunction to study possible isospin winding and/or stripe order, although we cannot exclude the possibility that the ground state maybe stabilized by other more general wavefunctions. We do point out, however, that if we include the mixing of  $((0, N), \uparrow)$  with  $((0, N+1), \downarrow)$ , then  $((0, N-1), \uparrow)$  mixing with  $((0, N+2), \downarrow)$  arises exactly in the same order in Coulomb interaction, but with a numerically larger energy gap for the unperturbed levels. Therefore, unlike the double well system at  $\nu = 4N+2$  (where the cyclotron resonance energy,  $\omega_\perp$ , can be assumed to be much larger than the tunneling energy and the Zeeman splitting), considering only states 3 and 4 and neglecting all the other levels in the wide well  $W2'$  case can not be energetically justified. In any case, our four-level coupling wavefunction agrees with the simple two-level coupling in the lowest order in Coulomb interaction, and we will show (in Section V) that its HF energy also gives the correct magnetoplasmon dispersion enabling us to study the possibility of a second order quantum phase transition to a state of broken spin symmetry [17]. Therefore we believe that Eq. (49) provides a reasonable trial wavefunction to describe the single wide well system for even filling factors — the fact that the numerical implementation of the Hartree-Fock calculation using Eq. (49) is relative easy is an additional motivation to study it in details.

### C. Stripe formation in the isospin coherent phase

In Section III A we have discussed some physical properties of a stripe phase, where  $\psi_k$  can be a periodic function of the guiding center coordinate, hence providing an oscillatory isospin polarization,  $\langle \mathcal{I}_z \rangle$ . A generic stripe phase discussed in this paper is provided by the hybridization of two crossing levels of different parity symmetries near the level crossing (or near degenerate) region, and therefore (at least) both parity (full space inversion) symmetry and translational symmetry are broken when a stripe phase is stabilized by Coulomb interaction. (Note that the spiral phase may also break translational symmetry without any stripe order; spin rotational symmetry around the total magnetic field direction may also be broken if the two coherent levels are of different spin directions in an even filling factor system.) Parity is broken in the non-fully polarized regions between the stripes that choose a spatial direction, and the translational symmetry is broken when the stripes choose their positions. Transitions between states of no-broken symmetries (i.e. fully isospin polarized states in our case) and states that break parity and translational symmetries simultaneously may happen in two ways. The first possibility is a direct first order transition when the in-plane magnetic field exceeds some critical value. To calculate the ground state wavefunction for this first order phase transition, we need to include many variational parameters in the theory (as shown in Fig. 6 and Appendix E) for the stripe phase function in addition to the spiral wavevector,  $\vec{Q}_\perp$ . The numerical calculation for this first order transition is very time-consuming in general. The second possibility is two consecutive transitions that break symmetries one by one: at the first transition (which could be either first order or second order) parity symmetry is broken through

a *uniform* superposition of the two crossing Landau levels, which have different parity symmetries, and no stripe order is present; at the second transition, the stripe order appears spontaneously with a concomitant breaking of the transitional symmetry via a second order phase transition. In this section we concentrate on the second scenario (two consecutive transitions) and develop a formalism for studying instabilities of an interlevel coherent phase toward the formation of stripe order. In some situations a spiral order may be stabilized in the first step, which, strictly speaking, breaks the translational symmetry even without a stripe order, see Section III A 3. Appearance of the stripe order from such a spiral phase can also be described by the perturbation theory that we develop below as long as the stripe order appears via a second order phase transition. In Appendix D we will show that our perturbation method for probing the existence of a stripe phase is actually equivalent to studying the finite wavevector mode softening of a collective mode inside the uniform isospin coherent phase. We mention, however, that in general the perturbation calculation is easier to carry out than the mode softening calculation.

The perturbation method consists of the following steps. First, we use the trial wavefunction in Eq. (36) to search for non-stripe phases (i.e. use  $\vec{Q}_\perp^*$ ,  $\gamma$ , and  $\psi_k = \psi_0$  as the variational parameters) that minimize the energy of the system. If the optimal configuration has  $\psi_0 = 0$  or  $\pi$ , then no uniform many-body phases are stabilized near the level crossing (or near degeneracy) region. Formation of the stripe phase is still possible, but if it does occur, it happens via the first order transition, and we need to consider the explicit variational forms for the stripe phases, and compare their energies to the energies of the uniform isospin polarized phases (see Appendix E). Alternatively, if the optimal nonstripe configuration has  $\psi_0 \neq 0, \pi$  (and possibly finite  $\vec{Q}_\perp^*$ ), the stripe phase may appear via a second order phase transition, which may be understood as the appearance of small oscillations in  $\psi_k$ . Therefore, we can choose the oscillation amplitude of  $\psi_k$  to be an order parameter, and approximate  $\psi_k$  by the following formula:

$$\psi_k = \psi_0^* + 4\Delta \cos(k\tilde{q}_0^2), \quad (50)$$

where  $|\Delta| \ll \psi_0^* \neq 0$ ;  $\tilde{q}$ , the characteristic wavevector of the stripe (the stripe period  $a = 2\pi/\tilde{q}$ ), is the only additional parameter we need in the perturbation theory. We then obtain the following expansion of  $\Theta_i(q_n)$  to the second order in  $\Delta$  using the definition given in Eq. (37):

$$\Theta_1(q_n) = \delta_{q_n,0} [\Theta_1^*(0) - 2\Delta^2 \cos(\psi_0^*)] - \Delta \sin(\psi_0^*) [\delta_{q_n,-\tilde{q}} + \delta_{q_n,\tilde{q}}] - \Delta^2 \cos(\psi_0^*) [\delta_{q_n,-2\tilde{q}} + \delta_{q_n,2\tilde{q}}] + \mathcal{O}(\Delta^3) \quad (51)$$

$$\Theta_2(q_n) = \delta_{q_n,0} [\Theta_2^*(0) + 2\Delta^2 \cos(\psi_0^*)] + \Delta \sin(\psi_0^*) [\delta_{q_n,-\tilde{q}} + \delta_{q_n,\tilde{q}}] + \Delta^2 \cos(\psi_0^*) [\delta_{q_n,-2\tilde{q}} + \delta_{q_n,2\tilde{q}}] + \mathcal{O}(\Delta^3) \quad (52)$$

$$\Theta_3(q_n) = \delta_{q_n,0} [\Theta_3^*(0) - 2\Delta^2 \sin(\psi_0^*)] + \Delta \cos(\psi_0^*) [\delta_{q_n,-\tilde{q}} + \delta_{q_n,\tilde{q}}] - \Delta^2 \sin(\psi_0^*) [\delta_{q_n,-2\tilde{q}} + \delta_{q_n,2\tilde{q}}] + \mathcal{O}(\Delta^3), \quad (53)$$

where  $\Theta_i^*(0)$  ( $i = 1, 2, 3$ ) are their extreme values. Putting Eqs. (51)-(53) in the expression of our HF energy as shown in the latter sections, we obtain the leading order (quadratic terms of  $\Delta$  only) energy perturbation of a stripe phase from the HF energy of the uniform phase,  $E_{\text{nonstripe}}^{\text{HF}}(\psi_0^*, \vec{Q}_\perp^*)$ . This result can be expressed as follows:

$$E_{\text{stripe}}^{\text{HF}}(\tilde{q}) = E_{\text{nonstripe}}^{\text{HF}}(\psi_0^*, \vec{Q}_\perp^*) + E_{\text{pert}}^{\text{HF}}(\tilde{q}; \psi_0^*, \vec{Q}_\perp^*)\Delta^2 + \mathcal{O}(\Delta^4), \quad (54)$$

where the sign of  $E_{\text{pert}}^{\text{HF}}(\tilde{q}; \psi_0^*, \vec{Q}_\perp^*)$  determines the existence of a stripe phase: if the minimum value of  $E_{\text{pert}}^{\text{HF}}(\tilde{q}; \psi_0^*, \vec{Q}_\perp^*)$  is negative *and* at a finite value of  $\tilde{q} = \tilde{q}^*$ , we can claim that the original uniform phase is not energetically favorable compared to the stripe phase, and the ground state can then be a stripe phase with iso(spin) winding vector  $\vec{Q}_\perp^*$  and stripe oscillation wavevector  $\tilde{q}^*$  along  $x$  axis (we are using Landau gauge,  $\vec{A}_{[y]}(\vec{r})$ ). On the other hand, if  $E_{\text{pert}}^{\text{HF}}(\tilde{q}; \psi_0^*, \vec{Q}_\perp^*)$  is positive for all  $\tilde{q}$ , then a stripe phase along  $y$  cannot be formed through a second order phase transition. If we want to study the possibility of stripe formation along  $x$  direction (i.e. stripe modulation is along  $y$  axis), we can do the same analysis as above, but using the Landau gauge,  $\vec{A}_{[x]}(\vec{r})$ . If both stripe phases are possible, we need to compare them and find the one of the lowest energy.

Finally we note that the same approach can be also applied to study possible stripe formation via a continuous transition in the double well systems at  $\nu = 4N + 2$  and wide well system at  $\nu = 2N + 2$ . In these cases we start with Eqs. (46) and (49) respectively, and use Eq. (50) and

$$\psi'_k = \psi_0'^* + 4\Delta' \cos(k\tilde{q}'l_0^2), \quad (55)$$

and expand the HF energy for small  $\Delta$  and  $\Delta'$ :

$$E_{\text{stripe}}^{\text{HF}}(\tilde{q}, \tilde{q}') = E_{\text{nonstripe}}^{\text{HF}}(\psi_0^*, \psi_0'^*, \vec{Q}_\perp^*, \vec{Q}'_\perp) + [\Delta, \Delta'] \cdot \mathbf{E}_{\text{pert}}^{\text{HF}}(\tilde{q}, \tilde{q}') \cdot \begin{bmatrix} \Delta \\ \Delta' \end{bmatrix} + \mathcal{O}(\Delta^4), \quad (56)$$

where  $\mathbf{E}_{\text{pert}}^{\text{HF}}(\tilde{q}, \tilde{q}')$  is a  $2 \times 2$  matrix (we have suppressed all other fixed parameters,  $\psi_0^*$ , etc. for notational simplicity). Therefore if the lowest eigenvalue of  $\mathbf{E}_{\text{pert}}^{\text{HF}}(\tilde{q}, \tilde{q}')$  is negative and located at finite  $(\tilde{q}^*, \tilde{q}'^*)$ , we can obtain a stripe phase

with total HF energy lower than the uniform coherent phases. On the other hand, if both eigenvalues of  $\mathbf{E}_{pert}^{HF}(\tilde{q}, \tilde{q}')$  are positive for the whole range of  $(\tilde{q}, \tilde{q}')$  or its minimum value is at  $(\tilde{q}, \tilde{q}') = (0, 0)$ , then we conclude that no stripe phase should arise via a second order phase transition. Once again we emphasize that, in general, it is possible that stripe phases at large value of  $\Delta$  are more favorable, for which the lowest order expansion in Eqs. (51)-(53) is not sufficient. But this would correspond to the first order transition to the stripe phase, and we do not have a better method to study its existence except for a direct numerical variational calculation (Appendix E).

#### IV. WIDE WELL SYSTEMS AT $\nu = 2N + 1$

In this section we calculate the Hartree-Fock variational energy obtained by the trial wavefunction of Eq. (36), and show the numerical results for a wide well system at odd filling factors,  $\nu = 2N + 1$ . As mentioned earlier, there are two classes of level coherence in a wide well system (see Fig. 1): one is for the intersubband level crossing at smaller  $B_{\parallel}$  (denoted by  $W1$ ), and the other one is the intrasubband “level near degeneracy” at larger  $B_{\parallel}$  region (denoted by  $W1'$ ). By “level near degeneracy”, we mean a small (but non-zero) gap between energy levels of noninteracting electrons, which is much smaller than the Coulomb interaction energy. This is not a true level crossing (which would imply a zero gap rather than a “small” gap), but as we will show below, it is sufficient for interlevel hybridization leading to non-trivial many-body ground states. For simplicity, we assume that the lowest  $2N$  levels do not have any interlayer coherence while the spin polarized top level is allowed to have interlevel coherence with the lowest empty level of the same spin polarization. In Figs. 2(a) and (b) we show the corresponding quantum numbers for the relevant Landau levels of these two kinds of level coherence we consider in this section: in the small  $B_{\parallel}$  region, we consider the intersubband level crossing between  $\vec{n}_1 = (1, 0)$  and  $\vec{n}_2 = (0, N)$ , and in the large  $B_{\parallel}$  region, we consider the level near degeneracy between  $\vec{n}_1 = (0, N)$  and  $\vec{n}_2 = (0, N + 1)$ . We note that this two level approximation is easily justified energetically in the  $W1$  case, where a level crossing always ensures the noninteracting energy gap between the two crossing levels is smaller than their energy separation with other levels. It is, however, less justifiable for the  $W1'$  case, where the finite gap between the two coherent levels is just numerically smaller than their energy separation from other lower filled or higher empty levels. For simplicity, in this paper we will restrict our analysis in the  $W1'$  case (intrasubband level near degeneracy) to  $N = 0$  ( $\nu = 1$ ) only, and speculate that the results for other odd filling factors ( $N \geq 1$ ) should be qualitatively similar. Note that in Fig. 1 there are more level crossings in the small  $B_{\parallel}$  region, e.g. crossing between  $(1, 1)$  and  $(0, 3)$ , and also more crossing in the large  $B_{\parallel}$  region (not shown in the figure), e.g. the between  $(0, N - 1)$  (spin down) and  $(0, N + 2)$  (spin up). For the sake of brevity, we will not discuss these additional level crossings in this paper. We believe the level crossings or level near degeneracy situations we consider in this paper are the most typical realistic ones for a wide well system, and the results for other level crossing situations should not be qualitatively different from the ones we discuss in this paper.

We use the trial state proposed in Eq. (36), and obtain the following expectation values:

$$\begin{aligned} & \langle \Psi_G^{W1} | c_{\vec{m}_1, s_1, k_1}^{W, \dagger} c_{\vec{m}_2, s_2, k_2}^W | \Psi_G^{W1} \rangle \\ &= \delta_{s_1, s_2} \delta_{k_1, k_2} \delta_{\vec{m}_1, \vec{m}_2} [\cos^2(\psi_{k_1+Q_y/2}/2) \delta_{\vec{m}_1, \vec{n}_1} \delta_{s_1, 1/2} + \sin^2(\psi_{k_1-Q_y/2}/2) \delta_{\vec{m}_1, \vec{n}_2} \delta_{s_1, -1/2} + \delta_{m_1, 0} \theta(N - m'_1)] \\ & \quad + \delta_{s_1, s_2} \delta_{s_1, 1/2} \delta_{k_1, k_2 - Q_y} \delta_{\vec{m}_1, \vec{n}_1} \delta_{\vec{m}_2, \vec{n}_2} e^{-iQ_x(k_2 - Q_y/2)l_0^2} \sin(\psi_{k_2-Q_y/2}/2) \cos(\psi_{k_2-Q_y/2}/2) e^{-i\gamma} \\ & \quad + \delta_{s_1, s_2} \delta_{s_1, 1/2} \delta_{k_2, k_1 - Q_y} \delta_{\vec{m}_1, \vec{n}_2} \delta_{\vec{m}_2, \vec{n}_1} e^{iQ_x(k_1 - Q_y/2)l_0^2} \sin(\psi_{k_1-Q_y/2}/2) \cos(\psi_{k_1-Q_y/2}/2) e^{i\gamma}, \end{aligned} \quad (57)$$

where  $\vec{m}_i = (m_i, m'_i)$  ( $i = 1, 2$ ), and  $\theta(x)$  is the Heaviside step function ( $= 1$  if  $x > 0$  and  $= 0$  otherwise).

#### A. Hartree-Fock variational energy

Using Eq. (57) we can calculate the single electron noninteracting energy from the noninteracting Hamiltonian of Eq. (6):

$$E_0^{W1} = E_{\vec{n}_1, \uparrow}^{0, W} \Theta_1(0) + E_{\vec{n}_2, \uparrow}^{0, W} \Theta_2(0) + \sum'_{\vec{m}, s} E_{\vec{m}, s}^{0, W}, \quad (58)$$

where  $\sum'$  means a summation over the core state. The Hartree (direct) energy per electron can also be obtained from the direct term of Eq. (8):

$$\begin{aligned}
E_H^{W1} &= \frac{N_\phi}{2\Omega_\perp} \sum_{q_n} \left\{ \tilde{V}_{\vec{n}_1\vec{n}_1, \vec{n}_1\vec{n}_1}^W(q_n, 0) \Theta_1(q_n)^2 + \tilde{V}_{\vec{n}_2\vec{n}_2, \vec{n}_2\vec{n}_2}^W(q_n, 0) \Theta_2(q_n)^2 + 2\tilde{V}_{\vec{n}_1\vec{n}_1, \vec{n}_2\vec{n}_2}^W(q_n, 0) \cos(q_n Q_y l_0^2) \Theta_1(q_n) \Theta_2(q_n) \right. \\
&\quad \left. + 4 \sum_{\vec{m}}' \left[ \tilde{V}_{\vec{n}_1\vec{n}_1, \vec{m}\vec{m}}^W(0, 0) \Theta_1(0) + \tilde{V}_{\vec{n}_2\vec{n}_2, \vec{m}\vec{m}}^W(0, 0) \Theta_2(0) \right] \right\} + \frac{2N_\phi}{2\Omega_\perp} \sum_{q_n} \tilde{V}_{\vec{n}_2\vec{n}_1, \vec{n}_1\vec{n}_2}^W(q_n, Q_y) \Theta_3(q_n - Q_x)^2 \\
&\quad + \delta_{Q_y, 0} \frac{2N_\phi}{2\Omega_\perp} \sum_{q_n} \operatorname{Re} \left[ \tilde{V}_{\vec{n}_1\vec{n}_2, \vec{n}_1\vec{n}_2}^W(q_n, 0) e^{i2\gamma} \right] \Theta_3(q_n - Q_x) \Theta_3(q_n + Q_x) \\
&\quad + \frac{4N_\phi \delta_{Q_y, 0}}{2\Omega_\perp} \sum_{q_n} \left\{ \operatorname{Re} \left[ \tilde{V}_{\vec{n}_1\vec{n}_2, \vec{n}_1\vec{n}_1}^W(q_n, 0) e^{i\gamma} \right] \Theta_3(q_n + Q_x) \Theta_1(q_n) + \operatorname{Re} \left[ \tilde{V}_{\vec{n}_1\vec{n}_2, \vec{n}_2\vec{n}_2}^W(q_n, 0) e^{i\gamma} \right] \Theta_3(q_n + Q_x) \Theta_2(q_n) \right\} \\
&= \frac{1}{2} \sum_{q_n} \left\{ E_{H1}^{W1}(q_n, 0) \Theta_1(q_n)^2 + E_{H2}^{W1}(q_n, 0) \Theta_2(q_n)^2 + 2E_{H3}^{W1}(q_n, 0; Q_y) \Theta_1(q_n) \Theta_2(q_n) \right\} \\
&\quad + 2 \left[ E_{H4}^{W1}(0, 0) \Theta_1(0) + E_{H5}^{W1}(0, 0) \Theta_2(0) \right] + \sum_{q_n} E_{H6}^{W1}(q_n, Q_y) \Theta_3(q_n - Q_x)^2 \\
&\quad + \delta_{Q_y, 0} \sum_{q_n} \mathcal{E}_H^{W1}(q_n, 0; 2\gamma) \Theta_3(q_n - Q_x) \Theta_3(q_n + Q_x) \\
&\quad + 2\delta_{Q_y, 0} \sum_{q_n} \left\{ \tilde{E}_{H1}^{W1}(q_n, 0; \gamma) \Theta_3(q_n + Q_x) \Theta_1(q_n) + \tilde{E}_{H2}^{W1}(q_n, 0; \gamma) \Theta_3(q_n + Q_x) \Theta_2(q_n) \right\}, \tag{59}
\end{aligned}$$

where in the last equation we have introduced  $E_{Hi}^{W1}$  ( $i = 1 \dots 6$ ),  $\mathcal{E}_H^{W1}$  and  $\tilde{E}_{Hj}^{W1}$  ( $j = 1, 2$ ) to label the Hartree energies contributed by each corresponding term for the convenience of later discussion. Their definition is obvious from Eq. (59). Here  $q_n = 2\pi n/a$  is the stripe wavevector with  $a$  being the period of the stripe. Note that there are three kinds of Hartree energies shown in Eq. (59): (i) the term  $E_{Hi}^{W1}$  ( $i = 1 \dots 6$ ), which have no explicit phase ( $\gamma$ ) dependence, are finite for all value of  $\vec{Q}_\perp$  in general; (ii) the term  $\mathcal{E}_H^{W1}$ , which has explicit  $e^{i2\gamma}$  dependence, is nonzero only when  $Q_y = 0$ ; (iii) the terms  $\tilde{E}_{Hj}^{W1}$  ( $j = 1, 2$ ), which have explicit  $e^{i\gamma}$  dependence, are nonzero only when  $Q_y = 0$  and for finite stripe order (when considering nonstripe phase,  $q_n = 0$ ,  $\tilde{V}_{\vec{n}_1\vec{n}_2, \vec{m}\vec{m}}^W(0, 0) = 0$ ). Since our explicitly numerical results show that the third kind of contribution ( $\tilde{E}_{Hj}^{W1}$ ) is always zero in the ground states we obtain near the level degeneracy region, we will neglect them throughout in our discussion. Comparing the  $E_{Hi}^{W1}$  ( $i = 1 \dots 6$ ) terms with the  $\mathcal{E}_H^{W1}$  term, we find that their distinction arises from the fundamental difference of the ordered phases at finite  $\vec{Q}_\perp$  and at  $\vec{Q}_\perp = 0$  when no stripe order is present (note that when  $\psi_k$  is a constant,  $\Theta_i(q_n) = \delta_{q_n, 0} \Theta_i(0)$  and  $\Theta_i(q_n \pm Q_x) = \delta_{q_n, \mp Q_x} \Theta_i(0)$  so that  $\mathcal{E}_H^{W1}$  term is proportional to  $\delta_{Q_y, 0} \delta_{Q_x, 0}$ ). For  $\vec{Q}_\perp$  finite, the state breaks translational symmetry and the invariance of energy with respect to  $\gamma$  reflects a freedom of choice of the origin (see Eq. (44) and the discussion in Section III A 3). It also signals the presence of a gapless Goldstone mode coming from the spontaneously broken continuous (translational) symmetry. On the other hand, for  $\vec{Q}_\perp = 0$ , the many-body state breaks only the discrete parity symmetry (see Eq. (43)). As a result there is an explicit dependence of energy on  $e^{i2\gamma}$  with  $\gamma = 0, \pi$  being the two degenerate minima (see also the discussion below and in Section VIII D). The ground state selects either  $\gamma = 0$  or  $\pi$  via the Ising type transition, which describes the breaking of parity symmetry. No Goldstone mode exists in this case since the broken symmetry is discrete (i.e. Ising type).

As for the Fock (exchange) energy per electron, we can have

$$\begin{aligned}
E_F^{W1} &= \frac{-1}{2\Omega_\perp} \sum_{\vec{q}_\perp} \left\{ \tilde{V}_{\vec{n}_1\vec{n}_1, \vec{n}_1\vec{n}_1}^W(\vec{q}) \sum_{q_n} \cos(q_n q_y l_0^2) \Theta_1(q_n)^2 + \tilde{V}_{\vec{n}_2\vec{n}_2, \vec{n}_2\vec{n}_2}^W(\vec{q}) \sum_{q_n} \cos(q_n q_y l_0^2) \Theta_2(q_n)^2 \right. \\
&\quad \left. + 2\tilde{V}_{\vec{n}_1\vec{n}_2, \vec{n}_2\vec{n}_1}^W(\vec{q}) \sum_{q_n} \cos(q_n (q_y + Q_y) l_0^2) \Theta_1(q_n) \Theta_2(q_n) \right. \\
&\quad \left. + 2 \sum_{\vec{m}}' \left[ \tilde{V}_{\vec{n}_1, \vec{m}, \vec{m}\vec{n}_1}^W(\vec{q}) \Theta_1(0) + \tilde{V}_{\vec{n}_2, \vec{m}, \vec{m}\vec{n}_2}^W(\vec{q}) \Theta_2(0) \right] \right\} \\
&\quad + 2\tilde{V}_{\vec{n}_1\vec{n}_1, \vec{n}_2\vec{n}_2}^W(\vec{q}) \cos((q_x Q_y - q_y Q_x) l_0^2) \sum_{q_n} \cos(q_n q_y l_0^2) \Theta_3(q_n)^2 \\
&\quad + 2\delta_{Q_y, 0} \operatorname{Re} \left[ \tilde{V}_{\vec{n}_1\vec{n}_2, \vec{n}_1\vec{n}_2}^W(\vec{q}) e^{i2\gamma} \right] \sum_{q_n} \cos(q_n q_y l_0^2) \Theta_3(q_n - Q_x) \Theta_3(q_n + Q_x)
\end{aligned}$$

$$\begin{aligned}
& + 4\delta_{Q_y,0} \left[ \sum_{q_n} \text{Re}[e^{-ip_n q_y l_0^2} \tilde{V}_{\vec{n}_1 \vec{n}_2, \vec{n}_1 \vec{n}_1}^W(\vec{q}_\perp) e^{i\gamma}] \Theta_1(q_n) \Theta_3(q_n + Q_x) \right. \\
& \quad \left. + \sum_{p_n} \text{Re}[e^{-ip_n q_y l_0^2} \tilde{V}_{\vec{n}_2 \vec{n}_2, \vec{n}_1 \vec{n}_2}^W(\vec{q}_\perp) e^{i\gamma}] \Theta_2(q_n) \Theta_3(q_n + Q_x) \right] \\
& = \frac{1}{2} \sum_{q_n} \{ E_{F1}^{W1}(q_n, 0) \Theta_1(q_n)^2 + E_{F2}^{W1}(q_n, 0) \Theta_2(q_n)^2 + 2E_{F3}^{W1}(q_n, 0; Q_y) \Theta_1(q_n) \Theta_2(q_n) \} \\
& \quad + [E_{F4}^{W1}(0, 0) \Theta_1(0) + E_{F5}^{W1}(0, 0) \Theta_2(0)] + \sum_{q_n} E_{F6}^{W1}(q_n, 0; Q_x, Q_y) \Theta_3(q_n)^2 \\
& \quad + \delta_{Q_y,0} \sum_{q_n} \mathcal{E}_F^{W1}(q_n, 0; 2\gamma) \Theta_3(q_n - Q_x) \Theta_3(q_n + Q_x) \\
& \quad + 2\delta_{Q_y,0} \sum_{q_n} \{ \tilde{E}_{F1}^{W1}(q_n, 0; \gamma) \Theta_3(q_n + Q_x) \Theta_1(q_n) + \tilde{E}_{F2}^{W1}(q_n, 0; \gamma) \Theta_3(q_n + Q_x) \Theta_2(q_n) \} \tag{60}
\end{aligned}$$

where  $E_{Fi}^{W1}$  ( $i = 1 \dots 6$ ),  $\mathcal{E}_F^{W1}$ , and  $\tilde{E}_{Fj}^{W1}$  ( $j = 1, 2$ ) are introduced to label each contribution of the exchange energy. The dependence of these exchange terms on the phase  $\gamma$  associated with possible broken symmetry behavior is the same as discussed earlier for the corresponding Hartree energy terms.

We think that it is worthwhile to emphasize again that Eqs. (59) and (60) are based on a specific choice of the Landau gauge for the vector potential,  $\vec{A}_{[y]}(\vec{r})$ , in which the particle momentum is conserved along  $y$  axis (perpendicular to the in-plane magnetic field). To obtain the HF variational energy for a stripe phase along  $x$  direction, we can choose the alternate gauge,  $\vec{A}_{[x]}(\vec{r})$ , in which particle momentum is conserved along  $x$  direction, to construct a many-body wavefunction similar to Eq. (36) (see details in Appendix A). If no stripe phase is stabilized, the results obtained in these two gauges are identical. To save space, we will not show the HF variational energy obtained in the second gauge throughout this paper, although we take it into consideration in our numerical calculations.

## B. Magnetoplasmon excitations

Before showing the results of minimizing the HF energy, it is instructive to address the close relationship between the HF variational energy shown in Eqs. (58)-(60) and the collective magnetoplasmon excitations of the conventional incompressible quantum Hall states (i.e. the isospin polarized states). In an integer quantum Hall system, magnetoplasmons are collective modes associated with magneto-exciton excitations above the Fermi energy that can be theoretically studied by using the generalized Hartree-Fock (or time-dependent Hartree-Fock) approximation [48,17,33], which is correct to the leading order of the ratio of the electron interaction energy to the noninteracting Landau energy separation. The softening of the magnetoplasmon mode indicates that the system may undergo a second order phase transition from a usual isospin polarized state (i.e. the uniform quantum Hall state) to a new symmetry-broken ground state, which is precisely the same as that obtained by minimizing the variational HF energy shown in Eqs. (58)-(60). Moreover, the full analytical expression of the magnetoplasmon dispersion can be obtained from the uniform variational HF energy (i.e. same as Eqs. (58)-(60) but considering  $\psi_k = \psi_0$  or equivalently  $\Theta_i(q_n) = \Theta_i(0)\delta_{q_n,0}$ ) by taking small  $|\psi_0|$  expansion from the isospin up ground state or by taking small  $|\pi - \psi_0|$  expansion from the isospin down ground state. For example, if we consider the  $W1$  case with isospin up state ( $\vec{n}_1 = (1, 0)$ ) being the highest filled level, the HF energy of Eqs. (58)-(60) can be expanded to the leading order of  $\Theta_2(0)$  (i.e. small  $\psi_0$ ) to obtain (using  $\Theta_3(0)^2 = \Theta_1(0)\Theta_2(0)$ ) the following total HF energy:

$$E_{HF}^{W1}(\psi_0) = E_{\vec{n}_1, \uparrow}^{W1} + E_{\vec{n}_1 \vec{n}_2}^{pl, W1}(\vec{Q}_\perp) \Theta_2(0) + \delta_{Q_x,0} \delta_{Q_y,0} \mathcal{E}_{\vec{n}_1 \vec{n}_2}^{a, W1}(\gamma) \Theta_2(0) + \mathcal{O}(\Theta_2(0)^2), \tag{61}$$

where the first term is the total electron energy of the isospin up state (the ground state), including the HF self-energy correction, the second term is the plasmon dispersion shown below, and the third one is the additional point energy shift associated with the broken parity symmetry. More explicitly we have

$$E_{\vec{n}_1, s}^{W1} = E_{\vec{n}_1, s}^{0, W} + \frac{1}{2} [E_{H1}^{W1}(0, 0) + E_{F1}^{W1}(0, 0)] + E_{H4}^{W1}(0, 0) + E_{F4}^{W1}(0, 0), \tag{62}$$

where the first term is the noninteracting energy, the second term is the self-energy produced by electrons within the top level ( $\frac{1}{2}$  is for double counting), and the third term is the self-energy produced by electrons in the core state (see

the definition of  $E_{H(F)i}^{W1}(0,0)$  in Eqs. (59) and (60)). The magnetoplasmon excitation energy in the right hand side of Eq. (61) gives

$$E_{\vec{n}_1 \vec{n}_2}^{pl,W1}(\vec{Q}_\perp) = E_{\vec{n}_2,\uparrow}^{0,W} - E_{\vec{n}_1,\uparrow}^{0,W} + \Sigma_{\vec{n}_2,\uparrow}^{W1} - \Sigma_{\vec{n}_1,\uparrow}^{W1} + E_{H6}^{W1}(Q_x, Q_y) + E_{F6}^{W1}(0,0; Q_x, Q_y), \quad (63)$$

where  $\Sigma_{\vec{n},s}^{W1}$  is the Hartree-Fock self-energy of level  $\vec{n}$  and spin  $s$ . Eq. (63) is exactly the same as the magnetoplasmon excitation energy of the incompressible (isospin up) quantum Hall state obtained directly from the time-dependent Hartree-Fock approximation (TDHFA) [17]. The contributions from the bubble diagrams (the direct term) and from the ladder diagrams (the exchange term) correspond to the last two terms of Eq. (63) respectively. Note that the energy of the  $\vec{Q}_\perp = 0$  point is disconnected from the rest of the spectrum due to the last term in Eq. (61),  $\mathcal{E}_{\vec{n}_1 \vec{n}_2}^{a,W1}(\gamma) = \mathcal{E}_H^{W1}(0,0;\gamma) + \mathcal{E}_F^{W1}(0,0;\gamma) < 0$ . This reflects the fact that a many-body state at  $\vec{Q}_\perp = 0$  breaks only a discrete symmetry and should not have Goldstone modes. Alternatively continuous dispersion for  $\vec{Q}_\perp \neq 0$  would break the continuous translational symmetry and lead to Goldstone modes. The plasmon dispersion obtained are based on the uniform integer quantum Hall state, or equivalently, the isospin polarized ground state, therefore Eq. (63) has to be changed if we want to study the dispersion of the collective modes *inside* the symmetry-broken ground state. We mention that such a complete equivalence between the Hartree-Fock ground state energetic calculation and the corresponding collective mode dispersion follows from the Ward identities, and has also been used extensively in Ref. [33] in discussing the canted anti-ferromagnetic state in bilayer systems.

### C. Results I: intersubband level crossing ( $W1$ case)

In Fig. 7(a) we first show the energy dispersion of the magnetoplasmon mode (in charge channel only) obtained from Eq. (63) for  $\nu = 5$ , near the intersubband level crossing point at  $B_{\parallel}^* \sim 2.33$  Tesla (after including the self-energy correction) for realistic GaAs 2D systems. We also use a filled circle to denote the excitation energy at  $\vec{q}_\perp = 0$ , that are disconnected from the rest of the spectrum by a negative energy shift,  $\mathcal{E}_{\vec{n}_1 \vec{n}_2}^{a,W1}$ , according to Eq. (63). In the system parameter range we consider here ( $B_{\perp} = 3$  T and the bare confinement energy,  $\omega_0$ , is 7 meV), this disconnected energy shift is very small ( $< 0.01$  meV). When the in-plane magnetic field is above  $B_{\parallel}^* = 2.25$  Tesla, the magnetoplasmon mode is softened at  $\vec{q}_\perp = 0$ , indicating a second order phase transition toward a many-body coherent state breaking the parity symmetry. Strictly speaking, only the disconnected point at  $\vec{q}_\perp = 0$  is softened at  $B_{\parallel}^*$ , and the whole collective mode dispersion will be modified for  $B_{\parallel} > B_{\parallel}^*$  inside the new symmetry-broken phase.

In Fig. 7(b), we show the HF energy calculated from Eqs. (58)-(60) around the intersubband level crossing point. We find an isospin coherent phase ( $\psi_k = \psi_0^* \neq 0, \pi$  with no spiral order ( $\vec{Q}_\perp^* = 0$ ) and no stripe order) in addition to the isospin polarized quantum Hall states within a small range of the in-plane magnetic field ( $2.25 < B_{\parallel} < 2.40$  T) for the chosen system parameters. According to the symmetry analysis discussed in Section III A 3, the coherent phase only breaks the parity symmetry of the system and therefore has no Goldstone mode. This is consistent with the result studied by the mode softening of the collective excitations shown in Fig. 7(a).

We note that the new coherent phase, breaking the discrete parity symmetry, is similar to the ferroelectric state observed in ferroelectric crystals [42]. More precisely, the electric dipole moment,  $\langle \vec{r} \rangle$ , is obviously zero if the ground state has a definite parity, while it can be nonzero if the ground state mixes two states of different parities. Therefore we think the simple coherent state we find above in the intersubband level crossing region of odd filling systems is a “ferroelectric” quantum Hall state with finite electric dipole moment. The recent experiments observing anomalies in the Shubnikov-de Haas oscillations of a wide parabolic well in the presence of a tilted magnetic field may be due to the existence of such coherent states [50], but more definite experimental work would be needed to settle this point.

### D. Results II: intrasubband level near degeneracy ( $W1'$ case)

In Fig. 8 we show a typical magnetoplasmon mode dispersion in the charge channel of a wide well at  $\nu = 1$  in the large  $B_{\parallel}$  region near the intrasubband level near degeneracy point, where the interaction energy is of the same order as the noninteracting energy separation. (Note that the bare confinement energy  $\omega_0$  is 3 meV here.) When  $B_{\parallel}$  is larger than 30 Tesla, we find a mode softening at a finite wavevector perpendicular to the in-plane magnetic field (i.e. along  $y$  axis). In the same figure, we use filled squares, triangles, and circles to denote the energies of the zero momentum excitation, which is different from the long wavelength limit of the plasmon curve by an energy  $|\mathcal{E}_{(0,0),(0,1)}^{a,W1}(0)| \sim 0.25$  meV (see Eq. (61)). In sharp contrast to the  $W1$  case shown in Fig. 7(a), the collective mode

softening occurs here at a finite wavevector,  $\vec{Q}_\perp = (0, \pm Q_y^*)$  rather than at  $\vec{Q}_\perp = 0$ , showing an isospin spiral order in this system. Therefore the ground state can be a spiral phase if only one of the ordering wavevectors,  $(0, \pm Q_y^*)$ , is present, or it can be a collinear spin density wave if there is an ordering at *both* wavevectors with equal amplitude. We have not been able to write a wavefunction for such a collinear phase to compare its energy with the spiral phase, and therefore we cannot rule out the possibility that a collinear phase can also be a ground state in the  $W1'$  case.

Now we have to investigate if such uniform coherent isospin spiral phase is stable against the formation of a stripe phase. We use the perturbation method developed in Section III C and calculate the perturbative energy  $E_{pert}^{HF}(q)$ . In Fig. 9 we show our numerical results for  $E_{pert}^{HF}(q)$  as a function of  $q$  for several different values of  $B_\parallel$ . Both gauges of the vector potential,  $\vec{A}_{[x]}(\vec{r})$  and  $\vec{A}_{[y]}(\vec{r})$ , are considered in calculating  $E_{pert}^{HF}(q)$  as indicated in the figure caption. When  $B_\parallel$  is larger than a critical value (it is also about 30 Tesla in this situation), the minimum of  $E_{pert}^{HF}(q)$  is located at a finite wavevector ( $q^* \sim 0.3 \times 10^6 \text{ cm}^{-1}$ ) along  $x$  axis, showing a stripe order with isospin  $I_z$  modulating in the  $x$  direction with a period  $2\pi/q^* \sim 2000 \text{ \AA}$ . Therefore, combining the two results above, we conclude that an isospin skyrmion stripe phase (see Section III A) can be stabilized, with the stripe normal vector along  $x$  direction and the spiral winding vector along  $y$  direction. In our numerical calculation, we do not see signature for any intermediate phase (e.g. isospin spiral phase without stripe order) between the isospin polarized (incompressible) quantum Hall state and the isospin skyrmion stripe phase — the local minimum of  $E_{pert}$  occurs at finite wavevector simultaneously with the plasmon mode softening. Therefore, following the results of Section III A 3, the spiral order breaks the translational symmetry along  $y$  direction, while the stripe order breaks the translational symmetry in  $x$  direction (parallel to the in-plane field). As discussed in our earlier paper [8], such skyrmion stripe has finite topological isospin density that leads to charge stripe order with stripes perpendicular to the in-plane field. This should lead to anisotropy in charge transport with larger conductivity along the stripes, i.e. perpendicular to  $B_\parallel$ .

In Fig. 10 we show the phase diagram of the wide well system at  $\nu = 1$  in a strong in-plane field. The usual incompressible integer quantum Hall state is favored at small well width (large bare confinement energy) and/or small  $B_\parallel$  values. At larger well width and/or stronger  $B_\parallel$  field, the system undergoes a second order phase transition toward an isospin skyrmion stripe phase with translational symmetries broken in both  $x$  and  $y$  directions (parity symmetry is of course also broken). In extremely large  $B_\parallel$  and large well width, we expect the isospin skyrmion stripe phase to evolve toward the Wigner crystal phase, which, however, is not included in our present theory.

## V. SINGLE WIDE WELL SYSTEM AT $\nu = 2N + 2$

For a wide well system at even filling factor,  $\nu = 2N + 2$ , we also consider two kinds of level crossings (see Figs. 1, 2(c) and (d)) : one is the intersubband level crossing between levels  $((1, 0), \downarrow (\uparrow))$  and  $((0, N), \uparrow (\downarrow))$  in the small  $B_\parallel$  region ( $W2$ ), and the other is the intrasubband level crossing between levels  $((0, N), \downarrow)$  and  $((0, N + 1), \uparrow)$  in the large  $B_\parallel$  region ( $W2'$ ). For simplicity, we do not discuss the system behavior at yet higher fields, for example, when there is a crossing between levels  $((0, N - 1), \downarrow)$  and  $((0, N + 2), \uparrow)$ . The main difference between a level crossing in an odd filling system and the one in an even filling system is the spin degree of freedom. In the odd filling situation, the two crossing levels are of the same spin so that only isospin degree of freedom affects the existence of a novel coherent phase via their different orbital wavefunctions (and the spin degree of freedom is essentially frozen). In even filling situation, however, the two crossing levels are of opposite spin polarization, so that a stabilized many-body coherent phase must also break the spin rotational symmetry. This fact leads important consequences, since spin and isospin are not equivalent in their roles: the Coulomb interaction does not flip spin polarization but may flip the isospin polarization of each scattered electron (see Fig. 5(b)). We will discuss this subject in more details in Section VIII B.

As shown in Section III B 2, when discussing possible many-body states around level crossings at  $\nu = 2N + 2$ , we will consider trial wavefunctions that mix the four closest levels around the Fermi energy, the two highest filled Landau levels and two lowest empty Landau levels, and will assume that the lower  $2N$  (core) levels are completely filled (frozen) and do not participate in the coherent hybridization process. Using Eq. (49), we obtain the following expectation value similar to Eq. (57):

$$\begin{aligned} & \langle \Psi_G^{W2} | c_{\vec{m}_1, \sigma_1, k_1}^{W, \dagger} c_{\vec{m}_2, \sigma_2, k_2}^W | \Psi_G^{W2} \rangle \\ &= \delta_{\vec{m}_1, \vec{m}_2} \delta_{\sigma_1, \sigma_2} \delta_{k_1, k_2} [\cos^2(\psi_{k+Q_y/2}/2) \delta_{\vec{m}_1, \vec{n}_1} \delta_{\sigma_1, -1/2} + \sin^2(\psi_{k-Q_y/2}/2) \delta_{\vec{m}_1, \vec{n}_2} \delta_{\sigma_1, 1/2} \\ & \quad + \cos^2(\psi'_{k+Q'_y/2}/2) \delta_{\vec{m}_1, \vec{n}_1} \delta_{\sigma_1, 1/2} + \sin^2(\psi'_{k-Q'_y/2}/2) \delta_{\vec{m}_1, \vec{n}_2} \delta_{\sigma_1, -1/2} + \delta_{m_1, 0} \theta(N - m'_1)] \\ & \quad + \delta_{\vec{m}_1, \vec{n}_1} \delta_{\vec{m}_2, \vec{n}_2} \delta_{\sigma_1, -1/2} \delta_{\sigma_2, 1/2} \delta_{k_1, k_2 - Q_y} e^{-iQ_x(k_2 - Q_y/2)l_0^2} \sin(\psi_{k_2 - Q_y/2}/2) \cos(\psi_{k_2 - Q_y/2}/2) e^{-i\gamma/2} \\ & \quad + \delta_{\vec{m}_1, \vec{n}_2} \delta_{\vec{m}_2, \vec{n}_1} \delta_{\sigma_1, 1/2} \delta_{\sigma_2, -1/2} \delta_{k_2, k_1 - Q_y} e^{iQ_x(k_1 - Q_y/2)l_0^2} \sin(\psi_{k_1 - Q_y/2}/2) \cos(\psi_{k_1 - Q_y/2}/2) e^{i\gamma/2} \end{aligned}$$

$$\begin{aligned}
& + \delta_{\vec{m}_1, \vec{n}_1} \delta_{\vec{m}_2, \vec{n}_2} \delta_{\sigma_1, 1/2} \delta_{\sigma_2, -1/2} \delta_{k_1, k_2 - Q'_y} e^{-iQ'_x(k_2 - Q'_y/2)l_0^2} \sin(\psi'_{k_2 - Q'_y/2}/2) \cos(\psi'_{k_2 - Q'_y/2}/2) e^{-i\gamma'/2} \\
& + \delta_{\vec{m}_1, \vec{n}_2} \delta_{\vec{m}_2, \vec{n}_1} \delta_{\sigma_1, -1/2} \delta_{\sigma_2, 1/2} \delta_{k_2, k_1 - Q'_y} e^{iQ'_x(k_1 - Q'_y/2)l_0^2} \sin(\psi'_{k_1 - Q'_y/2}/2) \cos(\psi'_{k_1 - Q'_y/2}/2) e^{i\gamma'/2},
\end{aligned} \tag{64}$$

where  $\vec{n}_1 = (1, 0)$  and  $\vec{n}_2 = (0, N)$  for  $W2$  case, while  $\vec{n}_1 = (0, N)$  and  $\vec{n}_2 = (0, N+1)$  for  $W2'$  case.

### A. Hartree-Fock variational energy

The noninteracting single electron energy can be obtained from Eq. (11):

$$E_0^{W2} = E_{\vec{n}_1, \downarrow}^{0,W} \Theta_1(0) + E_{\vec{n}_2, \uparrow}^{0,W} \Theta_2(0) + E_{\vec{n}_1, \uparrow}^{0,W} \Theta'_1(0) + E_{\vec{n}_2, \downarrow}^{0,W} \Theta'_2(0) + \sum_{l, \sigma} {}' E_{l, \sigma}^{0,W}, \tag{65}$$

where the last term is a constant energy shift from the frozen core states. The Hartree (direct) and the Fock (exchange) energies per electron are respectively

$$\begin{aligned}
E_H^{W2} = & \frac{N_\phi}{2\Omega_\perp} \sum_{q_n} \left\{ \tilde{V}_{\vec{n}_1 \vec{n}_1, \vec{n}_1 \vec{n}_1}^W(q_n) [\Theta_1(q_n)^2 + \Theta'_1(q_n)^2] + \tilde{V}_{\vec{n}_2 \vec{n}_2, \vec{n}_2 \vec{n}_2}^W(q_n) [\Theta_2(q_n)^2 + \Theta'_2(q_n)^2] \right. \\
& + 2\tilde{V}_{\vec{n}_1 \vec{n}_1, \vec{n}_2 \vec{n}_2}^W(q_n) [\Theta_1(q_n)\Theta_2(q_n) \cos(q_n Q_y l_0^2) + \Theta'_1(q_n)\Theta'_2(q_n) \cos(q_n Q'_y l_0^2)] \\
& + 2\tilde{V}_{\vec{n}_1 \vec{n}_1, \vec{n}_1 \vec{n}_1}^W(q_n) \Theta_1(q_n)\Theta'_1(q_n) \cos(q_n(Q_y - Q'_y)l_0^2/2) \\
& + 2\tilde{V}_{\vec{n}_2 \vec{n}_2, \vec{n}_2 \vec{n}_2}^W(q_n) \Theta_2(q_n)\Theta'_2(q_n) \cos(q_n(Q_y - Q'_y)l_0^2/2) \\
& + 2\tilde{V}_{\vec{n}_1 \vec{n}_1, \vec{n}_2 \vec{n}_2}^W(q_n) [\Theta_1(q_n)\Theta'_2(q_n) + \Theta_2(q_n)\Theta'_1(q_n)] \cos(q_n(Q_y + Q'_y)l_0^2/2) \\
& \left. + 4\delta_{q_n, 0} \sum_{\vec{m}} {}' \left[ \tilde{V}_{\vec{n}_1 \vec{n}_1, \vec{m} \vec{m}}^W(0) (\Theta_1(0) + \Theta'_1(0)) + \tilde{V}_{\vec{n}_2 \vec{n}_2, \vec{m} \vec{m}}^W(0) (\Theta_2(0) + \Theta'_2(0)) + \sum_{\vec{l}} {}' \tilde{V}_{\vec{m} \vec{m}, \vec{m}' \vec{m}'}^W(0) \right] \right\}, \tag{66}
\end{aligned}$$

and

$$\begin{aligned}
E_F^{W2} = & \frac{-1}{2\Omega} \sum_{\vec{q}_\perp} \left\{ \tilde{V}_{\vec{n}_1 \vec{n}_1, \vec{n}_1 \vec{n}_1}^W(\vec{q}_\perp) \sum_{q_n} \cos(q_n q_y l_0^2) [\Theta_1(q_n)^2 + \Theta'_1(q_n)^2] + \tilde{V}_{\vec{n}_2 \vec{n}_2, \vec{n}_2 \vec{n}_2}^W(\vec{q}) \sum_{q_n} \cos(q_n q_y l_0^2) [\Theta_2(q_n)^2 + \Theta'_2(q_n)^2] \right. \\
& + 2\tilde{V}_{\vec{n}_1 \vec{n}_2, \vec{n}_2 \vec{n}_1}^W(\vec{q}_\perp) \sum_{q_n} \cos(q_n q_y l_0^2) \cos(q_n(Q_y + Q'_y)l_0^2/2) [\Theta_1(q_n)\Theta'_2(q_n) + \Theta_2(q_n)\Theta'_1(q_n)] \\
& + 2 \sum_{\vec{m}} {}' \tilde{V}_{\vec{n}_1 \vec{m}, \vec{m} \vec{n}_1}^W(\vec{q}_\perp) [\Theta_1(0) + \Theta'_1(0)] + 2 \sum_{\vec{m}} {}' \tilde{V}_{\vec{n}_2 \vec{m}, \vec{m} \vec{n}_2}^W(\vec{q}_\perp) [\Theta_2(0) + \Theta'_2(0)] + 2 \sum_{\vec{m}_1, \vec{m}_2} \tilde{V}_{\vec{m}_1 \vec{m}_2, \vec{m}_2 \vec{m}_1}^W(\vec{q}) \\
& + \frac{-2}{2\Omega_\perp} \sum_{\vec{q}_\perp} \tilde{V}_{\vec{n}_1 \vec{n}_1, \vec{n}_2 \vec{n}_2}^W(\vec{q}_\perp) \cos((Q_x q_y - Q_y q_x)l_0^2) \sum_{q_n} \cos(q_n q_y l_0^2) \Theta_3(q_n)^2 \\
& + \frac{-2}{2\Omega_\perp} \sum_{\vec{q}_\perp} \tilde{V}_{\vec{n}_1 \vec{n}_1, \vec{n}_2 \vec{n}_2}^W(\vec{q}_\perp) \cos((Q'_x q_y - Q'_y q_x)l_0^2) \sum_{q_n} \cos(q_n q_y l_0^2) \Theta'_3(q_n)^2 \\
& \left. + \frac{-4\delta_{Q_y, -Q'_y}}{2\Omega_\perp} \sum_{\vec{q}_\perp} \text{Re}[\tilde{V}_{\vec{n}_1 \vec{n}_2, \vec{n}_1 \vec{n}_2}^W(\vec{q}_\perp) e^{i(\gamma + \gamma')}] \sum_{q_n} \Theta_3(q_n - Q_x) \Theta'_3(q_n + Q'_x) \cos((q_x Q_y - q_n q_y)l_0^2) \right\}, \tag{67}
\end{aligned}$$

where the last term in the exchange energy shows the interplay between the two isospinors as mentioned in Section III B 1, and this term is nonzero only when  $\vec{Q}'_\perp = -\vec{Q}_\perp$  (for simplicity, we have chosen their stripe wavevectors,  $\tilde{q}_n$  and  $\tilde{q}'_n$ , to be the same). Note that this is also the only term which depends on the phase,  $\gamma + \gamma'$ , in the Hartree-Fock energy. This is because, in the even filling systems, the two crossing levels are of different spin polarizations. Therefore, spin symmetry breaking of the coherent state gives a continuous energy degeneracy (i.e.  $\gamma - \gamma'$  is arbitrary), while the breaking of parity symmetry selects  $\gamma + \gamma' = 2m\pi$ , where  $m$  is an integer.

## B. Magnetoplasmon excitations

Using the arguments similar to those in Section IV B, we can also obtain the magnetoplasmon excitation energy of the even filling system in the usual incompressible quantum Hall ground state by taking small  $\Theta_2(0)$  and  $\Theta'_2(0)$  limits in the above Hartree-Fock variational energy, Eqs. (65)-(67). The result is equivalent to solving the eigenvalue problem of the following  $2 \times 2$  matrix:

$$\mathbf{E}_{\vec{n}_1 \vec{n}_2}^{pl,W2}(\vec{Q}_\perp) = \begin{bmatrix} \Delta E_{\vec{n}_2 \uparrow, \vec{n}_1 \downarrow}^{0,W} + \Delta \Sigma_{\vec{n}_2 \uparrow, \vec{n}_1 \downarrow}^{HF,W2} + E_X^{W2}(\vec{Q}_\perp) & E_{X'}^{W2}(\vec{Q}_\perp) \\ \left[ E_X^{W2}(\vec{Q}_\perp) \right]^* & \Delta E_{\vec{n}_2 \downarrow, \vec{n}_1 \uparrow}^{0,W} + \Delta \Sigma_{\vec{n}_2 \downarrow, \vec{n}_1 \uparrow}^{HF,W2} + E_X^{W2}(\vec{Q}_\perp) \end{bmatrix}, \quad (68)$$

where we have used  $\vec{Q}'_\perp = -\vec{Q}_\perp$ ;  $\Delta E_{\vec{n}_2 \uparrow(\downarrow), \vec{n}_1 \downarrow(\uparrow)}^{0,W} \equiv E_{\vec{n}_2, \uparrow(\downarrow)}^{0,W} - E_{\vec{n}_1, \downarrow(\uparrow)}^{0,W}$  and  $\Delta \Sigma_{\vec{n}_2 \uparrow(\downarrow), \vec{n}_1 \downarrow(\uparrow)}^{HF,W} \equiv \Sigma_{\vec{n}_2, \uparrow(\downarrow)}^{H,W} - \Sigma_{\vec{n}_1, \downarrow(\uparrow)}^{H,W} + \Sigma_{\vec{n}_2, \uparrow(\downarrow)}^{F,W} - \Sigma_{\vec{n}_1, \downarrow(\uparrow)}^{F,W}$  are respectively the noninteracting energy and the HF self-energy difference between the two relevant levels. The definition and the explicit expression of the HF self-energies,  $\Sigma_{\vec{m},s}^{H/F,W2}$ , are similar to those in the odd filling systems. The two electron-hole (exciton) binding energies are respectively

$$E_X^{W2}(\vec{Q}_\perp) = \frac{-1}{\Omega_\perp} \sum_{\vec{q}_\perp} \tilde{V}_{\vec{n}_1 \vec{n}_2, \vec{n}_2 \vec{n}_2}^W(\vec{q}_\perp) \cos((q_x Q_y - q_y Q_x) l_0^2) \quad (69)$$

and

$$E_{X'}^{W2}(\vec{Q}_\perp) = \frac{-1}{\Omega_\perp} \sum_{\vec{q}_\perp} \tilde{V}_{\vec{n}_1 \vec{n}_2, \vec{n}_1 \vec{n}_2}^W(\vec{q}_\perp) \cos((q_x Q_y - q_y Q_x) l_0^2). \quad (70)$$

We note that Eq. (68) is exactly the same as the magnetoplasmon dispersion matrix derived for the triplet spin channel in the time-dependent-Hartree-Fock approximation [17], demonstrating that our proposed four level trial wavefunction, Eq. (49), is adequate in investigating the existence of new broken symmetry phases. On the other hand, we note that the other two spin singlet magnetoplasmon modes [17] cannot be obtained in our theory, since the trial wavefunction of Eq. (49) is still not of the most general form for the four level degeneracy. As mentioned earlier, this fact will not affect any of our results or conclusions shown in this section, because these two singlet excitations are relatively higher energy excitations and are of different symmetries from the lowest one we consider here. For the purpose of understanding quantum phase transitions in the system, it is crucial to have the correct description for the low energy sector of the relevant Hilbert space, and clearly our four level trial wavefunction of Eq. (49) accomplished that very well. Since the 2D magnetoplasmon dispersion calculation of the integer quantum Hall system has been reported before [17], we will not further discuss the magnetoplasmon dispersion and just focus on the HF variational energy calculation.

## C. Results I: intersubband level crossing ( $W2$ case)

For level crossing in the small  $B_{\parallel}$  region, our numerical calculation shows that there is *no* many-body coherent phase with total energy lower than the (uniform) isospin polarized states within our Hartree-Fock approximation. In other words, we find that such level crossing always introduces a (trivial) first order phase transition with a sharp polarization change in the narrow region of level crossing tuned by  $B_{\parallel}$  (see Fig. 1). This is related to the resistance hysteresis recently observed and discussed in Refs. [51,52] — small domain walls may occur during the first order phase transition separating the two polarizations so that the resistance shows a hysteretic behavior when the external electric field is swapt. Although such domain wall physics associated with intersubband level crossing induced first order transition is of intrinsic interest, we do not include this possibility in our theory since our interest here is to classify the (second order) quantum phase transitions between nontrivial quantum Hall phases (see a brief discussion in Section VIII E).

## D. Results II: intrasubband level crossing ( $W2'$ case)

For the level crossing at large  $B_{\parallel}$  region, only one level crossing between  $\vec{n}_1 = (0, N)$  of spin down and  $\vec{n}_2 = (0, N+1)$  of spin up occurs and the next nearest two levels do not cross in the noninteracting energy spectrum. From Eqs. (65)-(67) we find that if we fix  $\psi_k = \psi_0$  to be uniform and finite ( $0 < \psi_k < \pi$ ), the HF energy is always minimized

at a finite winding wavevector along  $y$  direction,  $\vec{Q}_\perp = \pm(0, Q_y^*)$  with  $Q_y^* \sim 0.75 l_0^{-1}$  (the magnetic field is along  $x$  axis), so the optimum state of broken spin symmetry must have a spiral or a collinear spin order (the latter happens when  $\pm\vec{Q}$  components are present simultaneously). However, in optimizing the HF energy with respect to  $\psi_0$  we find that the minimum is always at  $\psi_0 = 0$  or  $\pi$ , so states with broken spin symmetry are not favored at the HF level. In Fig. 11 we compare the HF energies of the isospin spiral, isospin spiral stripe, and isospin skyrmion stripe phases, calculated using typical realistic system parameters (for GaAs 2D systems) and by employing a more general phase function,  $\psi_k$ , as shown in Fig. 6. For the sake of comparison we fix most parameters in the phase function of  $\psi_k$  and let  $\phi = \psi_1 - \psi_2$  to be the only free parameter for the stripe phases (we have tried different ranges of these variational parameters, but the results are qualitatively similar to Fig. 11 and no exotic many-body phase is found). In the horizontal axis of Fig. 11, we define the spin polarization to be  $\Theta_2(0)$ , which is proportional to the density of spin triplet excitons excited from the top filled level to the lowest empty level. Another coherence parameter,  $\Theta'_2(0)$ , is chosen to be zero in Fig. 11 because the results do not depend qualitatively on this choice. In Fig. 11 we choose  $B_\parallel = 11$  T in the calculation, slightly lower than the level crossing point at  $B_\parallel^* = 11.1$  Tesla (note that this is the renormalized level crossing field including the HF self-energy correction and is therefore lower than the noninteracting result). We find that, within our Hartree-Fock calculation, the energy of the spiral phase is a convex curve as a function of the polarization, and therefore has *no* energy minimum between  $\Theta_2(0) = 0$  (spin unpolarized state) and  $\Theta_2(0) = 1$  (spin polarized state), i.e. either the spin unpolarized or the spin polarized state is always the lowest energy ground state, depending on whether the magnetic field is smaller or larger than  $B_\parallel^* = 11.1$  Tesla.

Note that we have chosen the spiral wavevector to be  $\vec{Q}_\perp^* = (0, Q_y^*)$ , which is the extreme value for the lowest HF energy for  $0 < \Theta_2(0) < 1$ . Unsurprisingly, we find that this  $Q_y^*$  is the same as the wavevector obtained from the near softening point of the magnetoplasmon excitations [17]. (Therefore we can exclude the simple (incommensurate) isospin coherent (stripe) phases from the energy comparison, because they do not have spiral order and must have higher energy than the three cases shown in Fig. 11.) Among the three many-body states of spiral order, we find that the spiral phase always has the lowest energy. Our HF calculation therefore suggests a first order transition between spin polarized and unpolarized ground states with no intermediate broken symmetry phases in between (at least within the HF theory). We find, however, that the HF energy differences between simple incompressible states and exotic many-body states, such as the spiral phase and the skyrmion stripe phase, are very small ( $< 0.1$  meV). We therefore suggest (and speculate) that effects not included in our analysis, e.g. self-consistent calculation for the single electron wavefunction, lower level screening, and/or nonparabolic effects of the well confinement etc., may now well stabilize the many-body states. It is also plausible, given the smallness in the HF energy difference, that higher-order corrections beyond the HF theory could stabilize exotic quantum order in this situation.

In Ref. [15], Pan *et. al.* observed strong anisotropic longitudinal resistance when the in-plane field exceeded a certain critical value. This is very suggestive of the skyrmion stripe phase, since the latter has charge modulation in addition to the spin modulation, and therefore should lead to strong transport anisotropy. It is useful to point out that the direction of the charge modulation in the skyrmion stripe phase is fixed by the applied parallel magnetic field: the winding of the transverse components of spin,  $\langle \mathcal{I}_{x,y} \rangle$ , is set by  $\vec{Q}_\perp$  and is perpendicular to  $B_\parallel$ , while the modulation of  $\langle \mathcal{I}_z \rangle$  is along  $B_\parallel$ , so we have effectively a one-dimensional charge density wave that goes along  $B_\parallel$  (see also the discussion about skyrmion stripe phase in Section III A 2). Hence the expected “low” resistance direction of the skyrmion stripe phase is perpendicular to  $B_\parallel$ , which is what was observed in Ref. [15].

An alternative interpretation of the resistance anisotropy has been recently suggested in Ref. [53], where Chalker *et. al.* argued that surface disorder will form domains close to the first order phase transition, that have anisotropic shape due to the presence of the tilted magnetic field. Naive argument would suggest that these domains differ only in the spin structure and should not contribute appreciably to the transport anisotropy. Analysis presented in this paper suggests, however, that boundaries between different domains in this case should be accompanied by the topological spin density, which leads to change density modulation and may lead to large resistance anisotropy. In addition there is always the possibility (already mentioned in Section V C) that a direct first order phase transition from the spin unpolarized to the spin polarized phase will give rise to domains with different (up or down) spin polarizations in the (effectively Ising) ferromagnetic phase. Again, these domains, separated by domain walls, would differ only in the spin orientations, and it is unclear how this could give rise to the observed resistance anisotropy seen in the experiments [15,16]. Also, the domain structure should lead to hysteretic behavior in the observed resistance, which has not been reported. We emphasize, however, that the possibility of a direct first order (Ising type) transition in the experiment of Ref. [15] cannot be ruled out — in fact, our HF calculation does indeed predict such a transition (but with very fragile energetics) as discussed above.

To summarize, within our approximations we do not find any exotic phases as a true ground state close to the level crossing point of  $W2'$ . However, the exotic phases are very close in energy, and therefore we speculate that the resistance anisotropy observed in Ref. [15] may arise from the skyrmion stripe phase, which could be stabilized by effects not included in our theory.

## VI. DOUBLE WELL SYSTEM AT $\nu = 4N + 1$ (D1 CASE)

As mentioned in the Introduction, in the double well system at odd filling factor  $\nu = 4N + 1$ , many interesting phenomena have been explored, such as the interlayer coherence (and the commensurate-incommensurate phase transition) [22,26,54,31], unidirectional charge density wave (stripe) state [55,24,46,56], and the in-plane magnetic field induced charge imbalance phase [57] of the odd filling systems. Following our earlier work in Ref. [8], we will use a general trial wavefunction, Eq. (36), to include the isospin stripe order and the spiral order simultaneously, to obtain a rich quantum phase diagram within a single unified theory including all the effects mentioned above (which in the past have been studied in separate works using different techniques). In this section, we assume the following (reasonable) ordering of energy scales for the double well system:  $\omega_{\perp} \gg \omega_z \gg \Delta_{SAS}$  (see Eq. (15)), so that the lowest  $4N$  filled levels can be assumed to be frozen core states with no coherence effect, and only the top filled level has coherence with the lowest empty level of the same spin polarization (but opposite parity). Within this approximation it is more convenient to follow the standard convention in the literature and consider the isospin within the layer index basis to calculate the HF energy.

For the convenience of later discussion of the symmetry properties of the many-body wavefunction, we first write down the many-body state explicitly in the layer index ( $l = \pm$ ) basis (for notational simplicity, we suppress the Landau level index and the spin index throughout this section):

$$|\Psi_G^{D1}(\psi_k, \vec{Q}_{\perp}, \gamma)\rangle = \prod_k \left( e^{i(kQ_x l_0^2 + \gamma)/2} \cos(\psi_k/2) c_{+,k-Q_y/2}^{D,\dagger} + e^{-i(kQ_x l_0^2 + \gamma)/2} \sin(\psi_k/2) c_{-,k+Q_y/2}^{D,\dagger} \right) |LL\rangle. \quad (71)$$

We then obtain the following expectation value for the HF energy calculation:

$$\begin{aligned} & \langle \Psi_G^{D1} | c_{l_1, k_1}^{D,\dagger} c_{l_2, k_2}^D | \Psi_G^{D1} \rangle \\ &= \delta_{l_1, l_2} \delta_{k_1, k_2} \left[ \cos^2(\psi_{k_1+Q_y/2}/2) \delta_{l_1, +1} + \sin^2(\psi_{k_1-Q_y/2}/2) \delta_{l_1, -1} \right] \\ &+ \delta_{l_1, -l_2} \left[ \cos(\psi_{k_2-Q_y/2}/2) \sin(\psi_{k_2-Q_y/2}/2) \delta_{k_1+Q_y/2, k_2-Q_y/2} \delta_{l_1, +1} e^{-iQ_x(k_2-Q_y/2)l_0^2 - i\gamma} \right. \\ &+ \left. \sin(\psi_{k_1-Q_y/2}/2) \cos(\psi_{k_1-Q_y/2}/2) \delta_{k_1-Q_y/2, k_2+Q_y/2} \delta_{l_1, -1} e^{iQ_x(k_1-Q_y/2)l_0^2 + i\gamma} \right]. \end{aligned} \quad (72)$$

### A. Hartree-Fock variational energy

Neglecting the constant energies associated with Landau levels and Zeeman splittings, the noninteracting single electron energy is entirely the tunneling energy:

$$\begin{aligned} E_0^{D1} &= - \sum_k t \left[ e^{-ikP_y l_0^2} e^{-iQ_x k l_0^2 - i\gamma} + e^{ikP_y l_0^2} e^{iQ_x k l_0^2 + i\gamma} \right] \delta_{P_x, Q_y} \sin(\psi_k/2) \cos(\psi_k/2) \\ &= -\Delta_{SAS} \delta_{P_x, Q_y} \Theta_3(P_y + Q_x) \cos(\gamma). \end{aligned} \quad (73)$$

The Hartree and the Fock energies can be written as (obtained by using Eq. (13)):

$$E_H^{D1} = \frac{N_{\phi}}{2\Omega_{\perp}} \sum_{q_n} \left[ V_{NN,NN}^{D,++}(q_n) (\Theta_1(q_n)^2 + \Theta_2(q_n)^2) + 2V_{NN,NN}^{D,+-}(q_n) \cos(q_n Q_y l_0^2) \Theta_1(q_n) \Theta_2(q_n) \right], \quad (74)$$

and

$$E_F^{D1} = \sum_{q_n} \frac{-1}{2\Omega_{\perp}} \sum_{\vec{q}} \left\{ V_{NN,NN}^{D,++}(\vec{q}) \cos(q_n q_y l_0^2) \left[ \Theta_1(q_n)^2 + \Theta_2(q_n)^2 \right] + 2V_{NN,NN}^{D,+-}(\vec{q}) \cos((Q_x q_y - Q_y q_x) l_0^2) \cos(q_n q_y l_0^2) \Theta_3(q_n)^2 \right\}, \quad (75)$$

where we have used  $V_{NN,NN}^{D,++}(q_n) = V_{NN,NN}^{D,--}(q_n)$ , and neglected the constant energies associated with the frozen core levels. Combining Eqs. (73)-(75) we obtain the total HF energy as follows:

$$\begin{aligned} E_{HF}^{D1} &= -\Delta_{SAS} \delta_{P_x, Q_y} \Theta_3(P_y + Q_x) \cos(\gamma) + \frac{1}{2} \sum_{q_n} \left\{ [E_H^+(q_n) + E_F^+(q_n)] \cdot (\Theta_1(q_n)^2 + \Theta_2(q_n)^2) \right. \\ &+ \left. 2E_H^-(q_n; Q_y) \Theta_1(q_n) \Theta_2(q_n) + 2E_F^-(q_n; \vec{Q}_{\perp}) \Theta_3(q_n)^2 \right\}, \end{aligned} \quad (76)$$

where the definition is obvious by comparing Eq. (76) with Eqs. (73)-(75). The only  $\gamma$ -dependent term is from the tunneling amplitude, reflecting the fact that the isospin rotational symmetry is broken by electron tunneling. We will discuss the symmetry properties in details later.

## B. Commensurate, incommensurate, and charge imbalance phases

We first analytically discuss a special class of many-body states implied by Eq. (71) in the absence of any stripe order, i.e.  $\tilde{\psi}_k = \tilde{\psi}_0^*$  is a constant. Taking  $q_n = 0$  in Eq. (76), we obtain the following simplified HF energy ( $\tilde{\gamma}$  is set to be zero):

$$E_0^{HF}(\vec{Q}_\perp) = -\Theta_3(0) \left\{ \Delta_{SAS} \delta_{Q_y, P_x} \delta_{Q_x, -P_y} + E_\Delta(\vec{Q}_\perp) \Theta_3(0) \right\}, \quad (77)$$

where  $E_\Delta(\vec{Q}_\perp) = E_H^+(0) - E_H^-(0; Q_y) + E_F^+(0) - E_F^-(0; \vec{Q}_\perp)$ . We have used  $\Theta_1(0)\Theta_2(0) = \Theta_3(0)^2$  and neglected the irrelevant constant energy. Following the existing literature, we separate the discussion in two parts: systems in an incommensurate state (i.e. the coherent phase we defined in Section III A 2 with the extreme value of winding wavevector,  $\vec{Q}_\perp^* = 0$ ), and systems in a commensurate state (i.e. the spiral phase defined in Section III A 2 with  $\vec{Q}_\perp^* = (-P_y, P_x)$ ). When the system is in an incommensurate state, the tunneling amplitude is effectively zero according to Eq. (77), and therefore the extreme value of  $\tilde{\psi}_0$  is determined by the sign of  $E_\Delta(\vec{Q}_\perp^*)$ . For  $E_\Delta(\vec{Q}_\perp^*) > 0$  (i.e. the Hartree energy dominates the Fock energy), the minimum energy is at  $\Theta_3^*(0) = 1/2$  or  $\psi_0^* = \pi/2$ , indicating an equal population of electrons in the two layers. However, if  $E_\Delta(\vec{Q}_\perp^*) < 0$  (i.e. the Fock energy dominates the Hartree energy), the minimum value of  $E_0^{HF}(\vec{Q}_\perp)$  is at  $\Theta_3^*(0) = 0$  (i.e.  $\psi_0^* = 0$  or  $\pi$ ), and therefore we obtain a fully spontaneous charge imbalanced state [57], where all electrons like to accumulate in a single layer rather than distribute equally in the two layers (this is true, of course, only within the HF approximation where the correlation energy is totally neglected). In the commensurate state (i.e.  $Q_x = -P_y$  and  $Q_y = P_x$ ) and  $E_\Delta(\vec{Q}_\perp^*) < -\Delta_{SAS}$ , the total energy in Eq. (77) is minimized at  $0 < \Theta_3^*(0) = |\Delta_{SAS}/2E_\Delta(\vec{Q}_\perp^*)| < 1/2$ , showing a spontaneous partial charge imbalance phase. Otherwise, for  $E_\Delta(\vec{Q}_\perp^*) > -\Delta_{SAS}$ , the commensurate phase always has equal number of electrons in the two layers, i.e. the usual isospin paramagnetic phase. Therefore, the in-plane magnetic field can cause not only a commensurate-incommensurate phase transition, but also a spontaneous charge imbalance phase when the exchange energy is large. We note that such exchange driven spontaneous charge imbalance phases could arise even in the zero-field (i.e.  $B_{tot} = 0$ ) non-quantum-Hall bilayer 2D systems within a restricted HF approximation [68], but in the zero-field case the corresponding  $XY$  “isospin magnetic” state has been shown to be lower in the energy than the Ising-type charge imbalance phase for the long range Coulomb interaction.

In the present paper, we only consider the long-range Coulomb interaction, which gives  $E_H^+(0) - E_H^-(0; Q_y) = e^2/\epsilon l_0^2$  ( $\epsilon$  is the dielectric constant of the system), and therefore the Hartree electrostatic energy always dominates the Fock exchange energy (i.e.  $E_\Delta(\vec{Q}_\perp) > 0$ ), eliminating any spontaneous charge imbalance between the two layers. On the other hand, as will be shown later, we may obtain a commensurate stripe phase with a longer period ( $a \gg l_0$ ) in the small layer separation region, which is the asymptotic behavior of the charge imbalance phase recently discussed by Radzhovskiy *et. al.* [57].

## C. Numerical results and the stripe phases

Fig. 12(a) and (b) are the phase diagrams we obtain at zero temperature for  $\nu = 5$  for the in-plane magnetic field fixed in  $x$  direction. Using the isospin many-body phases defined in Section III, phase I is the coherent phase; phase II is the spiral phase, where the optimal spiral winding wavevector  $\vec{Q}_\perp^* = (0, Q_y^*) = (0, P_x)$  is perpendicular to the in-plane field direction; phase III is the coherent stripe phase, where the stripe direction can be in arbitrary direction, and phases IV and V correspond to the spiral stripe phase, where  $\vec{Q}_\perp^*$  is perpendicular to  $B_{\parallel}$  and the stripe is aligned in  $x$  direction (i.e.  $\langle \mathcal{I}_z \rangle$  modulates in  $y$  direction, parallel to  $\vec{Q}$ ). To obtain the stripe phase (phases III, IV and V), we numerically minimize the HF variational energy by using a general stripe phase function as shown in Fig. 6 and in Appendix E. (The perturbation method developed in Section III C also gives similar results, since the stripe formation in this system is a second order transition.) As mentioned in the beginning of Section III, to get the energy of a spiral stripe phase with stripe normal direction perpendicular to the in-plane field, we can just rotate the in-plane field direction from the  $x$  to the  $y$  axis. Therefore the results shown in 12(a) and (b) are gauge independent. Note that the stripe period of phase V is very large ( $a \gg l_0$ ), showing an asymptotic behavior of charge imbalance phase modified by the long-range Coulomb interaction. Using the existing terminology of the literature [46,22,26], phases I and II are the incommensurate and commensurate phases respectively, and phases III and IV are the incommensurate and commensurate stripe phases respectively. We will use this terminology as well as the isospin phases mentioned above (defined in Section III A 2) for later discussion in this paper.

We note, however, that our HF calculation does not incorporate the possibility of two decoupled compressible  $\nu = 2N + 1/2$  states in each layer, which could be energetically favored for smaller  $N$  (lower values of  $\nu$ , e.e.  $\nu = 1$ ). We expect that the phases discussed in this paper are more likely to be found for  $N > 0$ , when each of the layers becomes susceptible to forming a stripe phase [1,4,5], especially in the presence of a parallel magnetic field. Particle-hole symmetry implies that similar states should also occur at filling factors  $4N + 3$  by interchanging the role of holes and electrons in the top filled Landau level.

#### D. Symmetry properties of the commensurate and incommensurate states

Applying Eqs. (21) and (31)-(32) to the wavefunction,  $|\Psi_G^{D1}(\psi_k^*, \vec{Q}_\perp^*, \gamma^*)\rangle$  in Eq. (71) (where  $\psi_k^*$ ,  $\vec{Q}_\perp^*$ , and  $\gamma^*$  denote the extreme values to minimize the HF energy), we obtain

$$\begin{aligned} \hat{P}|\Psi_G^{D1}(\psi_k^*, \vec{Q}_\perp^*, \gamma^*)\rangle &= \prod_k \left( e^{i(kQ_x^*l_0^2 + \gamma^*)/2} \cos(\psi_k^*/2) c_{-, -k+Q_y^*/2}^{D,\dagger} + e^{-i(kQ_x^*l_0^2 + \gamma^*)/2} \sin(\psi_k^*/2) c_{+, -k-Q_y^*/2}^{D,\dagger} \right) |LL\rangle \\ &= (-i)^{N_\phi} |\Psi_G^{D1}(\psi_{-k}^* + \pi, \vec{Q}_\perp^*, -\gamma^* + \pi)\rangle \end{aligned} \quad (78)$$

$$\begin{aligned} \hat{T}_x(R_x)|\Psi_G(\psi_k^*, \vec{Q}_\perp^*, \gamma^*)\rangle &= \prod_k \left( e^{i(kQ_x^*l_0^2 + \gamma^* - R_x P_y)/2} \cos(\psi_k^*/2) c_{+, k+R_x/l_0^2 - Q_y^*/2}^{D,\dagger} \right. \\ &\quad \left. + e^{-i(kQ_x^*l_0^2 + \gamma^* - R_x P_y)/2} \sin(\psi_k^*/2) c_{-, k+R_x/l_0^2 + Q_y^*/2}^{D,\dagger} \right) |LL\rangle \\ &= |\Psi_G(\psi_{-R_x/l_0^2}^*, \vec{Q}_\perp^*, \gamma^* - R_x(Q_x^* + P_y))\rangle, \end{aligned} \quad (79)$$

$$\begin{aligned} \hat{T}_y(R_y)|\Psi_G(\psi_k^*, \vec{Q}_\perp^*, \gamma^*)\rangle &= \prod_k \left( e^{i(kQ_x^*l_0^2 + \gamma^* + R_y P_x)/2} e^{i(k-Q_y^*/2)R_y} \cos(\psi_k^*/2) c_{+, k-Q_y^*/2}^{D,\dagger} \right. \\ &\quad \left. + e^{-i(kQ_x^*l_0^2 + \gamma^* + R_y P_x)/2} e^{i(k+Q_y^*/2)R_y} \sin(\psi_k^*/2) c_{-, k+Q_y^*/2}^{D,\dagger} \right) |LL\rangle \\ &= |\Psi_G(\psi_k^*, \vec{Q}_\perp^*, \gamma^* - R_y(Q_y^* - P_x))\rangle, \end{aligned} \quad (80)$$

where we have used the fact that the guiding center coordinates,  $k$ , can be shifted and  $\sum_k k = 0$  in a completely filled Landau level.

Now we can study the symmetry properties of the many-body phases obtained earlier in the HF approximation. In-plane field,  $B_{\parallel}$ , is fixed along  $x$  axis and hence  $P_y = 0$ . According to Eqs. (78)-(80), we find that (i) for an incommensurate state (= coherent phase with neither isospin spiral nor stripe order:  $\psi_k^* = \pi/2$ ,  $\vec{Q}_\perp^* = 0$ , and  $\gamma^*$  = arbitrary),  $\hat{P}|\Psi_G^{D1}\rangle = \hat{T}_x|\Psi_G^{D1}\rangle = |\Psi_G^{D1}\rangle$  and therefore the parity symmetry and the translational symmetry in  $x$  direction are not broken. However, since  $\hat{T}_y(R_y)|\Psi_G(\psi_k^*, \vec{Q}_\perp^*, \gamma^*)\rangle = |\Psi_G(\psi_k^*, \vec{Q}_\perp^*, \gamma^* + R_y P_x)\rangle$  is in general not equal to the original wavefunction, and the HF energy is independent of phase  $\gamma^*$  (the tunneling term is effective absence in the incommensurate phase), the translational symmetry in  $y$  direction is therefore broken, with an oscillation period of  $2\pi/|P_x|$ . Note that the above translational symmetry breaking in the incommensurate phase is obtained within the mean field HF approximation, which is *not* the same as the soliton lattice ground state obtained in Ref. [31] by using an effective field theory to go beyond the mean field approximation. We should expect to see a gapless Goldstone mode associated with the broken translational symmetry in the time-dependent Hartree-Fock approximation. (ii) For a commensurate phase (= spiral phase:  $\psi_k^* = \pi/2$ ,  $\vec{Q}_\perp = (0, P_x)$ , and  $\gamma^* = 0$ ), we find that *no* symmetry is broken at all, since no distinct wavefunction is obtained after applying  $\hat{P}$ ,  $\hat{T}_x$  and  $\hat{T}_y$  operators. In other words, the commensurate (or spiral) phase is basically the same as an isospin polarized state from the symmetry point of view. It is not surprising because one can show that such commensurate (or isospin spiral) state is essentially the same as the noninteracting ground state,  $\prod_k a_{n,+s,k}^\dagger |LL\rangle$  (where  $a_{n,\alpha,s,k}^\dagger$  is defined in Eq. (14) for the noninteracting energy eigenstate), of the double well system, which is certainly an eigenstate of all of these symmetry operators. (iii) For an incommensurate stripe phase (= coherent stripe:  $\psi_k^* = \psi_{k+a/2\pi l_0^2}^*$ ,  $\vec{Q}_\perp = 0$ , and  $\gamma^*$  = arbitrary), we find that the translational symmetries in both  $x$  and  $y$  directions are broken. However, we note that another incommensurate stripe phase, whose isospin  $z$  component,  $\langle \mathcal{I}_z \rangle$ , modulates in  $y$  direction (perpendicular to  $B_{\parallel}$ ), is also a degenerate ground state at the mean field level, breaking the translational symmetry in  $y$  direction *only*. The wavefunction of this second incommensurate stripe phase cannot be simply described in the present Landau gauge,  $\vec{A}_{[y]}(\vec{r})$ , and therefore its energy is not shown in the equations presented in this section. We may, however, consider an equivalent state by assuming the in-plane magnetic field to be along  $y$  direction with stripe modulation along  $x$  so that the translational symmetry is broken only in the direction perpendicular to the in-plane field direction in this second type of incommensurate

stripe phase. Parity symmetry is, however, broken in both the incommensurate stripe phases. (iv) Finally, for a commensurate stripe (= spiral stripe:  $\psi_k^*$  modulates in  $y$  direction,  $\vec{Q}_\perp = (0, P_x)$ , and  $\gamma^* = 0$ ), its wavefunction cannot simply be described by the present gauge  $\vec{A}_{[y]}(\vec{r})$ , and we can obtain it by effectively rotating the in-plane field direction as described above. By changing the in-plane field direction from  $\hat{x}$  to  $\hat{y}$ , the spiral wavevector becomes  $\vec{Q}_\perp^* = (-P_y, 0)$ , and Eqs. (78)-(80) tell us that both parity symmetry and translational symmetry in  $x$  direction (now it is perpendicular to the in-plane field) are broken, while translational symmetry in  $y$  direction (parallel to the in-plane field) is preserved. We then conclude that the parity symmetry and the translational symmetry in the direction *perpendicular* to the in-plane field (i.e. in  $y$  axis) are both broken in this commensurate stripe phase in the presence of  $B_\parallel$  field (in  $x$  direction). This direction of broken translational symmetry is also parallel to the direction of isospin spiral wavefunction and the stripe oscillation (as defined for the spiral stripe phase in Section III A 3).

## VII. DOUBLE WELL SYSTEM AT $\nu = 4N + 2$ (D2 CASE)

For a double well system at even filling factor,  $\nu = 4N + 2$ , both spin and layer indices are involved in the level crossing region (see Fig. 2(f)), where the cyclotron resonance energy,  $\omega_\perp$ , is (realistically) assumed to be much larger than the tunneling energy ( $\Delta_{SAS}$ ) and the Zeeman energy ( $\omega_z$ ) so that the two top filled levels and the two lowest empty levels belong to the same orbital quantum number, well-separated from all other filled or empty levels, which are considered frozen and neglected from our consideration. As mentioned in Section II B, an appropriate basis for the isospinor for this system is the basis of noninteracting energy eigenstates, which have definite parity and spin symmetries. (Our definition of isospin coherent and isospin spiral phases in Section III A 2 then just corresponds to the fully commensurate and partially incommensurate phases in the literature [36]. For the convenience of comparison, we will use the conventional language for most of our discussion in this section.) We note that several interesting phenomena associated with the CAF phase in this system have been studied in the literature in the recent years [33–39]. A spin symmetry broken canted antiferromagnetic phase can be stabilized in this system in addition to the usual symmetric and fully ferromagnetic states in the  $B_\parallel = 0$  situation [33]. In the canted phase electrons in the two layers hold the same  $z$  component of spin polarization, while they have opposite spin direction in the  $x - y$  plane, showing a two-dimensional antiferromagnetic order. When an in-plane magnetic field is applied, such a canted phase remaining in a commensurate state and does not exhibit a commensurate-incommensurate phase transition at large  $B_\parallel$  as observed in  $\nu = 4N + 1$  case [36]. However, the possible stripe phase formation in the presence of an in-plane magnetic field for a larger layer separation has not yet been explored in the literature. For the sake of completeness, we will use the trial wavefunction proposed in Section III B and the perturbation method developed in Section III C to study the possibility of a stripe formation in the double well system at even filling factors.

For a double well system at  $\nu = 4N + 2$ , we have argued that the trial wavefunction proposed in Eq. (46), although not the most possible wavefunction, should be a reasonable approximation to describe the ground state in the presence of in-plane magnetic field. Thus we again start from calculating the following expectation value by using the trial wavefunction,  $|\Psi_G^{D2}\rangle$  shown in Eq. (46):

$$\begin{aligned}
& \langle \Psi_G^{D2} | a_{m_1, \alpha_1, \sigma_1, k_1}^\dagger a_{m_2, \alpha_2, \sigma_2, k_2} | \Psi_G^{D2} \rangle \\
&= \delta_{m_1, m_2} \delta_{\alpha_1, \alpha_2} \delta_{\sigma_1, \sigma_2} \delta_{k_1, k_2} [\cos^2(\psi_{k_1+Q_y/2}/2) \delta_{m_1, N} \delta_{\alpha_1, +1} \delta_{\sigma_1, 1/2} + \sin^2(\psi_{k_1-Q_y/2}/2) \delta_{m_1, N} \delta_{\alpha_1, -1} \delta_{\sigma_1, -1/2} \\
&\quad + \cos^2(\psi'_{k_1+Q'_y/2}/2) \delta_{m_1, N} \delta_{\alpha_1, +1} \delta_{\sigma_1, -1/2} + \sin^2(\psi'_{k_1-Q'_y/2}/2) \delta_{m_1, N} \delta_{\alpha_1, -1} \delta_{\sigma_1, 1/2} + \theta(N - m_1)] \\
&\quad + \delta_{m_1, N} \delta_{\alpha_1, -\alpha_2} \delta_{\sigma_1, -\sigma_2} [\cos(\psi_{k_2-Q_y/2}/2) \sin(\psi_{k_2-Q_y/2}/2) e^{-iQ_x(k_2-Q_y/2)l_0^2 - i\gamma} \delta_{k_1, k_2-Q_y} \delta_{\alpha_1, +1} \delta_{\sigma_1, +1/2} \\
&\quad + \cos(\psi_{k_1-Q_y/2}/2) \sin(\psi_{k_1-Q_y/2}/2) e^{iQ_x(k_1-Q_y/2)l_0^2 + i\gamma} \delta_{k_2, k_1-Q_y} \delta_{\alpha_1, -1} \delta_{\sigma_1, -1/2} \\
&\quad + \cos(\psi'_{k_2-Q'_y/2}/2) \sin(\psi'_{k_2-Q'_y/2}/2) e^{-iQ'_x(k_2-Q'_y/2)l_0^2 - i\gamma'} \delta_{k_1, k_2-Q'_y} \delta_{\alpha_1, +1} \delta_{\sigma_1, -1/2} \\
&\quad + \cos(\psi'_{k_1-Q'_y/2}/2) \sin(\psi'_{k_1-Q'_y/2}/2) e^{iQ'_x(k_1-Q'_y/2)l_0^2 + i\gamma'} \delta_{k_2, k_1-Q'_y} \delta_{\alpha_1, -1} \delta_{\sigma_1, 1/2}], \tag{81}
\end{aligned}$$

which is basically the same as Eq. (64) for a wide well system at  $\nu = 2N + 2$ , except for the different quantum numbers associated with the Landau levels.

### A. Hartree-Fock variational energy

The full Hartree-Fock energies (noninteracting, Hartree, and Fock energies respectively) can be obtained as follows:

$$E_0^{D2} = \frac{1}{2}(-\Delta_{SAS} + \omega_z)(\Theta_1(0) - \Theta_2(0)) + \frac{-1}{2}(\Delta_{SAS} + \omega_z)(\Theta'_1(0) - \Theta'_2(0)), \quad (82)$$

$$\begin{aligned} E_H^{D2} = & \frac{N_\phi}{2\Omega_\perp} \sum_{q_n \neq 0} V_{NN,NN}^I(q_n) [\Theta_1(q_n)^2 + \Theta_2(q_n)^2 + \Theta'_1(q_n)^2 + \Theta'_2(q_n)^2 \\ & + 2 \cos(Q_y q_n l_0^2) \Theta_1(q_n) \Theta_2(q_n) + 2 \cos(Q'_y q_n l_0^2) \Theta'_1(q_n) \Theta'_2(q_n) \\ & + 2 \cos((Q_y - Q'_y) q_n l_0^2 / 2) (\Theta_1(q_n) \Theta'_1(q_n) + \Theta_2(q_n) \Theta'_2(q_n)) \\ & + 2 \cos((Q_y + Q'_y) q_n l_0^2 / 2) (\Theta_1(q_n) \Theta'_2(q_n) + \Theta'_1(q_n) \Theta_2(q_n))] , \end{aligned} \quad (83)$$

and

$$\begin{aligned} E_F^{D2} = & \frac{-1}{2\Omega_\perp} \sum_{\vec{q}_\perp} V_{NN,NN}^I(\vec{q}_\perp) \sum_n \cos(q_n q_y l_0^2) [\Theta_1(q_n)^2 + \Theta_2(q_n)^2 + 2 \cos((Q_x q_y - Q_y q_x) l_0^2) \Theta_3(q_n)^2 \\ & + \Theta'_1(q_n)^2 + \Theta'_2(q_n)^2 + 2 \cos((Q'_x q_y - Q'_y q_x) l_0^2) \Theta'_3(q_n)^2] \\ & + \frac{-2}{2\Omega_\perp} \sum_{\vec{q}_\perp} V_{NN,NN}^o(\vec{q}_\perp) \sum_n \cos(q_n q_y l_0^2) \cos(q_n (Q_y + Q'_y) l_0^2) [\Theta_1(q_n) \Theta'_2(q_n) + \Theta_2(q_n) \Theta'_1(q_n)] \\ & + \frac{-4\delta_{Q_y, -Q'_y}}{2\Omega_\perp} \sum_{\vec{q}_\perp} V_{NN,NN}^o(\vec{q}_\perp) \cos(\gamma + \gamma') \sum_n \Theta_3(q_n - Q_x) \Theta'_3(q_n + Q'_x) \cos((q_x Q_y - q_n q_y) l_0^2) , \end{aligned} \quad (84)$$

where the last term of the exchange energy plays the same role as the last term of Eq. (67) in the wide well system at  $\nu = 2N + 2$ , coupling the nearest and the next nearest pairs of levels to stabilize a coherent phase. The minimum of the HF energy is achieved for  $\gamma + \gamma' = 2m\pi$  ( $m$  is an integer) and arbitrary  $\gamma - \gamma'$ .

## B. Nonstripe phases

For the sake of completeness and later discussion, here we first briefly review some results of the CAF phase in a double well system in the presence of in-plane magnetic field at even filling factors in our theory. We note that this system has also been studied recently in Ref. [36] by numerically solving a single electron HF equation. As has been mentioned in Section III B 1, in the energy eigenstate basis we use in Eq. (14), the in-plane magnetic field has been incorporated in the phase difference between the electrons in the right layer and in the left layer, so that a fully incommensurate state [36] has been automatically excluded in our trial wavefunction (see discussion in Section III B 1). The HF energy of such a fully incommensurate state, however, can still be calculated if we let tunneling and in-plane magnetic field to be zero in the above HF energy expression and let  $\vec{P}_\perp = \vec{Q}_\perp = \vec{Q}'_\perp = 0$ , since it is well-known that the tunneling energy is effectively absent when the in-plane field exceeds the critical value for the commensurate-to-incommensurate phase transition. The HF energy of a fully commensurate state is calculated by setting  $\vec{Q}_\perp = -\vec{Q}'_\perp = 0$  in the HF variational energy, and the energy of a partially commensurate/incommensurate state is obtained by setting  $\vec{Q}_\perp \neq -\vec{Q}'_\perp$  or  $\vec{Q}_\perp = -\vec{Q}'_\perp \neq 0$ . The stripe phase functions,  $\psi_k$  and  $\psi'_k$ , are just constant variational parameters for studying the nonstripe phases.

Inspecting the last term of Eq. (84)), it is easy to see that the minimum energy should be always at  $\vec{Q}_\perp = -\vec{Q}'_\perp$  to stabilize the CAF phase even in the absence of in-plane field, i.e. we need only consider  $\vec{Q}'_\perp = -\vec{Q}_\perp$  for both fully commensurate ( $\vec{Q}_\perp = 0$ ) and partially commensurate/incommensurate ( $\vec{Q}_\perp \neq 0$ ) states. (In the terminology defined in Section III A 2 of this paper, these are just the isospin coherent and isospin spiral phases respectively in the noninteracting energy eigenstate basis. As stated above, we are using the conventional terminology for most of our discussion in this section to avoid confusion.) Therefore, focusing on the nonstripe phase, the HF energy shown above can be simplified to be

$$\begin{aligned} E_{HF}^{D2,u}(\vec{Q}_\perp) = & (\Delta_{SAS} - \omega_z) \Theta_2(0) + (\Delta_{SAS} + \omega_z) \Theta'_2(0) \\ & + \frac{1}{2} E_F^I(0, 0) [\Theta_1(0)^2 + \Theta_2(0)^2 + \Theta'_1(0)^2 + \Theta'_2(0)^2] + E_F^I(\vec{Q}_\perp, 0) [\Theta_3(0)^2 + \Theta'_3(0)^2] \\ & + E_F^o(0, 0) [\Theta_1(0) \Theta'_2(0) + \Theta_2(0) \Theta'_1(0)] + 2 E_F^o(\vec{Q}_\perp, 0) \Theta_3(0) \Theta'_3(0) , \end{aligned} \quad (85)$$

where the analytic expression for  $E_{HF}^{I,o}(\vec{Q}_\perp, 0)$  is shown in Appendix F. From Eq. (85) we find that, as expected, the Hartree energy does not contribute to the HF energy of a uniform phase, and only exchange energy (negative value) is relevant.

By comparing the HF energy of the three different phases: fully incommensurate ( $\Delta_{SAS} = 0$  and  $\vec{P}_\perp = \vec{Q}_\perp = 0$ ), fully commensurate ( $\vec{Q}_\perp = 0$ ), and partially commensurate/incommensurate ( $\vec{Q}_\perp \neq 0$ ) phases, our numerical calculation shows that the ground state is always the fully commensurate phase (which has the lowest energy), i.e.  $\vec{Q}_\perp = \vec{Q}'_\perp = 0$  as an isospin coherent phase in the noninteracting eigenstate basis. Therefore we do not find the commensurate-incommensurate phase transition (as observed in the odd filling systems) in this even filling factor situation. Following the arguments in Section II C (see particularly Eqs. (43)-(45)), we find that this fully commensurate state breaks both parity and spin rotational symmetries (but not the translational symmetry). To understand that these are two separate broken symmetries one can consider a non-HF state that has uniform  $\psi_k$  and  $\psi'_k$ , and  $(\gamma, \gamma')$  fluctuating between  $(-\theta/2, \theta/2)$  and  $(\pi - \theta/2, \pi + \theta/2)$  with fixed  $\theta$ . Such a state clearly breaks the spin symmetry, but not parity (which changes  $\gamma$  and  $\gamma'$  by  $\pi$ , see Eq. (43)), and may be described as a spin nematic state.

The equation for the phase boundary between the fully commensurate phase (i.e. commensurate CAF phase) and the symmetric phase (both filled levels are orbital symmetric,  $\alpha = +$ , but with different spin directions) is

$$\omega_z(\Delta_{SAS}) = \sqrt{(\Delta_{SAS} - E_F^o(0,0))^2 - E_F^o(0,0)^2}, \quad (86)$$

where  $\omega_z$  is the Zeeman energy. Analogously the equation for the phase boundary between the commensurate CAF phase and the fully spin polarized state is

$$\omega_z^{cf}(\Delta_{SAS}) = \sqrt{E_F^o(0,0)^2 + \Delta_{SAS}^2} - E_F^o(0,0). \quad (87)$$

The calculated phase diagrams of different filling factors and different in-plane magnetic fields are shown in Fig. 13.

We can also use a similar method to calculate the triplet magnetoplasmon modes by taking  $\Theta_2(0)$  and  $\Theta'_2(0)$  to be small in Eq. (85), because the noninteracting Hamiltonian has been diagonalized in the energy eigenstate basis. However, since such calculations already exist in the literature both for zero in-plane magnetic field and in the presence of an in-plane field [40], we do not show the calculated magnetoplasmon dispersion in this paper.

### C. Exploration of the stripe formation

When considering the possible stripe formation via the periodic functions of  $\psi_k$  and  $\psi'_k$  in the trial wavefunction, we need to retain the Hartree energy, which is canceled in the uniform non-stripe phase discussed above. Assuming  $\vec{Q}_\perp = 0$  as in the uniform phase the Hartree-Fock energy in (Eqs. (82)-(84)) for the striped case becomes

$$\begin{aligned} E_{HF}^{D2,s}(0) = & (\Delta_{SAS} - \omega_z)\Theta_2(0) + (\Delta_{SAS} + \omega_z)\Theta'_2(0) \\ & + \frac{1}{2} \sum_{q_n \neq 0} E_H^I(q_n) [\Theta_1(q_n) + \Theta_2(q_n) + \Theta'_1(q_n) + \Theta'_2(q_n)]^2 \\ & - \frac{1}{2} \sum_{q_n} \{ E_F^I(0, q_n) [\Theta_1(q_n)^2 + \Theta_2(q_n)^2 + \Theta'_1(q_n)^2 + \Theta'_2(q_n)^2 + 2\Theta_3(q_n)^2 + 2\Theta'_3(q_n)^2] \\ & + 2E_F^o(0, q_n) [\Theta_1(q_n)\Theta'_2(q_n) + \Theta_2(q_n)\Theta'_1(q_n) + 2\Theta_3(q_n)\Theta'_3(q_n)] \}, \end{aligned} \quad (88)$$

where  $q_n = 2\pi n/a$  and  $a$  is the stripe period. We define  $E_H^I(q_n) = (2\pi l_0^2)^{-1} V_{NN,NN}^I(q_n)$  and  $E_F^I(q_n) = \Omega_\perp^{-1} \sum_{\vec{q}_\perp} V_{NN,NN}^I(\vec{q}_\perp) \cos(q_n q_y l_0^2)$ , and neglect the divergent Hartree energy at  $q_n = 0$ , which is canceled by the background positive charge (providing the overall charge neutrality). Using the perturbation method developed in Section III C, which is equivalent to studying the mode softening of the Goldstone mode inside the CAF phase, we obtain the following perturbation energy matrix (see Eq. (56)):

$$\mathbf{E}_{pert}^{HF}(\tilde{q}) = \begin{bmatrix} (\Delta_{SAS} - \omega_z) \cos(\psi_0^*) + [E_F^I(0) - E_F^I(\tilde{q})] - E_F^o(0) \cos(\psi_0^* + \psi_0'^*) \\ -E_F^o(\tilde{q}) \cos(\psi_0^* + \psi_0'^*) \\ -E_F^o(\tilde{q}) \cos(\psi_0^* + \psi_0'^*) \\ (\Delta_{SAS} + \omega_z) \cos(\psi_0'^*) + [E_F^I(0) - E_F^I(\tilde{q})] - E_F^o(0) \cos(\psi_0^* + \psi_0'^*) \end{bmatrix}, \quad (89)$$

where  $\psi_0^*$  and  $\psi_0'^*$  are the optimal values obtained from minimizing the total energy inside the commensurate canted phase region, and  $\tilde{q}$  is the wavevector of the test small stripe as shown in Eq. (50). For simplicity, we have assumed that the stripe periods of the two stripe phase functions,  $\psi_k$  and  $\psi'_k$ , are the same,  $2\pi/\tilde{q}$ . The sign of the eigenvalues

of Eq. (89) then determines the existence of stripe formation as discussed in Section III C. Our numerical calculation shows that both of the eigenvalues of  $\mathbf{E}_{pert}^{HF}(\vec{q})$  in Eq. (89) are always positive within the canted phase region, showing that *no* stripe phase should occurs with an energy lower than the commensurate CAF phase. We have also studied the possibility of first order phase transition to a stripe phase, which cannot be included in the perturbation theory, by directly comparing various ground state energies. We still find that no stripe phase can be stabilized energetically. Therefore, unlike the rich phase diagram shown in the odd filling factor double well system at  $\nu = 4N + 1$ , the system at even filling  $\nu = 4N + 2$  in the presence of in-plane field has neither the commensurate-to-incommensurate phase transition in the large  $B_{\parallel}$  region (see discussion below Eq. (85)) nor the uniform-to-stripe phase transition in the large layer separation region. The former result is also consistent with the recent result obtained in an effective field theory [39]. We discuss this result further in Section VIII.

## VIII. DISCUSSION

In this section, we discuss and compare the quantum phases obtained in different systems studied in this paper (as well as those already existing in the literature).

### A. Directions of isospin stripe and isospin spiral orders

In Table II we summarize the isospin spiral and isospin stripe directions obtained in the three different cases,  $W1'$ ,  $W2'$ , and  $D1$ , where at least a spiral or a stripe order exists in our HF calculation. For the convenience of discussion, we will define the isospin components to be in the layer index basis for the double well systems at  $\nu = 4N + 1$ , i.e. the isospin spiral/coherent (stripe) phases in  $D1$  case correspond to the conventional commensurate/incommensurate (stripe) states respectively. We do not include the commensurate CAF phase in  $D2$  system, because it also has a spiral order following the in-plane field in the layer index basis and therefore is similar to the commensurate state (isospin spiral phase) of  $D1$  system.

Note that although the definition of isospin components are different for these systems (see Table I), all the isospin spiral orders select a wavevector,  $\vec{Q}_{\perp}$  (but  $\pm\vec{Q}_{\perp}$  are degenerate for the wide well system), to be perpendicular to the in-plane magnetic field. The mechanisms for the spiral winding in wide wells and in double wells are very different. In a wide well system with a strong in-plane magnetic field, the electron wavefunction is distorted by the anisotropic field and therefore the electron-hole binding energy is the strongest if the isospin is winding along the direction perpendicular to the in-plane field [17]. More precisely, this is true only in the presence of a very strong perpendicular magnetic field or in wells which are not too wide, so that the effective cyclotron resonance energy,  $\omega_{\perp}$ , is comparable to or larger than the confinement energy,  $\omega_0$ . The direction of the spiral winding can change to the in-plane field direction if the perpendicular field is so weak that  $\omega_{\perp} \ll \omega_0$ . (We will show this result explicitly in below). This effect of spiral winding locking is less important in the weak  $B_{\parallel}$  region, leading to the isotropic phases observed in the intersubband level crossing region ( $W1$ ). In a double well system with zero well width, however, the in-plane magnetic field does not affect the single electron wavefunction, but only affects the tunneling amplitude through the Aharonov-Bohm phase factor, which selects a specific spiral wavevector,  $\vec{Q}_{\perp} = (0, P_x) = (0, edB_{\parallel}/c)$ , perpendicular to the in-plane magnetic field. When  $B_{\parallel}$  is weak, the isospin spiral order follows the wavevector of the tunneling amplitude, since it minimizes the tunneling energy and does not cost much in the Coulomb exchange energy. When  $B_{\parallel}$  exceeds a certain critical value, the energetic cost of winding from the point of view of exchange energy becomes prohibitively high, and the system goes into the incommensurate phase with no isospin winding. Therefore the origin of isospin spiral order in a wide well system and a double well system is very different, although both are perpendicular to the in-plane magnetic field.

Now we discuss the mechanism, which determines the directions of the isospin stripe orders (if it exists) in these systems. From Table II we note that the stripe modulation of  $I_z$  (i.e. the normal vector,  $\hat{n}$ ) of the stripe is along  $x$  axis, parallel to the  $B_{\parallel}$  field for a wide well system at both even and odd filling factors (for even filling system,  $W2'$ , we cannot stabilize a many-body phase within the HF approximation, but speculate, based on very small calculated HF energy differences, that the resistance anisotropy observed in the experiment [15] could result from a skyrmion stripe phase near the level crossing region, which could perhaps be stabilized by going beyond our approximation scheme (see Section V). But the stripe normal vector is along  $y$  axis, perpendicular to the  $B_{\parallel}$  field, for a double well system at  $\nu = 4N + 1$  (no stripes are found in a double well system at  $\nu = 4N + 2$ ). The different stripe directions in the two systems could be understood as a result of competition between two effects: one is the anisotropy energy (i.e. the total energy difference between a stripe perpendicular to the in-plane field and a stripe parallel to the in-plane field, see [11]) induced by the in-plane magnetic field via the anisotropic distortion of electron wavefunction, and the other

one is the exchange interaction between the spiral order (oscillation of  $\langle I_x \rangle$  and  $\langle I_y \rangle$ ) and the stripe order (oscillation of  $\langle I_z \rangle$ ). This effect reflects on the term,  $E_{F6}^{W1}(q_n, 0; Q_x, Q_y)$  of Eq. (60) for a wide well at  $\nu = 2N + 1$  and on the last term of Eq. (75) for a double well at  $\nu = 4N + 1$  (the similar terms in the even filling systems can be also found in Eq. (67) and Eq. (84) for wide well and double well systems respective: proportional to  $\Theta_3(q_n)^2$  and  $\Theta'_3(q_n)^2$ ). Such interaction between the spiral order and the stripe order prefers to keep the wavevectors of these two oscillations parallel with each other in order to optimize the exchange energy. On the other hand, the anisotropy energy induced by the anisotropic electron wavefunction in the finite width well prefers to form a stripe aligned perpendicular to the in-plane field direction, i.e. its normal direction is parallel to  $\hat{x}$  axis [58].

If the spiral-stripe exchange energy dominates the anisotropic energy (like in the double well system, where the zero-well-width electron wavefunction is isotropic and hence the anisotropy energy is zero), the stripe order prefers to select a normal wavevector parallel to the wavevector of the spiral order, resulting in a spiral stripe phase. The stripe direction in this case is governed by the spiral order, which is perpendicular to the in-plane field in the commensurate phase as we find in the numerical results shown in Section VI and in Fig. 12(a) (phase (IV) and (V)). When the in-plane field is so strong that the double well system undergoes a first order phase transition to an incommensurate phase, the spiral order disappears and therefore the stripe direction is not locked by the in-plane field, being in an arbitrary direction in the two-dimensional plane (phase (III) in Fig. 12) [24]. On the other hand, when we consider a single finite width well in the presence of in-plane field, the anisotropy energy is finite and competes with the spiral-stripe exchange energy. If the anisotropy energy dominates, the spiral-stripe exchange energy can *not* force the stripe and spiral orders to be parallel with each other (and hence perpendicular to the in-plane field). Therefore the density modulation of the stripe phase prefers to stay in the direction of in-plane field [58], having a direction perpendicular to the spiral order, resulting in a skyrmion stripe phase. Therefore the mechanism we discussed so far can explain all of the spiral and stripe directions obtained individually in the previous sections within the HF approximation.

As a final remark, we note that the HF energy difference between the spiral stripe phase and the skyrmion stripe phase are very small compared to the other energy scales in our numerical calculation, both in wide well systems and in double well systems. Therefore we expect that various effects (e.g. disorder and impurity scattering) ignored in our calculations could have strong influence in determining the eventual ground state of the system, providing an experimental stripe direction different from that obtained in our idea HF theory. The actual finite width effects of a double quantum well system in a realistic experiment could also lead to the stabilization of the skyrmion stripe (rather than a spiral stripe) phase, especially when the spiral-stripe coupling is weakened by the finite temperature and/or finite disorder effects.

## B. Role of spin degree of freedom in level crossing

From the results presented in Sections IV and V for wide well systems, we find that systems of odd filling factors ( $W1$  and  $W1'$ ) have more interesting coherent phases with exotic quantum order than the systems of even filling factor ( $W2$  and  $W2'$ ). As summarized in Table I, the HF trial wavefunction, Eq. (36), stabilizes an isospin coherent phase in  $W1$ , and an isospin skyrmion stripe phase in  $W1'$ . For systems at even filling factors, strictly speaking, no novel quantum phases are obtained in the wide well systems within our HF approximation (although sometimes the exotic phases are very quantum closeby in energy). Since the orbital wavefunctions of the two crossing levels in the even filling systems are the same as those in the odd filling systems, it is natural to attribute the important difference between the two systems to the additional spin degree of freedom of the two crossing (or degenerate) levels, that is present in the  $W1/W1'$  cases. More precisely, we can compare the formulae of the HF variational energy of an odd filling system shown in Section IV with the formulae of HF energy of even filling system in Section V, where we can simply take  $\psi'_k = 0$  in Eq. (49) and Eq. (64), and consider the trial wavefunction constructed by the two crossing levels only (instead of the four degenerate levels), similar to Eq. (36). In such situations, the real spin quantum number of the two isospin states are of opposite sign, different from the level crossing in the odd filling system. The resulting HF variational energy (denoted by underlines) then becomes (compared to Eqs. (58)-(60))

$$\underline{E}_0^{W2} = E_{\vec{n}_1, \downarrow}^{0, W} \Theta_1(0) + E_{\vec{n}_2, \uparrow}^{0, W} \Theta_2(0), \quad (90)$$

$$\underline{E}_H^{W2} = \frac{N_\phi}{2\Omega_\perp} \sum_{q_n} \left[ \tilde{V}_{\vec{n}_1 \vec{n}_1, \vec{n}_1 \vec{n}_1}^W(q_n) \Theta_1(q_n)^2 + \tilde{V}_{\vec{n}_2 \vec{n}_2, \vec{n}_2 \vec{n}_2}^W(q_n) \Theta_2(q_n)^2 + 2\tilde{V}_{\vec{n}_1 \vec{n}_1, \vec{n}_2 \vec{n}_2}^W(q_n) \Theta_1(q_n) \Theta_2(q_n) \cos(q_n Q_y l_0^2) \right], \quad (91)$$

$$\underline{E}_F^{W2} = \frac{-1}{2\Omega} \sum_{\vec{q}_\perp} \left[ \tilde{V}_{\vec{n}_1 \vec{n}_1, \vec{n}_1 \vec{n}_1}^W(\vec{q}_\perp) \sum_{q_n} \cos(q_n q_y l_0^2) \Theta_1(q_n)^2 + \tilde{V}_{\vec{n}_2 \vec{n}_2, \vec{n}_2 \vec{n}_2}^W(\vec{q}) \sum_{q_n} \cos(q_n q_y l_0^2) \Theta_2(q_n)^2 \right]$$

$$+ \frac{-2}{2\Omega_{\perp}} \sum_{\vec{q}_{\perp}} \tilde{V}_{\vec{n}_1 \vec{n}_1, \vec{n}_2 \vec{n}_2}^W(\vec{q}_{\perp}) \cos((Q_x q_y - Q_y q_x) l_0^2) \sum_{q_n} \cos(q_n q_y l_0^2) \Theta_3(q_n)^2, \quad (92)$$

where we have neglected those uniform terms (linearly proportional to  $\Theta_i(0)$  for  $i = 1, 2, 3$ ) for simplicity. Comparing Eqs. (90)-(92) with the HF energy of an odd filling system in Eqs. (58)-(60), we find that the odd filling factor systems have one additional term in both Hartree and Fock energies (i.e. the  $E_{H6}^{W1}$  and  $E_{F3}^{W1}$  terms) after neglecting the uniform terms and those singular terms proportional to  $\delta_{Q_y,0}$  shown in Eqs. (58)-(60)). These two additional terms result from the direct and the exchange contractions of the correlation,  $\langle c_{\vec{n}_1, \sigma}^{\dagger} c_{\vec{n}_2, \sigma} c_{\vec{n}_2, \sigma'}^{\dagger} c_{\vec{n}_1, \sigma'} \rangle$ , which is absent at even filling factors, because the two relevant levels,  $\vec{n}_1$  and  $\vec{n}_2$ , have opposite spin direction. Since such additional exchange energy is larger than the additional Hartree energy, a coherent phase near the level crossing point can be stabilized more easily in an odd filling system than in an even filling system. This mechanism explains the results we obtain in the wide well system within the HF approximation, although it does not exclude the possibility of having a many-body phase in an even filling system in more sophisticated theories.

Such effects of spin degree of freedom can also be observed from the results of the double well systems ( $D1$  and  $D2$ ). When considering only the two crossing levels in  $\nu = 4N + 2$  case, we will not obtain any many-body state for the same reason as mentioned above. The coherent phase (i.e. commensurate canted antiferromagnetic phase) obtained in the literature [33,34,36] and in this paper strictly relies on the incorporation of all the four degenerate levels (see Sections III B and VII). On the other hand, at least four different many-body phases (see discussion in Section VI and Fig. 12) are obtained as ground states at  $\nu = 4N + 1$  within the HF approximation. In the odd filling case, electrons in the top level equally occupy the two layers, and therefore when the layer separation is larger than the order of  $l_0$ , interlayer coherence becomes relatively weaker and a stripe formation may occur in order to optimize the intralayer exchange energy in each layer, reflecting the charge density wave instability studied in the high half-odd-integer single layer systems [4,5]. Such a simple mechanism, however, does not seem to apply to  $\nu = 4N + 2$  case, because every flux quantum is occupied by an electron in each layer — any nonuniform density modulation, as in a stripe phase, will have to pay a large direct energy for the double occupancy of electrons of opposite spins in each layer in each flux quantum. Since the commensurate canted phase can successfully lower the exchange energy by canting both spin and isospin degrees of freedom, a stripe phase becomes unlikely in the even filling factor  $\nu = 4N + 2$  bilayer case (at least in the absence of any external bias voltage). When an external gate voltage is applied in the growth direction of the two layers, the two layers become partially filled, and there might be some interesting stripe phase in this situation, at least for the following extreme case: when the gate voltage between the two layers is so large that the filling factor of the left layer is near  $2N + 1/2$  and of the right layer is near  $2N + 3/2$ , the two layers can form stripe phases individually similar to those well-known single layer systems at high half-odd-integer filling factors ( $N \geq 1$ ) [1] (especially if the layer separation is so large that the tunneling energy and interlayer interaction are negligible).

### C. Comparison with the exchange induced spin density wave in a very wide well

It is very interesting and instructive to compare our results of stripe phases with the spin density instabilities proposed first by Brey and Halperin (BH) [44] in a wide parabolic well system and by Das Sarma and Tamborenea [59] in a zero-field double quantum well system. In Ref. [44], it is found that when an in-plane magnetic field is applied (without any perpendicular magnetic field) to a very wide parabolic well (width is  $\sim 4000$  Å), Hartree energy between electrons inside the well modifies the electron density profile to be almost a uniform slab, making the parabolic well a good approximation of the 3D jellium model where electrons move in a constant positive charge background. Calculation of spin density correlation function shows that a divergent singularity occurs at a certain wavevector in  $x$  direction (parallel to the in-plane field),  $Q_x^{BH} = k_{F,\uparrow} + k_{F,\downarrow}$ , where  $k_{F,\sigma}$  is the Fermi wavevector of spin  $\sigma$  electrons. They proposed that such spin density wave instability is similar to those originally proposed by Celli and Mermin [60] in three-dimensional systems and may cause a resistance anisotropy in the  $x - y$  plane of the well. This result [44] seems to contradict the spiral direction suggested by the magneto-roton minimum of the magnetoplasmon mode [17] as well as our HF calculation in this paper for a wide parabolic well system at the even filling factor, where the softening of the spin triplet magnetoplasmon mode (i.e. the divergence of a spin density correlation function) is in  $y$  direction, perpendicular to the in-plane magnetic field. Besides, the wavevector of the BH spin density wave mode softening,  $Q_x^{BH}$ , depends mainly on the electron density and is almost independent of the magnetic field strength, while the wavevector of the mode softening in our calculation crucially depends on the in-plane magnetic field strength and is almost independent of the electron total density [17]. Here we analyze the superficial contradiction between our results in this paper and the BH results, providing a deeper understanding of these two calculations. We find that both results are correct, and their different characteristic spin density wave vectors arise entirely from considerations of different limits of system parameters in the two situations.

First we should clarify the energy scales of the wide well system we are going to discuss. For the quantum Hall situation of our interest in this paper, the perpendicular magnetic field is always finite ( $B_{\perp} \sim 3$  Tesla, i.e.  $\omega_{\perp} \sim 5$  meV) to ensure the existence of a discrete orbital Landau level spectrum. The well width is chosen to have a comparable ( $\omega_0 \sim \omega_{\perp}$ ) bare confinement energy  $\omega_0 \sim 7$  meV. The (iso)spin density wave instability (for both odd and even filling factor) in this system occurs in a very high in-plane magnetic field region ( $B_{\parallel} \sim 10 - 30$  T, or  $\omega_{\parallel} \sim 17 - 50$  meV). Therefore we can obtain the following approximate order of energy scales for the system of our interest in the current paper (using the even filling factor system as an example)

$$\omega_{\perp} \sim \omega_0 \ll \omega_{\parallel}, \text{ and } N_{\uparrow} \sim N_{\downarrow} \sim \mathcal{O}(1), \quad (93)$$

where  $N_{\sigma}$  is the Landau level index of the highest filled level of spin  $\sigma$ , and the total filling factor  $\nu = N_{\uparrow} + N_{\downarrow} + 2$  is of order of unity, A small parameter,  $\epsilon \equiv \text{Max}(\omega_{\perp}, \omega_0)/\omega_{\parallel} \ll 1$  can therefore be defined. In this limit, we have  $\omega_1 \rightarrow \omega_{\parallel}$  and  $\omega_2 \rightarrow \epsilon^2 \omega_{\parallel}$  for the two noninteracting Landau energy separation (see Eq. (2)). Besides, the two effective magnetic lengths,  $l_{1,2} \equiv \sqrt{1/m^* \omega_{1,2}}$ , defined in Eq. (5) (or see Ref. [17]) become  $l_0 \epsilon^{1/2}$  and  $l_0 \epsilon^{-1/2}$  respectively. On the other hand, for the system discussed by BH [44], no perpendicular magnetic field is applied and the predicted spin density wave instability occurs at an intermediate strength of  $B_{\parallel}$  ( $\sim 1$  Tesla, i.e.  $\omega_{\parallel} \sim 1.7$  meV) for a very wide well (for width about 4000 Å, the parabolic confinement energy  $\omega_0 < 0.05$  meV). Therefore we can obtain the following approximate order of energy scales for the BH system:

$$\omega_{\perp} \ll \omega_0 \ll \omega_{\parallel}, \text{ and } N_{\uparrow} \sim N_{\text{tot},\uparrow}, N_{\downarrow} \sim N_{\text{tot},\downarrow}, \quad (94)$$

where  $N_{\text{tot},\uparrow(\downarrow)}$  is the total electron number of spin up(down) (in the direction parallel to  $B_{\parallel}$ ), and hence the Landau level degeneracy,  $N_{\phi}$ , is only of the order of unity in this weak  $B_{\perp}$  limit. Therefore there are two small parameters we can construct for the BH system:  $\epsilon \equiv \text{Max}(\omega_{\perp}, \omega_0)/\omega_{\parallel} = \omega_0/\omega_{\parallel} \ll 1$  as defined earlier and  $\alpha \equiv (\omega_{\perp}/\omega_0)^2 \ll 1$ , which is of order unity in the system of our interest in this paper. In this limit (Eq. (94)),  $\omega_{1,2}$  are still the same as above (i.e. close to  $\omega_{\parallel}$  and  $\epsilon^2 \omega_{\parallel}$  respectively), while  $l_1 \rightarrow l_0 \epsilon^{1/2} \alpha$  and  $l_2 \rightarrow l_0 \epsilon^{-1/2} \alpha$ . Note that although both  $\epsilon$  and  $\alpha$  are small numbers for the BH system, an additional constraint,  $\alpha \ll \epsilon$ , exists also, to ensure the fact that no perpendicular magnetic field is applied. We will show below that this additional constraint (i.e.  $\alpha \ll \epsilon$ ) and the resulting small Landau level degeneracy ( $N_{\phi} \sim \mathcal{O}(1)$ ) are the key points needed to understand BH's result of SDW instability from the perspective of our theory.

For the convenience of comparison, we still consider the two level degeneracy on the top of the filled Landau levels and use the "core state" approximation for a qualitative discussion, although it is certainly a bad approximation in the limit of Eq. (94), where the Landau level energy separation goes to zero. To simplify our analysis, we calculate  $E_X^{W2}(\vec{Q}_{\perp})$  shown in Eq. (69) only, which corresponds to the electron-hole binding energy via ladder diagrams and gives rise to the roton minimum of the magnetoplasmon dispersion [17], and use a zero-range contact electron-electron interaction. We can obtain the following approximate  $E_X^{W2}(\vec{Q}_{\perp})$  by using the analytical expression of  $A(\vec{q})$  in Eq. (B1) and taking the  $\epsilon \rightarrow 0$  limit:

$$\begin{aligned} E_X^{W2}(\vec{Q}_{\perp}) &= \frac{-V_0}{\Omega} \sum_{\vec{q}} A_{\vec{n}_1 \vec{n}_1}^W(-\vec{q}) A_{\vec{n}_2 \vec{n}_2}^W(\vec{q}) \cos((q_x Q_y - q_y Q_x) l_0^2) \\ &\sim \frac{-V_0}{\Omega} \sum_{\vec{q}} \exp \left[ -\frac{\epsilon^2 \alpha (q_y l_0)^2 + (\epsilon \sqrt{\alpha} q_x l_0 - q_z l_0)^2 \epsilon^2 \alpha^4}{2\epsilon \alpha^2} \right] \exp \left[ -\frac{(q_y l_0)^2 + (q_x l_0 + \epsilon \sqrt{\alpha} q_z l_0)^2 \alpha^4 / \epsilon^2}{2\alpha^2 / \epsilon} \right] \\ &\quad \times L_{N_{\uparrow}+1}^0 \left( \frac{(q_y l_0)^2 + (q_x l_0 + \epsilon \sqrt{\alpha} q_z l_0)^2 \alpha^4 / \epsilon^2}{2\alpha^2 / \epsilon} \right) L_{N_{\downarrow}}^0 \left( \frac{(q_y l_0)^2 + (q_x l_0 + \epsilon \sqrt{\alpha} q_z l_0)^2 \alpha^4 / \epsilon^2}{2\alpha^2 / \epsilon} \right) \cos((q_x Q_y - q_y Q_x) l_0^2), \end{aligned} \quad (95)$$

where we have let  $\vec{n}_1 = (0, N_{\downarrow})$  and  $\vec{n}_2 = (0, N_{\uparrow} + 1)$  for the orbital level index of the top filled and the lowest empty levels respectively.

For the quantum Hall system of our interest in this paper,  $\alpha$  is of the order of unity (see Eq. (93)), and then the above equation can be simplified further (denoted by  $E_X^{W2,1}(\vec{Q}_{\perp})$ ) by keeping only the leading term in  $\epsilon$ :

$$\begin{aligned} E_X^{W2,1}(\vec{Q}_{\perp}) &\sim \frac{-V_0}{\Omega} \sum_{\vec{q}} \exp \left[ -\frac{(q_z l_0)^2 \epsilon \alpha^2}{2} \right] \exp \left[ -\frac{(q_x l_0)^2 \alpha^2}{2\epsilon} \right] L_{N_{\uparrow}+1}^0 \left( \frac{(q_x l_0)^2 \alpha^2}{2\epsilon} \right) L_{N_{\downarrow}}^0 \left( \frac{(q_x l_0)^2 \alpha^2}{2\epsilon} \right) \cos((q_x Q_y - q_y Q_x) l_0^2) \\ &\propto -\frac{V_0 \delta_{Q_x,0}}{2\pi} \int dq_x \exp \left[ -\frac{q_x^2 l_0^2}{2} \right] \left( \frac{q_x^2 l_0^2}{2} \right)^{2N+1} \cos(q_x Q_y l_0^2) \end{aligned} \quad (96)$$

where we have used  $L_n^0(x) \propto x^n$  for  $x \gg 1$ ,  $N_\uparrow = N_\downarrow = N = (\nu - 2)/2$  for even filling system, and  $l_2/l_0 \sim \alpha/\sqrt{\epsilon}$ . It is very easy to see from Eq. (96) that  $E_X^{W2,1}(\vec{Q}_\perp)$  is nonzero *only* at  $Q_x = 0$  and a finite  $Q_y$ . The extreme value of  $Q_y$  to optimize the exchange energy is given by the length scale generated by the competition between the exponential function and the power-law function, proportional to  $\sqrt{N}l_2^{-1}$ . This is consistent with our numerical results obtained either from the HF variational calculation in this paper or from the collective mode calculation in our earlier work [17].

On the other hand, if we take  $\alpha \rightarrow 0$  first in Eq. (95) as appropriate for the situation considered by BH, we obtain the electron-hole binding energy (denoted by  $E_X^{W2,2}(\vec{Q}_\perp)$ ) to be

$$\begin{aligned} E_X^{W2,2}(\vec{Q}_\perp) &\sim \frac{-V_0}{\Omega} \sum_{\vec{q}} \exp\left[-\frac{\epsilon(q_y l_0)^2}{2\alpha}\right] \exp\left[-\frac{\epsilon(q_y l_0)^2}{2\alpha^2}\right] L_{N_\uparrow+1}^0\left(\frac{\epsilon(q_y l_0)^2}{2\alpha^2}\right) L_{N_\downarrow}^0\left(\frac{\epsilon(q_y l_0)^2}{2\alpha^2}\right) \cos((q_x Q_y - q_y Q_x)l_0^2) \\ &\sim B - \delta_{Q_y,0} C \int_{l_2/l_0^2}^{+\infty} \frac{dq_y l_2}{q_y l_0^2} \cos(\sqrt{2N_\uparrow} q_y l_0^2/l_2) \cos(\sqrt{2N_\downarrow} q_y l_0^2/l_2) \cos(q_y Q_x l_0^2), \end{aligned} \quad (97)$$

where we have used the asymptotic formulae,  $L_n^0(x) \propto e^{x/2} x^{-1/4} \cos(2\sqrt{nx})$  for large  $n$  [61], and have let the constant contribution from integration of small  $q_y$  region to be denoted by  $B$ ;  $C$  is a constant factor. It is easy to see that the maximum electron-hole (exciton) binding energy occurs at  $Q_y = 0$  and  $Q_x \sim \pm(k_{F,\uparrow} + k_{F,\downarrow})$ , where the Fermi wavevector is determined by the Fermi energy,  $k_{F,\sigma} = \sqrt{2m^*(E_{F,\sigma} - E_{k=0})} \sim \sqrt{2m^*(E_{(0,N_\sigma),\sigma}^{0,W} - E_{(0,0),\sigma}^{0,W})} = \sqrt{2m^*N_\sigma\omega_2} = \sqrt{2N_\sigma}l_2^{-1}$ , for spin  $\sigma$  subband ( $E_k = k^2/2m^*$  is the usual free particle zero-field energy dispersion with effective mass  $m^*$ ). Therefore Eq. (97) is consistent with the result obtained by BH, showing a SDW instability along the in-plane field direction ( $x$ ) with a wavevector,  $Q_x = \pm(k_{F,\uparrow} + k_{F,\downarrow})$ . Note that the maximum  $E_X^{W2,2}(Q_x, 0)$  does not occur at  $Q_x = \pm(k_{F,\uparrow} - k_{F,\downarrow})$  because the decaying function,  $q_y^{-1}$  in Eq. (97) has higher contribution from the small  $q_y$  region, and hence a larger value of  $|Q_x|$  (i.e.  $|k_{F,\uparrow} + k_{F,\downarrow}|$ ) should give stronger electron-hole binding energy than a smaller value of  $|Q_x|$  (i.e.  $|k_{F,\uparrow} - k_{F,\downarrow}|$ ). This effect is enhanced for the long-ranged Coulomb interaction, which has a faster decaying function in  $q_y$ . Therefore our simple analysis above shows that the apparent inconsistency between of the SDW spiral winding direction studied in our work [17] and in the BH work [44] is just due to the different limits of interest in the two works: A quantum Hall situation with finite  $B_\perp$  in our case and the “zero-field”  $B_\perp = 0$  situation in Ref. [44].

We now summarize the above discussion on the spiral (spin-density-wave) order of a wide well system in the presence of in-plane magnetic field (along  $x$  axis): when a strong perpendicular magnetic field is applied so that only few Landau levels are occupied and the in-plane field is tuned to be close to a level crossing (or a level near degeneracy) point, the (iso)spin spiral winding prefers a specific wavevector in a direction ( $y$ ) perpendicular to the in-plane field, while the (iso)spin  $\langle I_z \rangle$  oscillates in  $x$  direction; when the perpendicular magnetic field is reduced to a very small value, the electron wavefunction near Fermi energy becomes a plane wave and strongly modifies the interaction matrix elements through the form function — the spin-flip exchange energy then stabilizes the spin density wave at a wavevector  $Q_x^* \sim \pm(k_{K,\uparrow} + k_{F,\downarrow})$ . The spin (or isospin) density wave state actually results from two different mechanisms in the two different limits of the same system. These results are independent of the gauge choice in the theory.

#### D. Effective Hamiltonian of wide well at $\nu = 2N + 1$ around intersubband level crossing point (W1 case)

In the previous sections, we have been using the concept of “isospin” to discuss the ground state wavefunction properties in both the wide well systems and the double well systems. Without losing generality, one can also apply the isospin concept to effectively represent the Hamiltonians of these systems so that some aspects of this physical properties (e.g. collective excitations or finite temperature effects) may be studied in a more comprehensive way. Here we will give the effective Hamiltonian of a wide well system at  $\nu = 2N + 1$  near the intersubband level crossing point in the isospin representation after projecting the whole system into the two crossing levels we consider in this paper. According to our HF calculation results presented in Section IV, only the uniform coherent phase is stabilized in this intersubband level crossing region, and therefore we will not consider the stripe order (modulation of isospin  $z$  component) here for simplicity.

For convenience of comparison, we redefine the isospin component to be (c.f. Eqs. (38) and (39)):

$$\tilde{\mathcal{I}}_\alpha^{W1}(\vec{r}_\perp) = \frac{1}{2\Omega_\perp} \sum_{\vec{q}_\perp} e^{i\vec{q}_\perp \cdot \vec{r}_\perp} \rho_{I_1 I_2}^{W1}(\vec{q}_\perp) \sigma_{I_1 I_2}^\alpha, \quad (98)$$

where  $\alpha = x, y, z$  and  $\sigma_{I_1 I_2}^\alpha$  is the Pauli matrix element. Therefore the low energy effective Hamiltonian for a wide well system at  $\nu = 2N + 1$  can be obtained from Eq. (9) by using Eq. (98) and considering the long wavelength limit:

$$\mathcal{H}_{eff}^{W1} = \int d\vec{r}_\perp \left\{ (h + g_{z0}) \tilde{\mathcal{I}}_z^{W1} + g_{zz} \left( \tilde{\mathcal{I}}_z^{W1} \right)^2 + [g_\perp + g_X \cos(2\gamma) + \tilde{g}_{\alpha\beta}(\gamma) (\nabla_\alpha \gamma) (\nabla_\beta \gamma)] \left( \tilde{\mathcal{I}}_\perp^{W1} \right)^2 \right\} \quad (99)$$

where we have used  $\tilde{\mathcal{I}}_x^{W1} = \tilde{\mathcal{I}}_\perp^{W1} \cos \gamma$  and  $\tilde{\mathcal{I}}_y^{W1} = \tilde{\mathcal{I}}_\perp^{W1} \sin \gamma$  to address the phase dependence in the isospin  $x - y$  components.  $\nabla_\alpha$  is the spatial derivative of phase  $\gamma$  in  $\alpha = x, y$  direction. The coefficients shown above are respectively

$$h = E_{\vec{n}_1, \uparrow}^{0,W} - E_{\vec{n}_2, \uparrow}^{0,W}, \quad (100)$$

$$g_{z0} = \frac{1}{2} [\mathcal{V}_{\uparrow\uparrow, \uparrow\uparrow}^W(0) - \mathcal{V}_{\downarrow\downarrow, \downarrow\downarrow}^W(0)], \quad (101)$$

$$g_{zz} = \frac{1}{2} [\mathcal{V}_{\uparrow\uparrow, \uparrow\uparrow}^W(0) + \mathcal{V}_{\downarrow\downarrow, \downarrow\downarrow}^W(0) - 2\mathcal{V}_{\uparrow\uparrow, \downarrow\downarrow}^W(0)], \quad (102)$$

$$g_\perp = 2\mathcal{V}_{\uparrow\downarrow, \downarrow\uparrow}^W(0), \quad (103)$$

$$g_X = \mathcal{V}_{\uparrow\downarrow, \uparrow\downarrow}^W(0), \quad (104)$$

$$\tilde{g}_{\alpha\beta}(\gamma) = \delta_{\alpha\beta} \partial_\alpha \partial_\beta \mathcal{V}_{\uparrow\downarrow, \downarrow\uparrow}^W(0) - |\partial_\alpha \partial_\beta \mathcal{V}_{\uparrow\downarrow, \downarrow\uparrow}^W(0)| \cos \left( 2\gamma + \frac{\pi}{2} (1 - \delta_{\alpha\beta}) \right), \quad (105)$$

where we have used the fact that  $\mathcal{V}_{\uparrow\downarrow, \uparrow\downarrow}^W(0)$  and  $\partial_{x(y)}^2 \mathcal{V}_{\uparrow\downarrow, \uparrow\downarrow}^W(0)$  ( $\partial_\alpha$  is the derivative in the  $\alpha = x(y)$  component of wavevector,  $\vec{q}_\perp$ ) are pure real, and  $\partial_x \partial_y \mathcal{V}_{\uparrow\downarrow, \uparrow\downarrow}^W(0)$  is pure imaginary giving an additional phase  $\pi/2$ . The effective interaction matrix element,  $\mathcal{V}_{I_1 I_2, I_3 I_4}^W(\vec{q}_\perp)$ , can be obtained within the Hartree-Fock theory:

$$\mathcal{V}_{I_1 I_2, I_3 I_4}^W(\vec{q}_\perp) \equiv \frac{1}{2\pi l_0^2} \tilde{V}_{I_1 I_2, I_3 I_4}^W(\vec{q}_\perp) - \frac{1}{\Omega_\perp} \sum_{\vec{p}_\perp} \tilde{V}_{I_1 I_4, I_3 I_2}^W(\vec{p}_\perp) e^{i(q_x p_y - p_x q_y) l_0^2}. \quad (106)$$

From the effective Hamiltonian in Eq. (99), we can see that the effective “Zeeman” energy,  $h + g_{z0}$ , is the same as the single electron energy gap between the two crossing levels (including the HF correction). Therefore when such “Zeeman” energy is dominant in Eq. (99) (i.e. the two levels are far from crossing region), the isospin direction must be polarized at  $\tilde{\mathcal{I}}_z^{W1} = \pm 1/2$  and hence the ground state has no transverse component, i.e.  $\tilde{\mathcal{I}}_\perp^{W1} = 0$ . These are the conventional integer QH states with electrons of the top filled Landau level being at level  $\vec{n} = (1, 0)$  (for isospin up) and at  $\vec{n} = (0, N)$  (for isospin down) respectively. In the intermediate region between the two states (see also Fig. 7(b)), where  $|h + g_{z0}|$  is small compared with the other energy scales, the transverse isospin component,  $\tilde{\mathcal{I}}_\perp^{W1}$  may become finite to minimize the energy so that the isospin polarization becomes canted. The prefactor,  $\cos(2\gamma)$ , of the  $g_X$  term in Eq. (99) selects  $\gamma = 0, \pi$  to be the two degenerate points of the lowest energy, showing that only  $\tilde{\mathcal{I}}_x^{W1}$  is finite and there is no isospin in  $y$  direction. This two-point degeneracy results from the fact that only the parity symmetry is broken in the intermediate region. The coefficient of the gradient term,  $\tilde{g}_{\alpha\beta}(\gamma)$ , is positive in such an intersubband level crossing case so that the optimal value of phase  $\gamma$  is always a constant in space, confirming the fact that no spiral order exists in the coherent phase.

For the convenience of comparison, here we also show the effective Hamiltonian of the double well system at  $\nu = 4N + 1$  using the same definition of isospins in the layer index basis ( $B_\parallel$  is along  $x$  axis):

$$\begin{aligned} \mathcal{H}_{eff}^{D1} = \int d\vec{r}_\perp & \left\{ -\Delta_{SAS} \cos(\gamma - P_{xy}) \tilde{\mathcal{I}}_\perp^{D1} + [\mathcal{V}_{\uparrow\uparrow, \uparrow\uparrow}^D(0) - \mathcal{V}_{\uparrow\uparrow, \downarrow\downarrow}^D(0)] \left( \tilde{\mathcal{I}}_z^{D1} \right)^2 \right. \\ & \left. + [2\mathcal{V}_{\uparrow\downarrow, \downarrow\uparrow}^D(0) + \partial_\alpha^2 \mathcal{V}_{\uparrow\downarrow, \downarrow\uparrow}^D(0) (\nabla_\alpha \gamma)^2] \left( \tilde{\mathcal{I}}_\perp^{D1} \right)^2 \right\}, \end{aligned} \quad (107)$$

where  $\mathcal{V}_{I_1 I_1, I_2 I_2}^D(\vec{q}_\perp)$  is similarly defined as Eq. (106) now for the double well system. Without losing generality, the effective Hamiltonian of the wide well system in Eq. (99) is similar to that of the double well system in Eq. (107) [26], except that in the former case the in-plane field is included implicitly in the interaction matrix element,  $\tilde{V}_{I_1 I_2, I_3 I_4}^W(\vec{q}_\perp)$  and the isospin stiffnesses in  $x$  and  $y$  directions depend on the isospin direction. The effective “tunneling” amplitude,  $g_X$ , in the wide well system originates from the Coulomb exchange energy and as such is not an independent physical quantity (in contrast to) the tunneling energy in the double well system, which is an independent physical parameter. When considering the intersubband level crossing in the small in-plane magnetic field range (i.e.  $W1$  case),  $\tilde{g}_{\alpha\beta}(\gamma)$  is always positive as mentioned above, so that the phase is fixed to be 0 or  $\pi$  similar to the commensurate phase

in the double well system at  $\nu = 4N + 1$ , where only  $\gamma = 0$  is chosen by the tunneling energy,  $\Delta_{SAS}$ . However, if we apply Eq. (99) to the *intrasubband* level near degeneracy case in the strong in-plane field region (i.e.  $W1'$  case),  $\tilde{g}_{\alpha\beta}(\gamma)$  may become negative, so that the total energy can be minimized at some finite isospin winding in the isospin  $x - y$  plane (say,  $\gamma = P_xy$  becomes a function of spatial coordinate). This result leads to the finite spiral order of the isospin skyrmion stripe phase as discussed in Section VI in the large in-plane field region. In such a case, the effective “tunneling” amplitude,  $g_X$ , becomes zero since the space average of  $\cos(2\gamma) = \cos(2P_xy)$  vanishes. Phenomenologically this situation is similar to the incommensurate state of the double well system, where the tunneling energy is dominated by the Coulomb exchange energy so that the phase is not fixed by the in-plane field. But in such intrasubband level near degeneracy case, we will also have to consider the stripe order (gradient term of  $\tilde{\mathcal{I}}_z^{W1}$ ) to obtain the a full effective Hamiltonian in describing the skyrmion stripe phase obtained in the HF calculation. Finally we note that in general, the interlevel(layer) scattering amplitude (proportional to  $\mathcal{V}_{\uparrow\downarrow,\uparrow\downarrow}^{W(D)}(\vec{q}_\perp)$ ) is finite in the wide well system, while it is zero in the double well system due to the layer separation. This gives the finite values of  $g_X$  and the second term of  $\tilde{g}_{\alpha\beta}(\gamma)$ , according to Eqs. (104)-(105), and leads to the major difference between a wide well system and a double well system.

From the experimental point of view, however, a smooth crossover from a wide well system to a double well system can be observed in the same semiconductor system by tuning some parameters, e.g. electron density [62] due to the Coulomb screening effects on the confinement potential. It is therefore very interesting to investigate such crossover from monolayer to bilayer systems from a more fundamental theory — they are usually assumed to be two different systems when studied in the literature (the inclusion of a modified form function to take into account the finite width effect in the double well system does not help in this comparison). The effective Hamiltonians shown above could be a good starting point for this problem, but we will not discuss it further here since it must incorporate one-electron self-consistent potential [45,59] in the confinement potential which is beyond the scope of our approximation scheme. We must emphasize that it is useful to remember that the bilayer and the wide well systems may be continuously tuned into each other by changing the system carrier density.

### E. Instability of the stripe phases and the domain wall formation

In a single well system at partial filling factors, another interesting kind of charge density wave ground state, the so-called “bubble phase”, may occur when the filling factor of the top level is away from the exact half odd integer values [1]. It is believed that when the filling factor of the top Landau level is below about 0.4, electrons in the top level may lower their potential energy by accumulating to become bubbles, rather than stripes, in the two dimensional plane [63]. The equivalent “bubbles of holes” may occur when the filling factor of the top level is between 0.6 and 1. This phase can be understood as the edge state instability of the stripe phase due to the backward scattering between the two nearest edges, leading to the breaking up of the stripes into segments. These segments of stripes then rearrange their shapes and positions to form bubbles in a lattice to lower their total energy. (The strong field Wigner crystal phase can be viewed as an extreme limit of the bubble phase — having only one electron in each “bubble”.) A possible experimental evidence for such an interesting phase is the reentrant integer quantum Hall effect observed recently [1,64]. Similar nonstripe density modulation may also occur in the integral quantum Hall systems discussed in this paper. Near the level degeneracy region, the edge state instability may be strong enough to break the stripe phase and form several “bubble-like” domain walls inside which the isospin  $\langle I_z \rangle$  is different from that outside the domain wall. Some spiral winding structure may appear at the surface of the domain wall to reduce the Hartree energy (see Fig. 14). Such domain wall structures could be stabilized by the presence of surface disorder as suggested in Ref. [53], and may also lead to the observed resistance anisotropy [15,16]. However, this domain wall phase cannot be included in the trial wavefunctions we propose in this paper [65], and we speculate that they may be important in understanding some other experimental results, such as the hysteretic behavior in the magnetoresistance experiments [51,52].

### F. The $\nu = 1$ bilayer system

There has been a great deal of recent experimental and theoretical interest in the (weak-tunneling) bilayer double well system at  $\nu = 1$ , i.e.  $N = 0$  case, which has essentially been left out of our consideration in this paper where we have mostly restricted ourselves to the case  $N \geq 1$ , with  $\nu = 4N + 1$  ( $D1$ ) or  $4N + 2$  ( $D2$ ), level crossing bilayer situation. (The  $\nu = 1$  bilayer case can be thought of as an isospin level crossing situation for  $N = 0$  in our notation.) Here we provide some brief comments on the  $\nu = 1$  bilayer situation in the context of our theoretical results presented in this paper. The specific issue we addresses is the nature of the phase transition in  $\nu = 1$  bilayer system as the

layer separation ( $d$ ) is increased in the zero (or weak) tunneling situation. It is commonly believed, not however based on any really compelling evidence, that the  $\nu = 1$  bilayer system undergoes a first order transition from an incompressible interlayer-coherent quantum hall state (presumably a Halperin (1,1,1) state [23]) to a compressible state (presumably two decoupled  $\nu = 1/2$  single-layer states) as  $d$  increases above a critical value (which depends on the tunneling strength). We want to suggest here another distinct possibility based on our results presented in this paper. It is in principle, possible for the transition to be a second order quantum phase transition (rather than a direct first order transition) to a many-body state with exotic quantum order, such as an isospin stripe phase discussed in this paper. Such an exotic phase will still be incompressible (for low value of disorder), but perhaps with a much smaller value of the incompressibility gap. (The system will make a transition to the compressible state of two decoupled  $\nu = 1/2$  layers at some still larger nonuniversal value of  $d$ .) We believe that there is already some evidence supporting our suggested “double-transition” scenario (a second order transition to a weakly incompressible stripe phase at  $d = d_{c1}$ , followed by a first order transition to the compressible decoupled  $\nu = 1/2$  layers at  $d = d_{c2} > d_{c1}$ ). In particular, the early calculation of Fertig [56] finding a finite wavevector magnetoplasmon mode softening in bilayer TDHF theory indicates the obvious possibility of an isospin stripe formation at the characteristic wavevector of mode softening. The second order quantum phase transition associated with this mode softening leads to an incompressible state (at low disorder) which has a finite quasiparticle gap (perhaps reduced from that in the uniform (1,1,1) phase). At some higher value of disorder the stripes would eventually be pinned independently in each layer, leading to an incompressible-to-compressible phase transition as a function of increasing disorder. (This is also consistent with experiment where all the interesting results are typically obtained in extremely high mobility bilayer samples.) The level crossing HF technique used in our current work is unfortunately unsuitable to investigate the  $\nu = 1$  bilayer case, which has to be studied by the direct numerical diagonalization technique. It is therefore encouraging that there is recent numerical evidence [66] in apparent support of the scenario as proposed here. The recent experimental results of inelastic light scattering [67], showing that the magneto-roton excitation is softened at a layer separation very close to the incompressible-to-compressible phase boundary, is also consistent with our scenario that there is an intermediate second order phase transition to a stripe phase before the system undergoes the first order transition to a compressible state. The magnetoresistance anisotropy measurement around the critical layer separation of the observed magneto-roton excitation softening (which is also very close to the incompressible-to-compressible phase transition boundary) should be a good test of such charge density wave order in the  $\nu = 1$  incompressible quantum Hall system.

## IX. SUMMARY

In this paper, we use the mean-field HF approximation to systematically study the possible spontaneous breaking of parity, spin, and translational symmetries in different integer quantum Hall systems in the presence of an in-plane magnetic field, concentrating on the level crossing situation in wide parabolic well and bilayer double well systems for both even and odd filling factors. We propose a general class of variational wavefunctions to include the isospin spiral and isospin stripe orders simultaneously, and discuss the symmetry breaking as well as the exotic quantum order properties of various many-body phases generated by our wavefunctions. Comparing the HF energies of these many-body phases, we find several of them can be stabilized near the level crossing or level near degeneracy regions of different systems, breaking certain system symmetries as listed in the last two columns of Table I: (i) for a wide well system at  $\nu = 2N + 1$ , we find an isospin coherent phase in the intersubband level crossing region (small  $B_{\parallel}$ ), breaking the parity symmetry only, and an isospin skyrmion stripe phase in the intrasubband level near degeneracy region (large  $B_{\parallel}$ ), breaking the parity and the translational symmetries in both  $x$  and  $y$  directions simultaneously and having finite topological isospin density, which leads to appreciable charge oscillations in the direction parallel to the in-plane field; (ii) for a wide well system at  $\nu = 2N + 2$ , we find direct first order phase transitions between simple (un)polarized QH states in both intersubband and intrasubband level crossing regions, but we suggest that the resistance anisotropy observed recently by Pan *et. al.* [15] may possibly be explained by a skyrmion stripe phase by going beyond the HF approximation; (iii) for a double well system at  $\nu = 4N + 1$ , we stabilize the coherent, spiral, coherent stripe, and spiral stripe phases in different parameter regions of the phase diagram (see Fig. 12), and critically discuss the broken symmetries and the exotic quantum order of these many-body phases in Section VID; (iv) for a double well system at  $4N + 2$ , only a coherent phase (= commensurate CAF phase in the literature) is stabilized, breaking parity and spin rotational symmetries simultaneously. We also compare our HF results for these different systems in details, and discuss the influence of wavefunction anisotropy, spiral-stripe coupling, spin degree of freedom and finite well width in Section VIII, manifesting the nontrivial effects of Coulomb interactions in the multi-component quantum Hall systems.

## X. ACKNOWLEDGMENT

This work is supported by the NSF grant DMR 99-81283, DMR 01-32874, US-ONR, DARPA, and ARDA. We thank B. I. Halperin for helpful discussion and critical reading of the manuscript. We also acknowledge useful discussions with C. Kallin, S. Kivelson, A. Lopatnikova, A. MacDonald, C. Nayak, K. Park, D. Podolsky, L. Radzihovsky, and S. Sachdev.

## APPENDIX A: THE VARIATIONAL WAVEFUNCTION FOR STRIPES PARALLEL TO THE IN-PLANE FIELD

In this section we derive a variational trial wavefunction, which describes a stripe phase parallel to the in-plane field in a wide well system. As mentioned in Section III, we choose the Landau gauge,  $\vec{A}_{[x]}(\vec{r}) = (-B_{\perp}y, -B_{\parallel}z, 0)$ , in which particle momentum is conserved along  $x$  axis. We will use the notation " $\bar{O}$ " to denote quantities,  $O$ , in this gauge in order to avoid confusion. The noninteracting Hamiltonian, Eq. (6), becomes

$$\bar{H}_0^W = \frac{1}{2m^*} \left( p_x - \frac{eB_{\perp}y}{c} \right)^2 + \frac{1}{2m^*} \left( p_y - \frac{eB_{\parallel}z}{c} \right)^2 + \frac{p_z^2}{2m^*} + \frac{1}{2}m^*\omega_0^2z^2 - \omega_z S_z. \quad (\text{A1})$$

Setting  $p_x = k$  to be a good quantum number, we can obtain the single electron wavefunction similar to the form of Eq. (4):

$$\bar{\phi}_{\vec{n},s,k}^W(\vec{r}) = \frac{e^{ikx}}{\sqrt{L_x}} \bar{\Phi}_{\vec{n}}^W(y - l_0^2 k, z), \quad (\text{A2})$$

where  $\bar{\Phi}_{\vec{n}}(y, z)$  satisfies the following wave equation:

$$\left[ \frac{1}{2}m^*\omega_{\perp}^2y^2 + \frac{1}{2m^*} \left( p_y - \frac{eB_{\parallel}z}{c} \right)^2 + \frac{p_z^2}{2m^*} + \frac{1}{2}m^*\omega_0^2z^2 - \omega_z S_z \right] \bar{\Phi}_{\vec{n}}^W(y, z) = E_{\vec{n},s}^{0,W} \bar{\Phi}_{\vec{n}}^W(y, z). \quad (\text{A3})$$

If we define an auxiliary function,  $\bar{\Phi}_{\vec{n}}^{W'}(pl_0^2, z)$  to be

$$\bar{\Phi}_{\vec{n}}^{W'}(pl_0^2, z) = \frac{1}{\sqrt{2\pi}l_0} \int dy \bar{\Phi}_{\vec{n}}^W(y, z) e^{-ipy}, \quad (\text{A4})$$

then it is easy to show that  $\bar{\Phi}_{\vec{n}}^{W'}(pl_0^2, z)$  satisfies exactly the same equation as  $\bar{\Phi}_{\vec{n}}^W(x, z)$  in Eq. (1) by redefining  $x = x + kl_0^2$ . Therefore we could write down the complete solution of Eq. (A3) to be

$$\bar{\Phi}_{\vec{n}}^W(y, z) = \frac{l_0}{\sqrt{2\pi}} \int dp e^{ipy} \psi_{n_1}^{(1)}(pl_0^2 \cos \theta - z \sin \theta) \cdot \psi_{n_2}^{(2)}(pl_0^2 \sin \theta + z \cos \theta), \quad (\text{A5})$$

where  $\psi_n^{(i)}(x)$  has been defined in Eq. (5). Note that the energy quantum number,  $\vec{n}$ , is the same as before because the energy eigenvalue is independent of the gauge we choose.

Similar to our analysis in Section III A, we can construct the following trial wavefunction for the possible many-body ground state near the degeneracy point of the two crossing levels (or of the two nearly degenerate levels):

$$|\bar{\Psi}_G\rangle = \sum_k \bar{c}_{1,k}^{\dagger} |LL\rangle$$

$$\begin{bmatrix} \bar{c}_{1,k}^{\dagger} \\ \bar{c}_{2,k}^{\dagger} \end{bmatrix} = \begin{bmatrix} e^{-ik\bar{Q}_y l_0^2/2 - i\bar{\gamma}/2} \cos(\bar{\psi}_k/2) & e^{ik\bar{Q}_y l_0^2/2 + i\bar{\gamma}/2} \sin(\bar{\psi}_k/2) \\ -e^{-ik\bar{Q}_y l_0^2/2 - i\bar{\gamma}/2} \sin(\bar{\psi}_k/2) & e^{ik\bar{Q}_y l_0^2/2 + i\bar{\gamma}/2} \cos(\bar{\psi}_k/2) \end{bmatrix} \cdot \begin{bmatrix} \bar{c}_{\uparrow,k-\bar{Q}_x/2}^{\dagger} \\ \bar{c}_{\downarrow,k+\bar{Q}_x/2}^{\dagger} \end{bmatrix}. \quad (\text{A6})$$

Then the isospin components can be obtained easily in the new ground state wavefunction:

$$\langle \bar{\mathcal{I}}_z(\vec{q}_{\perp}) \rangle = \frac{1}{2} N_{\phi} \delta_{q_x,0} \left[ \bar{A}_{\uparrow\uparrow}^W(\vec{q}_{\perp}, 0) e^{iq_y \bar{Q}_x l_0^2/2} \Theta_1(q_y) - \bar{A}_{\downarrow\downarrow}^W(\vec{q}_{\perp}, 0) e^{-iq_y \bar{Q}_x l_0^2/2} \Theta_2(q_y) \right] \quad (\text{A7})$$

and

$$\langle \bar{\mathcal{I}}_+(\vec{q}_\perp) \rangle = N_\phi \delta_{q_x, \bar{Q}_x} \bar{A}_{\uparrow\downarrow}^W(\vec{q}_\perp, 0) \Theta_3(q_y - \bar{Q}_y) e^{i\bar{\gamma}}. \quad (\text{A8})$$

Therefore the stripe phase constructed in this method is along  $x$  axis and the spiral direction is determined by  $\vec{\bar{Q}}_\perp$ .

Finally it is instructive to point out that the form function obtained from the noninteracting electron wavefunction in Eq. (7) is *invariant* under such gauge transformation. Defining the form function in the new gauge similar to Eq. (7), we have

$$\begin{aligned} \bar{A}_{\vec{n}_1 \vec{n}_2}^W(\vec{q}) &= \int dy \int dz e^{-iq_y y} e^{-iq_z z} \bar{\Phi}_{\vec{n}_1}^W(y - l_0^2 q_x/2, z) \bar{\Phi}_{\vec{n}_2}^W(y + l_0^2 q_x/2, z) \\ &= \frac{l_0^2}{2\pi} \int dy \int dz e^{-iq_y y} e^{-iq_z z} \int dp e^{ip(y - l_0^2 q_x/2)} \bar{\Phi}_{\vec{n}_1}^{W'}(p l_0^2, z) \int dp' e^{ip'(y + l_0^2 q_x/2)} \bar{\Phi}_{\vec{n}_2}^{W'}(p' l_0^2, z) \\ &= \int dx \int dz e^{-iq_x x} e^{-iq_z z} \Phi_{\vec{n}_1}^W(x - l_0^2 q_y/2, z) \Phi_{\vec{n}_2}^W(x + l_0^2 q_y/2, z) = A_{\vec{n}_1 \vec{n}_2}^W(\vec{q}), \end{aligned} \quad (\text{A9})$$

where we have changed the integration variables:  $p = q_y/2 + x/l_0^2$  and  $p' = q_y/2 - x/l_0^2$  in the last equation. Therefore the interaction matrix element,  $\bar{V}_{\vec{n}_1 \vec{n}_2, \vec{n}_3 \vec{n}_4}^W(\vec{q})$  does not change in the new gauge, and the HF variational energies for the wide well system in the new gauge,  $\bar{A}_{[x]}(\vec{r})$ , can be obtained by doing the following simple transformation in Eqs. (59), (60), (66), and (67):  $\bar{V}_{\vec{n}_1 \vec{n}_2, \vec{n}_3 \vec{n}_4}^W(q_n, 0) \rightarrow \bar{V}_{\vec{n}_1 \vec{n}_2, \vec{n}_3 \vec{n}_4}^W(0, q_n)$ ,  $\bar{V}_{\vec{n}_1 \vec{n}_2, \vec{n}_3 \vec{n}_4}^W(q_n, Q_y) \rightarrow \bar{V}_{\vec{n}_1 \vec{n}_2, \vec{n}_3 \vec{n}_4}^W(Q_y, q_n)$ ,  $\Theta_3(q_n - Q_x) \rightarrow \Theta_3(q_n - Q_y)$ ,  $\cos(q_n q_y l_0^2) \rightarrow \cos(q_n q_x l_0^2)$ ,  $\cos(q_n (q_y + Q_y) l_0^2) \rightarrow \cos(q_n (q_x + Q_x) l_0^2)$ ,  $\cos(q_n Q_y l_0^2) \rightarrow \cos(q_n Q_x l_0^2)$ ,  $\cos(q_n (Q_y \pm Q'_y) l_0^2) \rightarrow \cos(q_n (Q_x \pm Q'_x) l_0^2)$ ,  $\Theta_3(q_n \pm Q_x^{(\prime)}) \rightarrow \Theta_3(q_n \pm Q_y^{(\prime)})$ , and  $\cos((q_x Q_y - q_n q_y) l_0^2) \rightarrow \cos((q_y Q_x - q_n q_x) l_0^2)$ . Note that all other physical features of stripe phases (for example, the charge oscillation induced by the topological spin density of a skyrmion stripe phase in Appendix C and the perturbation theory for the stripe formation in Section III C, etc.) developed in the main text for the stripe aligned along  $y$  axis can also directly apply to the stripe phase along  $x$  axis in a similar way. The stripe phases constructed in a four level coherent trial wavefunction as shown in Section III B for even filling systems can also be obtained similarly.

## APPENDIX B: ANALYTICAL EXPRESSION OF THE FORM FUNCTION

The explicit formula for the form function,  $A_{\vec{n}_\alpha \vec{n}_\beta}^W(\vec{q})$ , defined in Eq. (7) can be evaluated analytically via a special function [17]. Here we just show the analytical results (for convenience, we define  $\vec{n}_\alpha = (n_\alpha, n'_\alpha)$  and  $\vec{n}_\beta = (n_\beta, n'_\beta)$  to be the Landau level indices of a parabolic wide well system):

$$\begin{aligned} A_{\vec{n}_\alpha \vec{n}_\beta}^W(\vec{q}) &= \sqrt{\frac{n_{\alpha\beta,min}!}{n_{\alpha\beta,max}!} \cdot \frac{n'_{\alpha\beta,min}!}{n'_{\alpha\beta,max}!}} \\ &\times \exp\left[-\frac{\cos^2 \theta(q_y l_0)^2 + (\cos \theta q_x l_0 - \sin \theta q_z l_0)^2 \lambda_1^2}{4\lambda_1}\right] \exp\left[-\frac{\sin^2 \theta(q_y l_0)^2 + (\sin \theta q_x l_0 + \cos \theta q_z l_0)^2 \lambda_2^2}{4\lambda_2}\right] \\ &\times \left(\frac{\mp \cos \theta(q_y l_0) - i(\cos \theta q_x l_0 - \sin \theta q_z l_0) \lambda_1}{\sqrt{2\lambda_1}}\right)^{m_{\alpha\beta}} \left(\frac{\mp \sin \theta(q_y l_0) - i(\sin \theta q_x l_0 + \cos \theta q_z l_0) \lambda_2}{\sqrt{2\lambda_2}}\right)^{m'_{\alpha\beta}} \\ &\times L_{n_{\alpha\beta,min}}^{m_{\alpha\beta}}\left(\frac{\cos^2 \theta(q_y l_0)^2 + (\cos \theta q_x l_0 - \sin \theta q_z l_0)^2 \lambda_1^2}{2\lambda_1}\right) L_{n'_{\alpha\beta,min}}^{m'_{\alpha\beta}}\left(\frac{\sin^2 \theta(q_y l_0)^2 + (\sin \theta q_x l_0 + \cos \theta q_z l_0)^2 \lambda_2^2}{2\lambda_2}\right), \end{aligned} \quad (\text{B1})$$

where  $\pm$  is the sign of  $n_\alpha^{(\prime)} - n_\beta^{(\prime)}$  for each bracket,  $n_{\alpha\beta,min(max)}^{(\prime)} \equiv \text{Min}(\text{Max})(n_\alpha^{(\prime)}, n_\beta^{(\prime)})$ , and  $m_{\alpha\beta}^{(\prime)} \equiv |n_\alpha^{(\prime)} - n_\beta^{(\prime)}|$ ;  $\lambda_{1,2} = l_{1,2}^2/l_0^2 = \omega_\perp/\omega_{1,2}$  are dimensionless parameters,  $L_n^m(x)$  is the generalized Laguerre polynomial [61] and  $\tan(2\theta) \equiv -2\omega_\perp \omega_\parallel / (\omega_b^2 - \omega_\perp^2)$ .

As for a double well system with zero well width, we note that the noninteracting single electron wavefunction in Eq. (4) becomes  $L_y^{-1/2} e^{iky} \psi_n^{(0)}(x + l_0^2 k) \sqrt{\delta(z)}$  for  $\omega_0 \rightarrow +\infty$ , where  $\psi_n^{(0)}(x)$  is the same as Eq. (5) with  $l_i$  replaced by the magnetic length,  $l_0$ . Separating the  $z$  component and integrating  $q_z$  first, we obtain the following isotropic form function:

$$A_{n_\alpha n_\beta}^D(\vec{q}_\perp) = \sqrt{\frac{n_{\alpha\beta,min}!}{n_{\alpha\beta,max}!}} \exp\left[-\frac{q^2 l_0^2}{4}\right] \left(\frac{\pm q_y l_0 - i q_x l_0}{\sqrt{2}}\right)^m L_{n_{min}}^m\left(\frac{q^2 l_0^2}{2}\right), \quad (\text{B2})$$

where  $q = |\vec{q}_\perp|$ , and all other notations are the same as above.

## APPENDIX C: TOPOLOGICAL CHARGE DENSITY IN SKYRMION STRIPE PHASE

According to Ref. [54], the charge density induced by the topological isospin density in the double well system at  $\nu = 1$  can be obtained from the isospin density function,  $\vec{m}(\vec{r}_\perp)$ :

$$\rho_{topo}(\vec{r}_\perp) = -\frac{1}{\pi} \varepsilon_{\mu\nu} \vec{m}(\vec{r}_\perp) \cdot [\partial_\mu \vec{m}(\vec{r}_\perp) \times \partial_\nu \vec{m}(\vec{r}_\perp)], \quad (C1)$$

where the magnitude of  $\vec{m}(\vec{r}_\perp)$  has been normalized to  $\frac{1}{2}$ . In this section we will show that the extra electron charge density,  $\rho_{ex}(\vec{r}_\perp)$ , obtained in Eq. (42) for a skyrmion stripe phase is related to the induced charge density fluctuation calculated by Eq. (C1). Using the isospin density operator defined in coordinate space, Eq. (98), and the trial wavefunction in Eq. (36), we obtain the mean values of the isospinor in the 2D well plane after renormalization by the electron average density,  $(2\pi l_0^2)^{-1}$ :

$$\langle \mathcal{I}_z(\vec{r}_\perp) \rangle = \frac{1}{2} \left\{ 1 - \sum_{q_x} \Theta_2(q_x) [A_{\uparrow\uparrow}(q_x, 0, 0) \cos(q_x(x - Q_y l_0^2/2)) + A_{\downarrow\downarrow}(q_x, 0, 0) \cos(q_x(x + Q_y l_0^2/2))] \right\}, \quad (C2)$$

and

$$\langle \mathcal{I}_+^W(\vec{r}_\perp) \rangle = \langle \mathcal{I}_-^W(\vec{r}_\perp) \rangle^* = \sum_{q_x} \Theta_3(q_x - Q_x) A_{\uparrow\downarrow}(q_x, Q_y, 0) e^{i(q_x x + Q_y y - \gamma)}. \quad (C3)$$

Since Eq. (C1) is valid only to the leading order in (weak) isospin density modulation [54], we should take the limits of small isospin spiral and stripe orders (i.e.  $\tilde{q}l_0 \ll 1$  and  $\tilde{q}Q_y l_0^2 \ll 1$  for  $\tilde{q} = q_x$ ) in above equations and obtain

$$\langle \mathcal{I}_z(\vec{r}_\perp) \rangle \sim \frac{1}{2} \{ \cos(\psi_0) - 4\Delta \sin(\psi_0) \cos(\tilde{q}Q_y l_0^2/2) \cos(\tilde{q}x) \} = \frac{1}{2} \cos(\psi_x/l_0^2), \quad (C4)$$

where we have used  $\psi_k = \psi_0 + 4\Delta \cos(k\tilde{q}l_0^2)$  (Eq. (50)) for the last equation, and

$$\langle \mathcal{I}_+(\vec{r}_\perp) \rangle = \langle \mathcal{I}_-(\vec{r}_\perp) \rangle^* \sim \frac{1}{2} A_{\uparrow\downarrow}(\vec{Q}_\perp, 0) \sin(\psi_x/l_0^2) e^{i\vec{Q}_\perp \cdot \vec{r}_\perp - i\gamma}. \quad (C5)$$

Note that the long wavelength limit behavior of  $\langle \mathcal{I}_\pm(\vec{r}_\perp) \rangle$  is different in wide and double well systems: for the former case, the two isospin states,  $\uparrow$  and  $\downarrow$ , have different Landau level indices,  $\vec{n}_1$  and  $\vec{n}_2$ , and therefore  $A_{\uparrow\downarrow}(\vec{Q}_\perp, 0) = A_{\vec{n}_1 \vec{n}_2}^W(\vec{Q}_\perp, 0) \rightarrow 0$  as  $|\vec{Q}_\perp| \rightarrow 0$  (see Eq. (B1)). However, for the latter case, the two levels of different isospins are of the *same* Landau level index,  $N$ , and hence  $A_{\uparrow\downarrow}(\vec{Q}_\perp, 0) = A_{NN}^D(\vec{Q}_\perp, 0) \rightarrow 1$  as  $|\vec{Q}_\perp| \rightarrow 0$ . As a result, Eq. (C5) implies that the total magnitude of the isospin density in a wide well system is not a constant of winding vector, while it is a constant for a double well system. Therefore, in order to apply Eq. (C1) to the wide well system, we have to project the isospin vector onto the unit sphere by renormalizing its magnitude to 1/2 with a space independent constant and redefining the following isospin density vector,  $\vec{m}(\vec{r}_\perp)$ :

$$\begin{aligned} m_x(\vec{r}_\perp) &= \frac{1}{2} \sin(\psi_x/l_0^2) \cos(Q_x x + Q_y y - \gamma), \\ m_y(\vec{r}_\perp) &= \frac{1}{2} \sin(\psi_x/l_0^2) \sin(Q_x x + Q_y y - \gamma), \\ m_z(\vec{r}_\perp) &= \frac{1}{2} \cos(\psi_x/l_0^2), \end{aligned} \quad (C6)$$

which leads to the following charge density modulation via Eq. (C1):

$$\begin{aligned} \rho_{topo}(\vec{r}_\perp) &= -\frac{2}{\pi} \vec{m}(\vec{r}_\perp) \cdot \partial_x \vec{m}(\vec{r}_\perp) \times \partial_y \vec{m}(\vec{r}_\perp) \\ &= -\frac{Q_y}{4\pi l_0^2} \sin(\psi_x/l_0^2) \frac{\partial \psi_k}{\partial k} \Big|_{k=x/l_0^2} \\ &\sim Q_y \Delta \tilde{q} \sin(\psi_0) \sin(\tilde{q}x)/\pi. \end{aligned} \quad (C7)$$

In the same weak isospin density modulation limit, the extra local charge density shown in Eq. (42) becomes

$$\begin{aligned}
\rho_{ex}(\vec{r}_\perp) &\sim -\frac{1}{2\pi l_0^2} \sum_{q_x} \Theta_2(q_x) [A_{\uparrow\uparrow}(q_x, 0, 0) \cos(q_x(x - Q_y l_0^2/2)) - A_{\downarrow\downarrow}(q_x, 0, 0) \cos(q_x(x + Q_y l_0^2/2))] \\
&\sim -\frac{2}{2\pi l_0^2} \Delta \sin(\psi_0) [\cos(\tilde{q}(x - Q_y l_0^2/2)) - \cos(\tilde{q}(x + Q_y l_0^2/2))] \\
&\sim -Q_y \Delta \tilde{q} \sin(\psi_0) \sin(\tilde{q}x)/\pi,
\end{aligned} \tag{C8}$$

which is the same as the charge density shown in Eq. (C8) above (but with an opposite sign). Such long wavelength charge density modulation is nonzero only when both the spiral order and stripe order are finite, and when the spiral winding vector is perpendicular to the stripe normal vector. Therefore this charge density modulation induced by the topological isospin density can be realized as a feature of isospin skyrmion stripe phase.

#### APPENDIX D: RELATIONSHIP BETWEEN THE PERTURBATION STUDY OF THE STRIPE FORMATION AND THE COLLECTIVE MODE SOFTENING AT FINITE WAVEVECTOR

In Section III C we discuss the suitability of the perturbation method to study the stripe formation if it results from an instability of a uniform phase via a two-step phase transition. In this section we will show that this method is equivalent to studying the stripe formation via the mode softening of a finite wavevector collective mode *inside* an isospin coherent or spiral phase, which is known as a standard method to investigate the stripe phase instability in a double well system [27,24]. Before we investigate the relationship between these two methods, it is instructive to mention that in general the collective mode dispersion can be obtained from the HF energy calculated by using a trial wavefunction similar to Eq. (36) but based on the symmetry-broken phase. More precisely, we can start from the following trial wavefunction, which is based on the rotated isospin basis,  $\tilde{c}_{1(2),k}^\dagger$ , obtained in Eq. (36):

$$\begin{aligned}
|\tilde{\Psi}_G\rangle &= \sum_k \tilde{c}_{1,k}^\dagger |LL\rangle \\
\begin{bmatrix} \tilde{c}_{1,k}^\dagger \\ \tilde{c}_{2,k}^\dagger \end{bmatrix} &= \begin{bmatrix} e^{ik\tilde{Q}_x l_0^2/2} \cos(\tilde{\psi}_0/2) & e^{-ik\tilde{Q}_x l_0^2/2} \sin(\tilde{\psi}_0/2) \\ -e^{ik\tilde{Q}_x l_0^2/2} \sin(\tilde{\psi}_0/2) & e^{-ik\tilde{Q}_x l_0^2/2} \cos(\tilde{\psi}_0/2) \end{bmatrix} \cdot \begin{bmatrix} \tilde{c}_{1,k-\tilde{Q}_y/2}^\dagger \\ \tilde{c}_{2,k+\tilde{Q}_y/2}^\dagger \end{bmatrix},
\end{aligned} \tag{D1}$$

where we use  $\tilde{c}_{1(2),k}^\dagger$ ,  $\tilde{\psi}_0$ , and  $\tilde{Q}_\perp$  to denote the new state and the relevant variational parameters for this *second* rotation. For simplicity, we have taken the phase  $\tilde{\gamma} = \gamma = 0$  in the following discussion. As discussed before, we just need to consider a uniform  $\tilde{\psi}_0$  to study the collective mode dispersion, i.e. when we take  $\tilde{\psi}_0$  to be small, the coefficient in front of leading order (quadratic of  $\tilde{\psi}_0$ ) term of the HF variational energy calculated by the new many-body wavefunction,  $|\tilde{\Psi}_G\rangle$ , can give the dispersion of a low-lying collective mode. This method is basically equivalent to the conventional time-dependent Hartree Fock theory used in the integer quantum Hall system [17,33].

The study of stripe formation from the collective mode softening at finite wavevector inside the coherent phase region can be realized in the following isospin rotation picture: When the system has no coherence (i.e. the conventional uniform QH state), the isospin is polarized along isospin  $z$  axis. The trial wavefunction of a many-body phase shown in Eq. (36) can be understood as a result of a rotation in isospin space, tilting the isospin polarization from  $+\hat{z}$  to  $+\hat{z}$  (see Fig. 3(a)) with a tilting angle,  $\psi_0$ . If the spiral winding wavevector is not zero (i.e. a spiral phase), the isospin polarization vector changes its  $x$  and  $y$  components in the old isospin space with respect to the guiding center coordinate,  $k$ , but keeps its  $z$  component,  $\langle I_z \rangle$ , as a constant along the original  $z$  axis, i.e. no stripe order. When we apply a similar rotation, Eq. (D1), onto the existing coherent or spiral phase, the isospin polarization vector prefers to have a second tilting angle,  $\tilde{\psi}_0$ , about the  $\hat{z}$  axis (see Fig. 3(b)). As shown in Fig. 3(b), if the isospin vector winds about the new axis,  $\hat{z}$ , (i.e.  $\tilde{Q}_\perp \neq 0$ ) the isospin projection onto the original  $\hat{z}$  axis becomes periodically oscillating, showing a stripe structure in the original isospin space. The amplitude of such stripe phase is proportional to the amplitude of the second tilting angle,  $\tilde{\psi}_0$ , if it is small. Combining with the fact we mentioned above that the collective mode can be obtained from the HF variational energy by taking small  $\tilde{\psi}_0$  in the coherent phase, we can conclude that the stripe formation, if it results from a two-step second order phase transition, can be investigated by the mode softening of the collective mode at a finite wavevector *inside* the coherent (or spiral) phase. On the other hand, if this collective mode is always gaped at finite wavevector, we can conclude that there is no second order phase transition for a stripe formation, and the only possible stripe phase is that from the first order transition.

To understand better the relationship between the method of studying the stripe formation from the collective mode softening at finite wavevector and the method of the perturbation theory developed in Section III C, we can apply Eq. (D1) to Eq. (36) (assuming the first tilting angle,  $\psi_0^* \neq 0$ , for the first rotation is nonzero and known by

minimizing the HF energy without stripe order in  $\psi_0$ ), and let the second tilting angle  $\tilde{\psi}_0$  to be small. Using  $\tilde{c}_{1(2),k}^\dagger$  as an intermediate isospin basis, and considering the conventional Landau gauge,  $\tilde{A}_{[y]}(\vec{r})$ , with the second spiral winding wavevector being along  $\hat{x}$ , i.e.  $\tilde{\vec{Q}}_\perp = (\tilde{Q}_x, 0)$ , we obtain

$$\begin{aligned}\tilde{c}_{1,k}^\dagger &= e^{ik\tilde{Q}_x l_0^2/2} \tilde{c}_{1,k}^\dagger + e^{-ik\tilde{Q}_x l_0^2/2} (\tilde{\psi}_0/2) \tilde{c}_{2,k}^\dagger \\ &= e^{ik\tilde{Q}_x l_0^2/2} \left[ e^{ikQ_x l_0^2/2} \left( \cos(\psi_0^*/2) - \sin(\psi_0^*/2)(\tilde{\psi}_0/2) e^{-ik\tilde{Q}_x l_0^2} \right) c_{1,k-Q_y/2}^\dagger \right. \\ &\quad \left. + e^{-ikQ_x l_0^2/2} \left( \sin(\psi_0^*/2) + \cos(\psi_0^*/2)(\tilde{\psi}_0/2) e^{-ik\tilde{Q}_x l_0^2} \right) c_{2,k+Q_y/2}^\dagger \right].\end{aligned}\quad (D2)$$

Similarly we can obtain the following energetically degenerate state by using  $\tilde{\vec{Q}}_\perp = (-\tilde{Q}_x, 0)$ :

$$\begin{aligned}\tilde{c}'_{1,k}^\dagger &= e^{-ik\tilde{Q}_x l_0^2/2} \left[ e^{ikQ_x l_0^2/2} \left( \cos(\psi_0^*/2) - \sin(\psi_0^*/2)(\tilde{\psi}_0/2) e^{ik\tilde{Q}_x l_0^2} \right) c_{1,k-Q_y/2}^\dagger \right. \\ &\quad \left. + e^{-ikQ_x l_0^2/2} \left( \sin(\psi_0^*/2) + \cos(\psi_0^*/2)(\tilde{\psi}_0/2) e^{ik\tilde{Q}_x l_0^2} \right) c_{2,k+Q_y/2}^\dagger \right].\end{aligned}\quad (D3)$$

Then we can define a new operator by adding above two equations together in the leading order of  $\tilde{\psi}_0$ :

$$\begin{aligned}d_{1,k}^\dagger &\equiv \frac{1}{2} \left[ e^{-ik\tilde{Q}_x l_0^2/2} \tilde{c}_{1,k}^\dagger + e^{ik\tilde{Q}_x l_0^2/2} \tilde{c}'_{1,k}^\dagger \right] \\ &= e^{ikQ_x l_0^2/2} \left( \cos(\psi_0^*/2) - \sin(\psi_0^*/2)(\tilde{\psi}_0/2) \cos(k\tilde{Q}_x l_0^2) \right) c_{1,k-Q_y/2}^\dagger \\ &\quad + e^{-ikQ_x l_0^2/2} \left( \sin(\psi_0^*/2) + \cos(\psi_0^*/2)(\tilde{\psi}_0/2) \cos(k\tilde{Q}_x l_0^2) \right) c_{2,k+Q_y/2}^\dagger \\ &\sim e^{ikQ_x l_0^2/2} \cos(\psi_k/2) c_{1,k-Q_y/2}^\dagger + e^{-ikQ_x l_0^2/2} \sin(\psi_k/2) c_{2,k+Q_y/2}^\dagger,\end{aligned}\quad (D4)$$

where

$$\psi_k \equiv \psi_0^* + \tilde{\psi}_0 \cos(k\tilde{Q}_x l_0^2) \quad (D5)$$

for  $\tilde{\psi}_0 \ll 1$ . We note that Eq. (D5) is exactly the same as Eq. (50) shown in Section III C ( $4\Delta = \tilde{\psi}_0$ ). Therefore we have shown that studying the stripe formation instability by using Eq. (50) is equivalent to studying the finite wavevector mode softening of the collective mode *inside* a coherent or a spiral phase. Note that another kind of stripe phase with  $I_z$  modulation along  $y$  direction can be obtained by the similar method using the other gauge,  $\tilde{A}_{[x]}(\vec{r})$ , in which particle momentum is conserved along  $x$  direction. Therefore the perturbative method for the stripe formation developed in Section III C is justified and can be applied in a more general situation.

## APPENDIX E: A GENERAL STRIPE PHASE FUNCTION, $\psi_k$

In general, we can use the following periodic function for  $\psi_k$  in Eqs. (36), (46) and (49):

$$\psi_k = \begin{cases} \psi_1 & \text{for } 0 \leq |kl_0^2/a - m| < \xi(1 - \eta)/2 \\ -\frac{\varphi}{\xi\eta}(k - \xi/2) + \psi_0 & \text{for } \xi(1 - \eta)/2 \leq |kl_0^2/a - m| \leq \xi(1 + \eta)/2, \\ \psi_2 & \text{for } \xi(1 + \eta)/2 < |kl_0^2/a - m| \leq 1/2 \end{cases} \quad (E1)$$

where  $\psi_0 = (\psi_1 + \psi_2)/2$  and  $\varphi = \psi_1 - \psi_2$ .  $0 < \xi, \eta < 1$ ,  $0 \leq \psi_1, \psi_2 \leq \pi$  and  $m$  is an integer. The meaning of these variational parameters can be understood more clearly from Fig. 6. Note that when  $\eta = 0$ , we have a rectangular function, while for  $\eta \neq 0$ , we have a smooth  $\psi_k$  to the linear order. To calculate  $\Theta_i(q_n)$  ( $i = 1, 2, 3$ ) for such  $\psi_k$ , we can first evaluate the following quantity (let  $k' = kl_0^2/a$ ,  $q'_x = q_x a$ ):

$$\begin{aligned}\Theta &\equiv \frac{1}{N_\phi} \sum_{k>0} \cos(kq_x l_0^2) e^{i\psi_k} \\ &= \int_0^{\xi(1-\eta)/2} dk' \cos(k'q'_x) e^{i\psi_1} + \int_{\xi(1-\eta)/2}^{\xi(1+\eta)/2} dk' \cos(k'q'_x) e^{-i\varphi(k'-\xi/2)/\xi\eta+i\psi_0} + \int_{\xi(1+\eta)/2}^{1/2} \cos(k'q'_x) e^{i\psi_2}\end{aligned}$$

$$\begin{aligned}
&= (\cos(\psi_1) + i \sin(\psi_1)) \frac{\sin(\xi(1-\eta)q'_x/2)}{q'_x} + (\cos(\psi_2) + i \sin(\psi_2)) \left( \frac{\sin(q'_x/2)}{q'_x} - \frac{\sin(\xi(1+\eta)q'_x/2)}{q'_x} \right) \\
&\quad + \frac{2\xi\eta \cos(q'_x\xi/2) \cos(\psi_0) [\xi\eta q'_x \cos(\varphi/2) \sin(\xi\eta q'_x/2) - \varphi \cos(\xi\eta q'_x/2) \sin(\varphi/2)]}{\xi^2\eta^2 q'^2 - \varphi^2} \\
&\quad + \frac{2\xi\eta \sin(q'_x\xi/2) \sin(\psi_0) [-\varphi \cos(\varphi/2) \sin(\xi\eta q'_x/2) + \xi\eta q'_x \cos(\xi\eta q'_x/2) \sin(\varphi/2)]}{\xi^2\eta^2 q'^2 - \varphi^2} \\
&\quad - i \frac{2\xi\eta \cos(q'_x\xi/2) \sin(\psi_0) [-\xi\eta q'_x \cos(\varphi/2) \sin(\xi\eta q'_x/2) + \varphi \cos(\xi\eta q'_x/2) \sin(\varphi/2)]}{\xi^2\eta^2 q'^2 - \varphi^2} \\
&\quad - i \frac{2\xi\eta \sin(q'_x\xi/2) \cos(\psi_0) [-\varphi \cos(\varphi/2) \sin(\xi\eta q'_x/2) + \xi\eta q'_x \cos(\xi\eta q'_x/2) \sin(\varphi/2)]}{\xi^2\eta^2 q'^2 - \varphi^2}.
\end{aligned} \tag{E2}$$

Then we have

$$\Theta_2(q_x) = \frac{2}{N_\phi} \sum_{k>0} \cos(kq_x l_0^2) \sin^2(\psi_k/2) = \frac{1}{N_\phi} \sum_{k>0} \cos(kq_x l_0^2) (1 - \cos(\psi_k)) = \frac{1}{2} \delta_{q_x,0} - Re[\Theta], \tag{E3}$$

and

$$\Theta_3(q_x) = \frac{2}{N_\phi} \sum_{k>0} \cos(kq_x l_0^2) \sin(\psi_k/2) \cos(\psi_k/2) = \frac{1}{N_\phi} \sum_{k>0} \cos(kq_x l_0^2) \sin(\psi_k) = Im[\Theta]. \tag{E4}$$

When replacing  $q'_x = q_n a = 2\pi n$ , we have  $\sin(q'_x/2)/(q'_x/2) = \delta_{n,0}$ .

## APPENDIX F: EVALUATION OF $E_{H,F}^{I,o}$

Here we show the analytical formula of the exchange energies used in Section VII for a double well system at  $\nu = 4N + 2$ . For convenience, we let  $\vec{Q}'_\perp \equiv \vec{Q}_\perp l_0$ ,  $\vec{P}' \equiv \vec{P} l_0$ , and  $d' = d/l_0$ ,  $q' = q l_0$  to be dimensionless. We have

$$\begin{aligned}
E_F^{I,o}(\vec{0}, 0) &= \frac{-1}{\Omega_\perp} \sum_{\vec{q}} V_{NN,NN}^{I,o}(\vec{q}_\perp) = \frac{-e^2}{l_0} \int_0^\infty dq' e^{-q'^2/2} \left[ L_N^0 \left( \frac{q'^2}{2} \right) \right]^2 \times \frac{1}{2\pi} \int_0^{2\pi} \frac{d\theta}{2} \left( 1 \pm \cos(q'(P'_x \cos \theta + P'_y \sin \theta)) e^{-q' d'} \right) \\
&= -\frac{e^2}{l_0} \int_0^\infty dq' e^{-q'^2/2} \left[ L_N^0 \left( \frac{q'^2}{2} \right) \right]^2 \times \frac{1}{2} \left[ 1 \pm J_0(q' P') e^{-q' d'} \right],
\end{aligned} \tag{F1}$$

$$\begin{aligned}
E_F^{I,o}(\vec{Q}_\perp, 0) &= \frac{-1}{\Omega_\perp} \sum_{\vec{q}} V_{NN,NN}^{I,o}(\vec{q}_\perp) \cos((Q_x q_y - Q_y q_x) l_0^2) \\
&= -\frac{e^2}{l_0} \int_0^\infty dq' e^{-q'^2/2} \left[ L_N^0 \left( \frac{q'^2}{2} \right) \right]^2 \times \frac{1}{2\pi} \int_0^{2\pi} \frac{d\theta}{2} \left( 1 \pm \cos(q'(P'_x \cos \theta + P'_y \sin \theta)) e^{-q' d'} \right) \cos(q'(Q'_x \sin \theta - Q'_y \cos \theta)) \\
&= -\frac{e^2}{l_0} \int_0^\infty dq' e^{-q'^2/2} \left[ L_N^0 \left( \frac{q'^2}{2} \right) \right]^2 \times \frac{1}{2} [J_0(q' Q')] \\
&\quad \pm \frac{1}{2} \left[ J_0 \left( q' \sqrt{(P'_x - Q'_y)^2 + (P'_y + Q'_x)^2} \right) + J_0 \left( q' \sqrt{(P'_x + Q'_y)^2 + (P'_y - Q'_x)^2} \right) \right] e^{-q' d'},
\end{aligned} \tag{F2}$$

and

$$\begin{aligned}
E_F^{I,o}(\vec{0}, q_n) &= \frac{-1}{\Omega_\perp} \sum_{\vec{q}} V_{NN,NN}^{I,o}(\vec{q}_\perp) \cos(q_n q_y l_0^2) \\
&= -\frac{e^2}{l_0} \int_0^\infty dq' e^{-q'^2/2} \left[ L_N^0 \left( \frac{q'^2}{2} \right) \right]^2 \underbrace{\frac{1}{2\pi} \int_0^{2\pi} \frac{d\theta}{2} \left( 1 \pm \cos(q'(P'_x \cos \theta + P'_y \sin \theta)) e^{-q' d'} \right) \cos(q'_n q' \sin \theta)}_{\frac{1}{2} \left[ J_0(q' q'_n) \pm \frac{e^{-q' d'}}{2} \left( J_0 \left( q' \sqrt{P'^2_x + (P'_y + q'_n)^2} \right) + J_0 \left( q' \sqrt{P'^2_x + (P'_y - q'_n)^2} \right) \right) \right]}.
\end{aligned} \tag{F3}$$

The most general expression of the exchange energy including both spiral and stripe orders ( $E_F^{I,o}(\vec{Q}_\perp, q_n) = 1\Omega_\perp^{-1} \sum_{\vec{q}} V_{NN,NN}^{I,o}(\vec{q}_\perp) \cos(q_n q_y l_0^2) \cos((Q_x q_y - Q_y q_x) l_0^2)$ ) can be obtained similarly via the same strategy.

---

- [1] For a review, see Michael M. Fogler, cond-mat/0111001, to be published in *Trends in High Magnetic Fields*, Lecture Notes for the Summer School (Cargese, France, 2001) and references therein.
- [2] R. Moessner and J. T. Chalker, Phys. Rev. B **54**, 5006 (1996).
- [3] M.M. Fogler and A.A. Koulakov, Phys. Rev. B **55**, 9326 (1997).
- [4] M.P. Lilly, K.B. Cooper, J.P. Eisenstein, L.N. Pfeiffer, and K.W. West, Phys. Rev. Lett. **82**, 394 (1999).
- [5] R.R. Du, D.C. Tsui, H.L. Stormer, L.N. Pfeiffer, K.W. Baldwin, and K.W. West, Solid State Commun. **109**, 389 (1999).
- [6] A.H. MacDonald, and M.P.A. Fisher, Phys. Rev. B **61**, 5724 (2000).
- [7] A. Lopatnikova, S.H. Simon, B.I. Halperin, and X.G. Wen, Phys. Rev. B **64**, 155301 (2001).
- [8] E. Demler, D.W. Wang, S. Das Sarma and B.I. Halperin, Solid State Comm. **123**, 243 (2002).
- [9] H.A. Fertig, Phys. Rev. Lett. **82**, 3693 (1999); E. Fradkin and S.A. Kivelson, Phys. Rev. B **59**, 8065 (1999).
- [10] W. Pan, T. Jungwirth, H.L. Stormer, D.C. Tsui, A.H. MacDonald, S.M. Girvin, L. Smrka, L.N. Pfeiffer, K.W. Baldwin, and K.W. West, Phys. Rev. Lett. **85**, 3257 (2000).
- [11] T. Jungwirth, A.H. MacDonald, L. Smrka, and S.M. Girvin, Phys. Rev. B **60**, 15574 (1999).
- [12] J. Zhu, W. Pan, H.L. Stormer, L.N. Pfeiffer, and K.W. West, Phys. Rev. Lett. **88**, 116803 (2002).
- [13] J.P. Eisenstein, K.B. Cooper, L.N. Pfeiffer, and K.W. West, Phys. Rev. Lett. **88**, 076801 (2002).
- [14] S.-Y. Lee, V.W. Scarola, and J.K. Jain, Phys. Rev. Lett. **87**, 256803 (2001).
- [15] W. Pan, H.L. Stormer, D.C. Tsui, L.N. Pfeiffer, K.W. Baldwin, and K.W. West, Phys. Rev. B **64**, 121305 (2001).
- [16] U. Zeitler, H.W. Schumacher, A.G.M. Jansen, and R.J. Haug, Phys. Rev. Lett. **86**, 866 (2001).
- [17] D.W. Wang, S. Das Sarma, E. Demler, and B.I. Halperin, Phys. Rev. B **66**, 195334 (2002).
- [18] S.L. Sondhi, A. Karlhede, S.A. Kivelson, and E.H. Rezayi, Phys. Rev. B **47**, 16419 (1993); A. Karlhede, S.A. Kivelson, K. Leijnell, and S.L. Sondhi, Phys. Rev. Lett. **77**, 2061 (1996).
- [19] L. Brey, Phys. Rev. B **44**, 3772 (1991).
- [20] G. Murthy, Phys. Rev. Lett. **85**, 1954 (2000).
- [21] X.G. Wen and A. Zee, Phys. Rev. Lett. **69**, 1811 (1992); Phys. Rev. B **47**, 2265 (1993).
- [22] S.M. Girvin and A.H. MacDonald, in *Perspectives in Quantum Hall Effects* edited by S. Das Sarma and A. Pinczuk (John Wiley & Sons, New York, 1997); J.P. Eisenstein, *ibid.*
- [23] B.I. Halperin, Helvetica Physica Acta **56**, 75 (1983).
- [24] L. Brey and H. Fertig, Phys. Rev. B **62**, 10268 (2000).
- [25] Y.B. Kim, C. Nayak, E. Demler, N. Read, and S. Das Sarma, Phys. Rev. B **63**, 205315 (2001);
- [26] K. Yang, K. Moon, L. Zheng, A. H. MacDonald, S. M. Girvin, D. Yoshioka, and S.-C. Zhang, Phys. Rev. Lett. **72**, 732 (1994); E. Demler, C. Nayak, and S. Das Sarma, Phys. Rev. Lett. **86**, 1853 (2001).
- [27] J. Yang and W.-P. Su, Phys. Rev. B **51**, 4626 (1995)
- [28] A. Stern, S. Das Sarma, M. P. A. Fisher, and S. M. Girvin, Phys. Rev. Lett. **84**, 139 (2000)
- [29] S.Q. Murphy, J.P. Eisenstein, G.S. Boebinger, L.N. Pfeiffer, and K.W. West, Phys. Rev. Lett. **72**, 728 (1994).
- [30] I.B. Spielman, J.P. Eisenstein, L.N. Pfeiffer, and K.W. West, Phys. Rev. Lett. **87**, 036803 (2001).
- [31] C.B. Hanna, A.H. MacDonald, and S.M. Girvin, Phys. Rev. B **63**, 125305 (2001).
- [32] K. Nomura and D. Yoshioka, cond-mat/0204461.
- [33] L. Zheng, R.J. Radtke, and S. Das Sarma, Phys. Rev. Lett. **78**, 2453 (1997); S. Das Sarma, S. Sachdev, and L. Zhang, Phys. Rev. B **58**, 4672 (1998); Phys. Rev. Lett. **79** 917 (1997).
- [34] A.H. MacDonald, R. Rajaraman, and T. Jungwirth, Phys. Rev. B **60**, 8817 (1999).
- [35] S. Das Sarma and E. Demler, Solid State Commun. **117** 141 (2001), and references therein.
- [36] A.A. Burkov and A.H. MacDonald, Phys. Rev. B **66**, 115323 (2002).
- [37] V. Pellegrini, A. Pinczuk, B.S. Dennis, A.S. Plaut, L.N. Pfeiffer, and K.W. West, Science **281** 799 (1998); Phys. Rev. Lett. **78**, 310 (1997).
- [38] A. Sawada, Z.F. Ezawa, H. Ohno, Y. Horikoshi, Y. Ohno, S. Kishimoto, F. Matsukura, M. Yasumoto, and A. Urayama, Phys. Rev. Lett. **80**, 4534 (1998); V.S. Khrapai, E.V. Deviatov, A.A. Shashkin, V.T. Dolgopolov, F. Hastedt, A. Wixforth, K.L. Campman, and A.C. Gossard, Phys. Rev. Lett. **84**, 725-728 (2000).
- [39] M.-F. Yang and M.-C. Chang, Phys. Rev. B, **60**, R13985 (1999).
- [40] A. Lopatnikova, private communication.
- [41] E. Papa, J. Schliemann, A.H. MacDonald, and M.P.A. Fisher, cond-mat/0209173 (unpublished).
- [42] For ferroelectric crystals, see for example, C. Kittel, *Introduction to Solid State Physics* (Wiley, New York, 1971).

[43] Note that the intersubband crossing may not exist if electron filling factor is so small (or the subband energy separation,  $\omega_1$  is so large) that no higher subband levels are occupied in the whole range of  $B_{\parallel}$  field. The criterion to have such crossing is  $N > N^* = \text{Max}(\omega_0/\omega_{\perp}, \omega_{\perp}/\omega_0)$ .

[44] L. Brey and B.I. Halperin, Phys. Rev. B **40**, 11634 (1989).

[45] J. Dempsey and B. Halperin, Phys. Rev. B **47**, 4662 (1993), Phys. Rev. B **47**, 4674 (1993); M.P. Stopa and S. Das Sarma, Phys. Rev. B **40**, 10048 (1989); P.I. Tamborenea and S. Das Sarma, Phys. Rev. B **49**, 16593 (1994).

[46] R. Cote, H.A. Fertig, J. Bourassa, and D. Bouchiha, Phys. Rev. B **66**, 205315 (2002).

[47] We note that the generalized Laguerre polynomial in the effective tunneling amplitude,  $t_{n,P}$ , may reverse the sign of tunneling amplitude for  $n > 0$  and hence reduce the tunneling effects when layer separation or  $B_{\parallel}$  is in a certain range [46]. But we will not consider this situation for simplicity and all of our results should be correct without losing generality.

[48] K. Kallin and B. Halperin, Phys. Rev. B **30**, 5655 (1984).

[49] We note that a generalized two-dimensional translation operator,  $\hat{\mathcal{T}}(\vec{R}_{\perp}) \equiv \exp(-i\vec{R}_{\perp} \cdot \hat{\mathcal{M}})$ , does not form a close translational group if both  $R_x$  and  $R_y$  are nonzero. This is because in general  $\hat{\mathcal{T}}(\vec{R}_{\perp}) \cdot \hat{\mathcal{T}}(\vec{R}'_{\perp})$  cannot be equivalently obtained by the third translation,  $\hat{\mathcal{T}}(\vec{R}''_{\perp})$  by an additional phase factor, which follows from the fact that  $\mathcal{T}_x(R_x)$  and  $\mathcal{T}_y(R_y)$  do not commute with each other. However, it is easy to see that  $\mathcal{T}_x(R_x)$  and  $\mathcal{T}_y(R_y)$  individually can form close translational groups in  $x$  and  $y$  direction respectively. Therefore we write them separately to avoid any confusion.

[50] C.S. Sergio, G.M. Gusev, A.A. Quivy, T.E. Lamas, J.R. Leite, O. Estibals, and J.C. Portal, Braz. J Phys. **32** 347 (2002).

[51] K.B. Cooper, M.P. Lilly, J.P. Eisenstein, L.N. Pfeiffer, and K.W. West, Phys. Rev. B **60**, R11285 (1999); V. Piazza, V. Pellegrini, F. Beltram, W. Wegscheider, T. Jungwirth, and A. MacDonald, Nature **402**, 638 (1999); E.P. De Poortere, E. Tutuc, S.J. Papadakis, and M. Shayegan, Science **290**, 1546 (2000).

[52] T. Jungwirth and A.H. MacDonald, Phys. Rev. Lett. **87**, 216801 (2001).

[53] J.T. Chalker, D.G. Polyakov, F. Evers, A.D. Mirlin, and P. Wolfle, cond-mat/0208024 (unpublished).

[54] K. Moon, H. Mori, K. Yang, S. M. Girvin, and A. H. MacDonald, L. Zheng, D. Yoshioka, and S.-C. Zhang, Phys. Rev. B **51**, 5138 (1995).

[55] A.H. MacDonald, P.M. Platzman and G.S. Boebinger, Phys. Rev. Lett. **65**, 775 (1990).

[56] H. A. Fertig, Phys. Rev. B **40**, 1087 (1989).

[57] L. Radzihovsky, Phys. Rev. Lett. **87**, 236802 (2001); M. Abolfath, L. Radzihovsky, and A.H. MacDonald, Phys. Rev. B **65**, 233306 (2002).

[58] This is because the electron Hartree energy in each Landau level has nodes in  $x$  direction, but quiet uniform in  $y$  direction due to the anisotropic distortion of the electron wavefunction in the strong in-plane magnetic field. A simple scenario to understand this is to view an isospin stripe phase as a two independent (incoherent) stripes in the two degenerate levels, each of which is partially filled, and therefore the stripe longitudinal direction must be aligned to be perpendicular to the in-plane field direction to optimize the anisotropy energy in each level, similar to the stripes at half filling factors extensively studied in the literature [10,11]. When we turn on the interlevel coherence between the two degenerate levels, a spiral order is introduced also and competes with the anisotropy energy to determine the direction of stripe phase at integer filling factors.

[59] S. Das Sarma and P.I. Tamborenea, Phys. Rev. Lett **73**, 1971 (1994).

[60] V. Celli and N.D. Mermin, Phys. Rev. **140**, A839 (1965).

[61] I.S. Gradshteyn and I.M. Ryzhik, *Table of Integrals, Series, and Products* (Academic Press, New York, 1965).

[62] Y.W. Suen, J. Jo, M.B. Santos, L.W. Engel, S.W. Hwang, and M. Shayegan, Phys. Rev. B **44**, 5947 (1991); C.S. Sergio, G.M. Gusev, J.R. Leite, E.B. Olshanetskii, A.A. Bykov, N.T. Moshegov, A.K. Bakarov, and A.I. Toropov, Phys. Rev. B **64**, 115314 (2001).

[63] X. Ren, S. Yang, Y. Yu, and Z. Su, J. Phys.:Condens. Matter **14** 3931 (2002).

[64] J.P. Eisenstein, K.B. Cooper, L.N. Pfeiffer, and K.W. West, Phys. Rev. Lett. **88**, 076801 (2002).

[65] E.H. Rezayi, T. Jungwirth, A.H. MacDonald, and F.D.M. Haldane, cond-mat/0302271 (unpublished).

[66] K. Park, private communication.

[67] S. Luin, V. Pellegrini, A. Pinczuk, B.S. Dennis, L.N. Pfeiffer, K.W. West, cond-mat/0301295 (unpublished).

[68] L. Zheng, M. Ortalano, and S. Das Sarma, Phys. Rev. B **55**, 4506 (1997); S. Das Sarma, M. Ortalano, and L. Zheng, *ibid* **58**, 7453 (1998).

label	system	$\nu$	isospin $\uparrow$ ( $I = 1$ )	isospin $\downarrow$ ( $I = -1$ )	many-body phases	broken symmetries
$W1$	wide well (intersubband)	$2N + 1^\ddagger$	$\vec{n}_1 = (1, 0), s = \uparrow$	$\vec{n}_2 = (0, N), s = \uparrow$	coherent	parity
$W1'$	wide well (intrasubband)	$2N + 1$	$\vec{n}_1 = (0, N), s = \uparrow$	$\vec{n}_2 = (0, N + 1), s = \uparrow$	skyrmion stripe	parity & trans. in $x$ and $y$ directions
$W2$	wide well (intersubband)	$2N + 2^\ddagger$	$\vec{n}_1 = (1, 0), s = \downarrow (\uparrow)$	$\vec{n}_2 = (0, N), s = \uparrow (\downarrow)$	no	no
$W2'$	wide well (intrasubband)	$2N + 2$	$\vec{n}_1 = (0, N), s = \downarrow$	$\vec{n}_2 = (0, N + 1), s = \uparrow$	(skyrmion stripe) $^\dagger$	(parity, spin & trans. in $x$ and $y$ directions) $^\dagger$
$D1$	double well	$4N + 1$	$N, l = +1, s = \uparrow$	$N, l = -1, s = \uparrow$	coherent spiral coherent stripe	trans. in $y$ no parity & trans. in $x$ (and $y$ ) direction
$D2$	double well	$4N + 2$	$N, \alpha = +1, s = \downarrow$	$N, \alpha = -1, s = \uparrow$	spiral stripe coherent $^\S$	parity & trans. in $y$ parity & spin

TABLE I. Table of the isospin notations and the many-body phases of different systems discussed in this paper.  $\vec{n} = (n, n')$  is the orbital level index of the energy eigenstate of an electron in a parabolic well subject to an in-plane magnetic field (see Eq. (2)).  $s = \pm 1/2$  and  $l = \pm 1$  are spin and layer indices respectively.  $\alpha = \pm 1$  is for the symmetric(antisymmetric) state of the double well system. The many-body phases of  $D1$  case are described in the layer index basis (see Section VI), while they are described in the symmetry-antisymmetry (noninteracting eigenstate) basis in the  $D2$  case. The in-plane magnetic field is fixed to be in  $+\hat{x}$  direction.

$\ddagger$ : Such level crossing exists only when  $N > N^*$  for  $N^* = \text{Max}(\omega_c/\omega_\perp, \omega_\perp/\omega_c)$ , see Ref. [43].

$\dagger$ : We do not really obtain a many-body phase within the HF approximation, but the experimental data of Ref. [15] suggests that a skyrmion stripe phase may exist in the  $W2'$  system (see Section V).

$\S$ : = "commensurate canted antiferromagnetic phase" in the literature with spiral order in the layer index basis (see Section VII).

systems	In-plane magnetic field, $B_{\parallel}$ , is along $+ \hat{x}$ ( $\rightarrow$ )				
	$W1'$	$W2'$	$D1$	$D1$	$D1$
anisotropic phases	skyrmion stripe	skyrmion stripe	spiral	spiral stripe	coherent stripe
isospin spiral					
winding vector, $\vec{Q}_\perp$	$\uparrow\downarrow$	$(\uparrow\downarrow)$	$\uparrow$	$\uparrow$	$\times$
isospin stripe					
normal vector, $\hat{n}$	$\leftrightarrow$	$(\leftrightarrow)$	$\times$	$\uparrow\downarrow$	arbitrary

TABLE II. A table summarizing the directions of the spiral and the stripe orders in different systems. The in-plane magnetic field is fixed in  $+ \hat{x}$  axis. For  $W2'$  system (wide well at even filling), we speculate that the skyrmion stripe is a possible ground state according to the experimental results and our analysis in Section VII. Note that in a wide well system, the spiral order is degenerate at  $\vec{Q}_\perp^* = (0, \pm Q_y^*)$ , while in a double well system, it is fixed along  $+ \hat{y}$  only in the commensurate state. Winding of the phases in  $D1$  system is set by the in-plane magnetic field, and does not imply breaking of the translational symmetry (see discussion in Section VID).

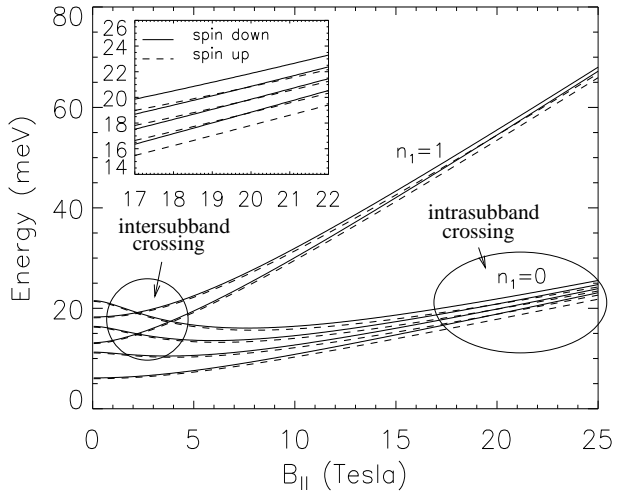


FIG. 1. Noninteracting Landau level energy spectra of a parabolic quantum well as a function of the parallel (in-plane) magnetic field,  $B_{\parallel}$ . We choose following system parameters:  $B_{\perp} = 3$  T ( $\omega_{\perp} = 5.2$  meV),  $\omega_0 = 7$  meV, and  $|g| = 0.44$  for GaAs material.  $n_1$  is the first Landau level index of  $\vec{n}$ . Regions of intersubband and intrasubband level crossings are indicated by circles (see text).

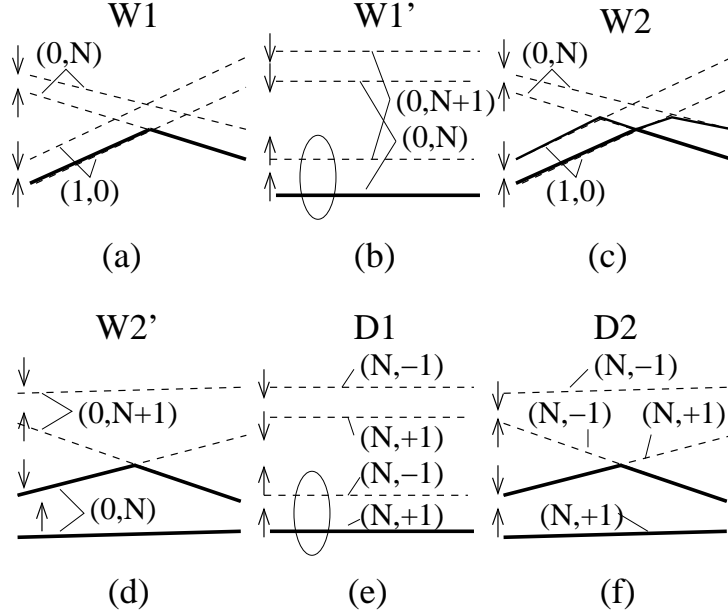


FIG. 2. Schematic pictures of the noninteracting energy configuration in the regions of level crossing (or level near degeneracy) for the six systems discussed in this paper: (a) intersubband level crossing of a wide well at  $\nu = 2N + 1$ , (b) intrasubband level near degeneracy of a wide well at  $\nu = 2N + 1$ , (c) intersubband level crossing of a wide well at  $\nu = 2N + 2$ , (d) intrasubband level crossing of a wide well at  $\nu = 2N + 2$ , (e) interlayer level near degeneracy of a double well at  $\nu = 4N + 1$ , and (f) level crossing of a double well at  $\nu = 4N + 2$ . Solid(dashed) lines are for filled(empty) levels. The horizontal axis is the strength of in-plane magnetic field. Up(down) arrows denote the electron spin states. Note that the level indices for (a)-(d) are  $\vec{n} = (n, n')$  for a parabolic wide well system, while they are  $(n, l)$  for (e) and  $(n, \alpha)$  for (f) (see Table I) for different definitions of isospin indices. The circles in (b) and (e) denote the two near degenerate levels we consider.

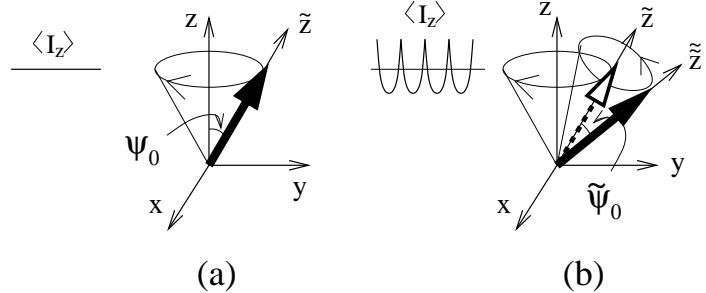


FIG. 3. (a) Isospin polarization in a coherent or spiral phase: the new polarization axis is along  $\tilde{z}$  axis with an angle  $\psi_0$  tilted from the original  $z$  axis. Finite winding wavevector causes  $\langle \mathcal{I}_{x,y} \rangle$  oscillating in the real space but keeps  $\langle \mathcal{I}_z \rangle$  as a constant. (b) If the isospin coherent (or spiral) phase is unstable to form a new isospin spiral phase based on the rotated coordinate, the isospin winding about the new polarization axis,  $\tilde{z}$ , will cause a new periodically oscillating  $\langle \mathcal{I}_z \rangle$  in the isospin projection onto the original  $z$  axis, showing a character of stripe phase.

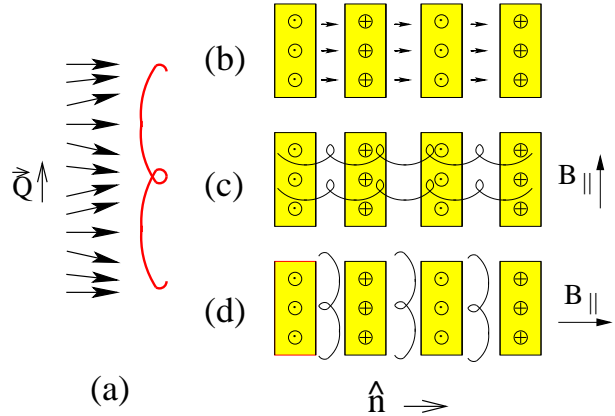


FIG. 4. (a) A cartoon for the isospin spiral structure. Horizontal arrows denote the isospin direction and the spiral curve indicate the transverse isospin ( $\mathcal{I}_x, \mathcal{I}_y$ ) order parameter. (b), (c) and (d) are the isospin coherent stripe phase, isospin spiral stripe phase, and isospin skyrmion stripe phase respectively. Shaded areas show isospin up ( $\odot$ ) and down ( $\oplus$ ) domains, and arrows in the right hand side show the directions of  $B_{\parallel}$ .  $\hat{n}$  is the normal vector of the stripes, which denotes the direction of isospin  $\langle \mathcal{I}_z \rangle$  modulation. For isospin coherent stripe in (b), there is no spiral order and therefore, in general, the stripe can have arbitrary direction with respect to the in-plane field.

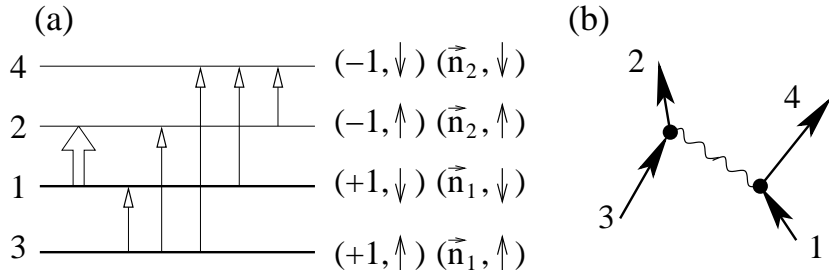


FIG. 5. (a) A schematic noninteracting energy configuration for a general four level degeneracy of an even filling system. Level 1 is the highest filled level, level 2 is the lowest empty level, level 3 is the second highest level, and level 4 is the second lowest empty level as defined in Section III B.  $(\alpha, s)$ , in the right hand side denotes the quantum numbers of each level in the double well system ( $\alpha$  is the parity quantum number and  $s$  is the electron spin), while  $(\vec{n}_i, s)$  is the quantum number for levels in the wide well systems (see Table I). Thick(thin) horizontal lines denote the filled(empty) levels. The thick upward arrow represents the density operator,  $\rho_{2,1}$ , which annihilates one electron in level 1 and creates another one in level 2. This is the main mechanism and the order parameter for the many-body phases of the four level system near the level crossing region. The other upward arrows denote the density operators for  $\rho_{1,3}$ ,  $\rho_{2,3}$ ,  $\rho_{4,3}$ ,  $\rho_{4,1}$  and  $\rho_{4,2}$  respectively from the left to the right. (b) The exchange interaction diagram for the coupling between  $\rho_{2,1}$  and  $\rho_{4,3}$ . The parity quantum number,  $\alpha$ , has sign changed at the vertex. This is the main mechanism to stabilize the canted antiferromagnetic phase in the double well system at  $\nu = 4N + 2$ .

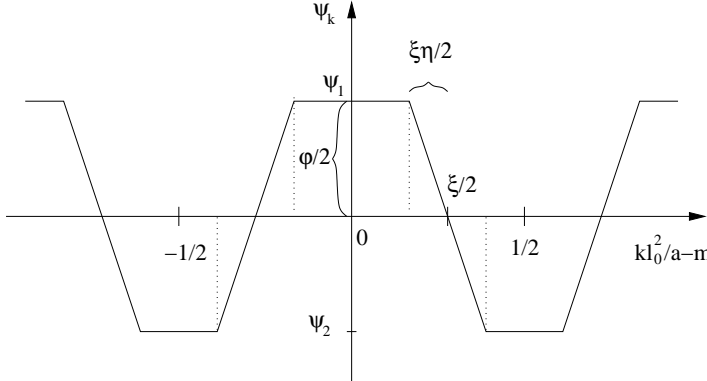


FIG. 6. A trial periodic function of the stripe phase function,  $\psi_k$ , in Eq. (36).  $\psi_1$ ,  $\psi_2$ ,  $\varphi$ ,  $\xi$ ,  $\eta$ , and stripe period,  $a$ , are variational parameters (not all of them are independent). Its mathematical expression is shown in Appendix E.

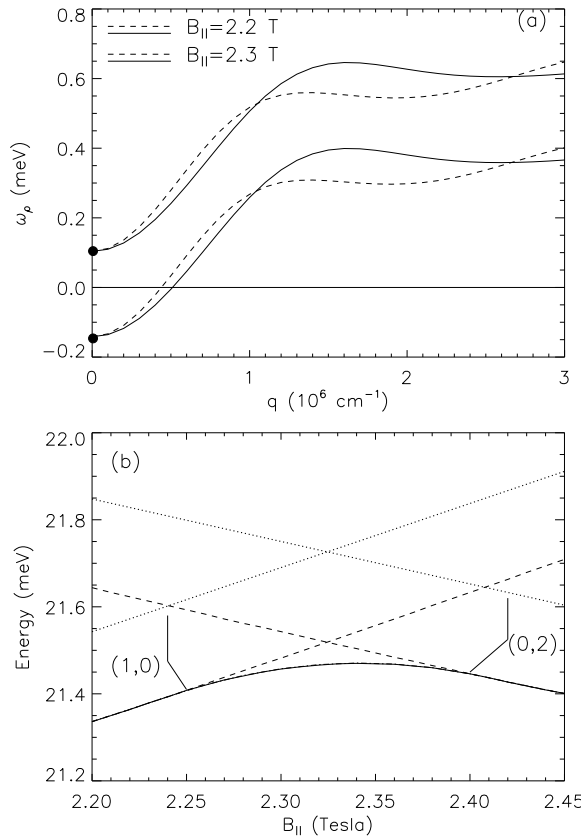


FIG. 7. (a) Magnetoplasmon dispersion near intersubband level crossing region of a wide well system at  $\nu = 5$  (system parameters are the same as in Fig. 1). The upper(lower) curves are for  $B_{\parallel} = 2.2$  and 2.3 Tesla respectively. (The latter is calculated based on the isospin polarized basis and its negative energy at zero wavevector indicates a mode softening in a symmetry breaking phase. The correct curve for such plasmon mode should be modified based on the new coherent state as mentioned in the text.) Solid(dashed) lines are for dispersion along  $y$  and  $x$  axes respectively. The filled circle at  $q = 0$  denotes the energy of disconnected excitations, softening of which is a signature of parity symmetry breaking. Note that the energy of the circle is just slightly lower ( $< 0.01$  meV) than the asymptotic magnetoplasmon energy in the long wavelength ( $q \rightarrow 0^+$ ). (b) Single particle energy as a function of in-plane magnetic field,  $B_{\parallel}$ , of the same system. The dashed(dotted) lines are the spin up(down) levels of the two crossing isospin polarized states (including HF self-energy correction), while the solid lines are the energies of the many-body isospin coherent state, which breaks the parity symmetry of the system for 2.2 Tesla  $< B_{\parallel} <$  2.40 Tesla.

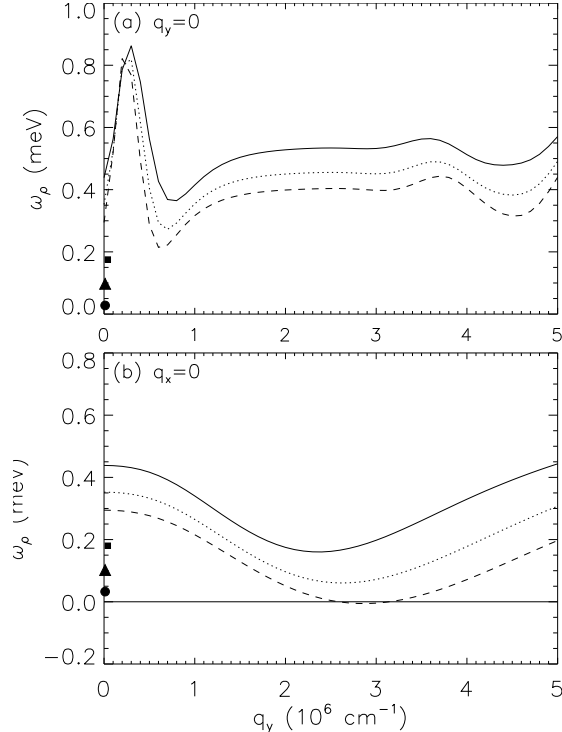


FIG. 8. Magnetoplasmon dispersion of a wide well system at  $\nu = 1$  with large in-plane magnetic field. The perpendicular magnetic field ( $B_{\perp}$ ) is 3 Tesla and the bare parabolic confinement potential ( $\omega_0$ ) is 3 meV. Solid, dotted, and dashed lines are for  $B_{\parallel} = 20, 25$ , and 30 Tesla respectively. When  $B_{\parallel} > 30$  Tesla, the plasmon mode is softened at a finite wavevector in  $y$  direction (perpendicular to the in-plane field). The filled squares, triangles, and circles denote the energies of the disconnected excitation energy at  $\vec{q}_{\perp} = 0$  for  $B_{\parallel} = 20, 25$  and 30 Tesla respectively.

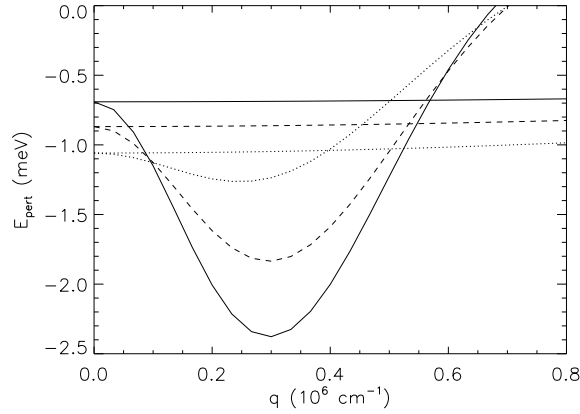


FIG. 9. Perturbative energy,  $E_{pert}^{HF}(q)$ , for the stripe formation in a wide well system at  $\nu = 1$  in large magnetic field region. Dotted, dashed, and solid lines are for in-plane magnetic field,  $B_{\parallel} = 31, 35$ , and  $40$  Tesla respectively. Thick and thin lines are obtained in Landau gauges,  $\vec{A}_{[y]}(\vec{r})$  and  $\vec{A}_{[x]}(\vec{r})$ , respectively. This result clearly shows that a stripe phase can always be stabilized to be along  $y$  direction (stripe modulation is in  $x$  direction) for  $B_{\parallel} > 30$  Tesla. System parameters are the same as used in Fig. 8.

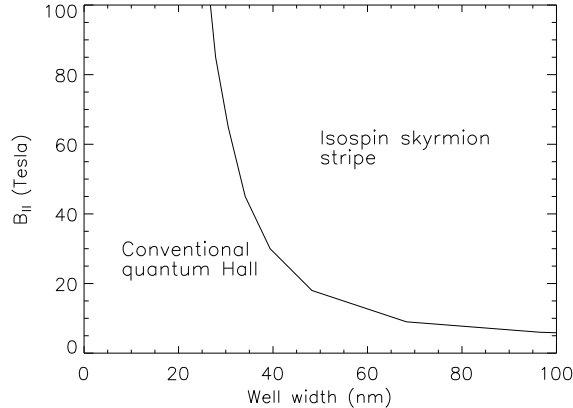


FIG. 10. Phase diagram of a wide well system at  $\nu = 1$ . System parameters are the same as used in Figs. 8 and 9 but with different confinement potential,  $\omega_0$ , leading to different well widths. The well width is estimated from the size of the single electron wavefunction in the lowest subband of the parabolic confinement potential in the absence of in-plane magnetic field, i.e.  $2(m^*\omega_0)^{-1/2}$ .

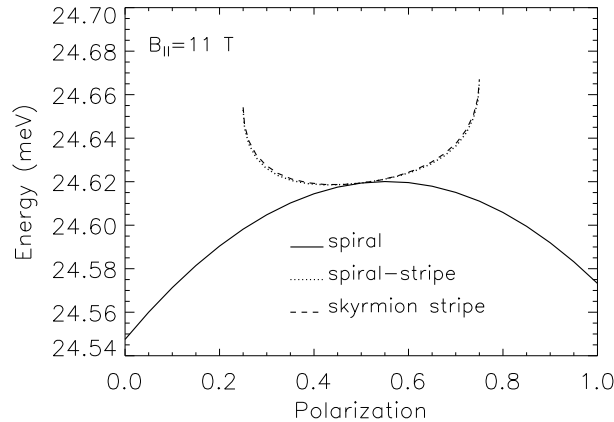


FIG. 11. Comparison of energies between three many-body phases of a wide well system at  $\nu = 6$  near the level crossing point ( $B_{\parallel}^* = 11.1$  T) : spiral (solid line), spiral stripe (dotted line) and skyrmion stripe (dashed line). The system parameters are chosen to be the same as those in Fig. 1. The polarization is defined by  $\Theta_2(0)$  (see Eq. (37) and the text), which is zero for the isospin up state (spin unpolarized) and is one for the isospin down state (spin fully polarized). For all three many-body phases, the isospin winding wavevector  $\vec{Q}_{\perp} = -\vec{Q}'_{\perp}$  has been chosen to be  $0.75 l_0^{-1}$  in  $y$  direction (perpendicular to the in-plane field) and zero in the  $x$  direction, which is the optimal value to minimize the HF energy if  $\Theta_2(0) \neq 0, 1$ . (It can be also obtained from the wavevectors of the roton minimum in the magnetoplasmon excitations as calculated in Ref. [17].) The phases,  $\gamma$  and  $\gamma'$  in Eq. (49) are set to be zero. For the spiral stripe and skyrmion stripe phase, the stripe phase function,  $\psi_k$ , is calculated variationally by using equations in Appendix E and parameters defined in Fig. 6. For the convenience of comparison, here we have fixed  $\psi_0 = \pi/2$ ,  $\xi = 0.5$ ,  $\eta = 0$  and stripe period  $a = 0.67 l_0 = 10^{-6}$  cm, and only  $\varphi$  is allowed to vary from  $-\pi/2$  to  $+\pi/2$ . When  $\varphi = 0$ , the energies of the stripe phases are the same as the spiral phase. (Note that the directions of the spiral stripe and the skyrmion stripe are different: the former one is along  $x$  direction while the latter one is along  $y$  direction, see Sections III A 2 and V.) We have checked that using other values does not change the figure qualitatively, and also cannot stabilize any of these many-body phases. In our calculation shown in this figure, the lowest energy state is always the conventional QH state (i.e. either spin unpolarized or spin fully polarized states at  $\Theta_2(0) = 0$  or 1 respectively). However, we find that the energy differences between these states with the three many-body states (spiral, spiral stripe and skyrmion stripe) are very small, and the lowest energy of the stripe phase curve (in both spiral stripe and skyrmion stripe) is at finite  $\varphi$ , showing that if only a uniform spiral phase is stabilized by some more sophisticated approximations, the stripe order may also be stabilized with energy even lower than the uniform spiral phase. The stabilization of a skyrmion stripe may be responsible to the resistance anisotropy observed in Ref. [15] in the strong in-plane field region (see text).

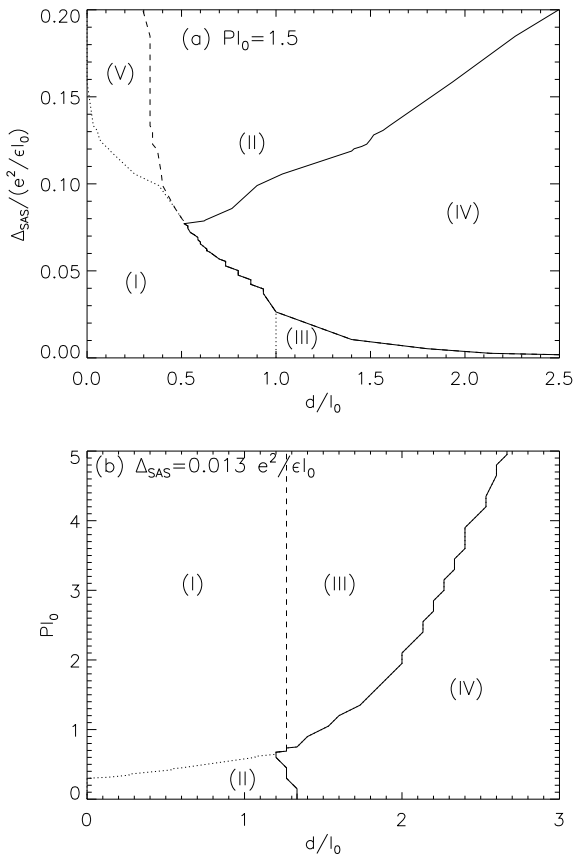


FIG. 12. Phase diagram of the bilayer system at  $\nu = 5$  in the presence of parallel magnetic field. (a) for fixed in-plane magnetic field ( $Pl_0 = 2\pi B_{\parallel} d l_0 / \Phi_0 = 1.5$ ), and (b) for fixed tunneling amplitude ( $\Delta_{SAS} = 0.013 e^2 / \epsilon_0$ ). In isospin language defined by layer index basis, phase I is an isospin coherent phase, phase II is an isospin spiral phase, phase III is an isospin stripe phase, phases IV and V are isospin spiral stripe phases. Note that phase V has a very long stripe period, and is related to the charge imbalance phase for the short-ranged interaction (see text).

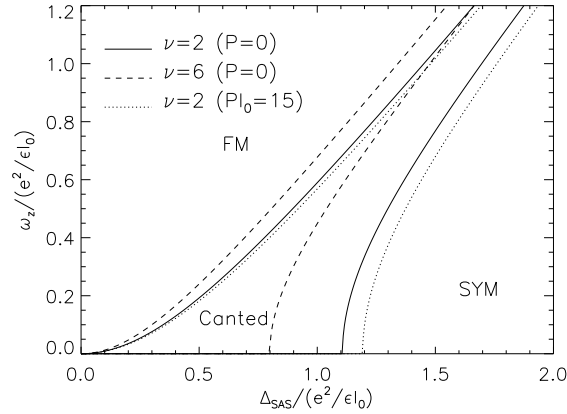


FIG. 13. Phase diagram of double well systems at  $\nu = 4N + 2$  in the presence of an in-plane magnetic field. The solid and dashed lines are for  $\nu = 2$  ( $N = 0$ ) and  $\nu = 6$  ( $N = 1$ ) without in-plane magnetic field, while the dotted lines are for  $\nu = 2$  with strong in-plane magnetic field ( $Pl_0 = 15$ ). The layer separation,  $d$ , is  $0.067l_0$ . FM is the ferromagnetic state with both filled levels being in the same spin polarized direction, and SYM is the symmetric state, where both spin indices are equally occupied in a symmetric orbital Landau level. In the middle is the canted antiferromagnetic phase, which breaks the spin and parity symmetries and is a commensurate state when finite in-plane magnetic field is applied.

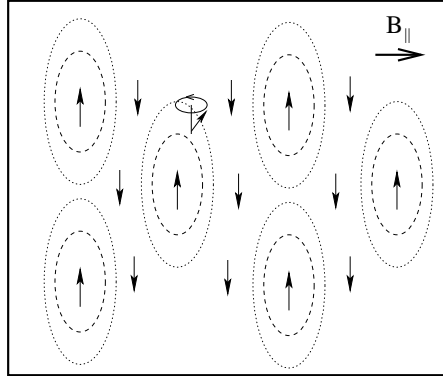


FIG. 14. Possible domain wall structure in integral quantum Hall system near level degeneracy region. Arrows denote the isospin polarization (see Fig. 3(a)). In the surface of each domain, isospin hybridization may be generated, resulting a coherent spiral order. The in-plane magnetic field is in  $+\hat{x}$  direction.